AD-A090 981 FOREIGN TECHNOLOGY DIV WRIGHT-PATTERSON AFB OH F/G 13/1
DE-ICING SYSTEMS OF FLIGHT VEHICLES. BASES OF DESIGN METHODS FO--ETC(U)
SEP 79 R K TENISHEV, B A STROGANOV, V S SAVIN
UNCLASSIFIED FTD-ID(RS)T-1163-79-PT-2 NL

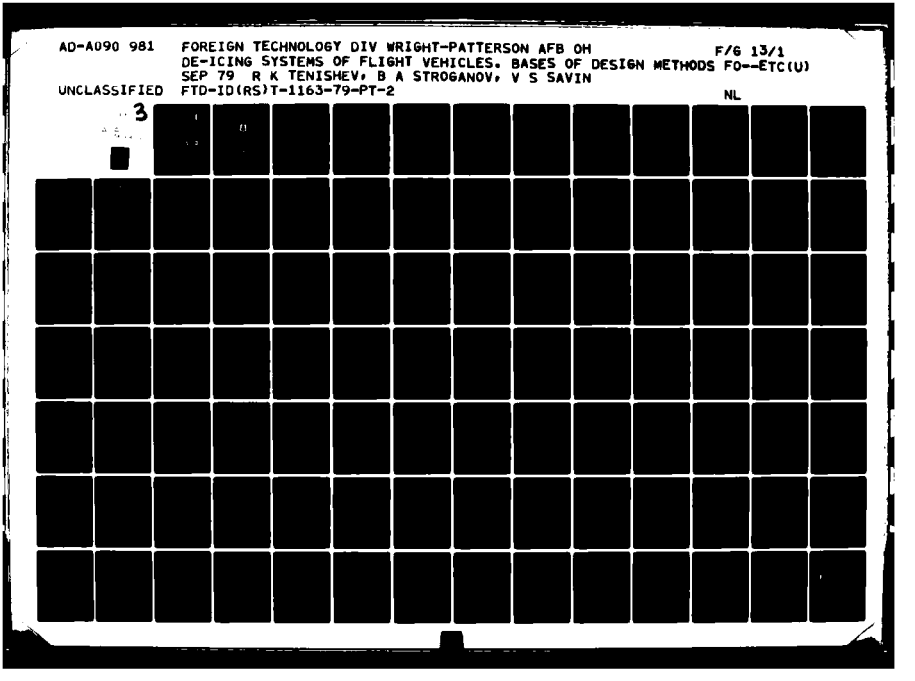

PHOTOGRAPH THIS SHEET

AD A090981

DTIC ACCESSION NUMBER

LEVEL

INVENTORY

FTD-ID(RS)T-1163-79, Part 2 of 2

DOCUMENT IDENTIFICATION

DISTRIBUTION STATEMENT A
Approved for public release;
Distribution Unlimited

DISTRIBUTION STATEMENT

ACCESSION FOR	
NTIS	GRA&I
DTIC	TAB
UNANNOUNCED	
JUSTIFICATION	
BY	
DISTRIBUTION /	
AVAILABILITY CODES	
DIST	AVAIL AND/OR SPECIAL
A	

DISTRIBUTION STAMP

DTIC
ELECTE
S OCT 3 1 1980 D
D

DATE ACCESSIONED

DATE RECEIVED IN DTIC

PHOTOGRAPH THIS SHEET AND RETURN TO DTIC-DDA-2

DTIC FORM OCT 79 70A

DOCUMENT PROCESSING SHEET

FTD-ID(RS)T-1163-79
Part 2 of 2

FOREIGN TECHNOLOGY DIVISION

DE-ICING SYSTEMS OF FLIGHT VEHICLES. BASES OF DESIGN METHODS FOR TESTING

by

R.Kh. Tenishev, B.A. Stroganov, et al

FTD- ID(RS)T-1163-79

UNEDITED MACHINE TRANSLATION

FTD-ID(RS)T-1163-79 7 September 1979

MICROFICHE NR: FTD-79-C-001215

DE-ICING SYSTEMS OF FLIGHT VEHICLES. BASES OF DESIGN METHODS FOR TESTING

By: R.Kh. Tenishev, B.A. Stroganov, et al

English pages: 681

Source: Protivoobledenitel'nyye Sistemy Letatel'nykh Apparatov. Osnovy Proyektirovaniya i Metody Ispytaniy, Izd-vo "Mashinostroyeniye", Moscow, 1967, pp. 1-320

Country of origin: USSR
This document is a machine translation
Requester: AEDC
Approved for public release; distribution unlimited.

PREPARED BY:

TRANSLATION DIVISION
FOREIGN TECHNOLOGY DIVISION
WP-AFB, OHIO.

Table of Contents

Page 198.

Chapter VII.

Calculation of air-heat deicers [1].

FOOTNOTE [1]. It is written by V. S. Savin. ENDFOOTNOTE.

The calculation of air-heat POS should be begun with the construction of the standard flight profile of the projected/designed aircraft. For example, it is necessary to examine such phases of flight as the climb, cruise flight, reduction/descent, circling flight and pre-landing glide. For each phase of flight is determined the flow rate of hot air, air-heat POS required for a work. It is obvious that this value must be lower than available air flow rates per all phases of flight. Furthermore, when selecting of one or the other system designer must consider its coefficient of heat efficiency, weight, simplicity and reliability of construction/design. The coefficient of the heat efficiency of deicer is found from the following expression:

$$\eta_т = \frac{t_{вх} - t_{вых}}{t_{вх} - t_{п.в}}, \qquad (7.1)$$

where $t_{вх}$ and $t_{вых}$ - temperature of hot air respectively at entry and outpet from the deicer;

$\tilde{t}_{п.ов}$ - mean temperature of the shielded surface during the steady supply of hot air.

For example, if the coefficient of the heat efficiency of the first four standard diagrams, given in Fig. 3.20, usually does not exceed 0.5 the for two latter/last diagrams of this coefficient can reach value on the order of 0.75.

7.1. Determination of the required flow rate of hot air and extent of zone heating.

For determining the required flow rates of hot air for the de-icing systems of permanent action can be used two methods: estimated and designing.

Calculation according to the first method is fulfilled on the basis of the following assumptions:

- flow conditions in boundary layer is turbulent above the entire shielded surface;

- temperature of surface $t_п$ is permanent by the area;

- aerodynamic heating of surface is equal to 0;

- entire/all shielded surface is represented in the form of flat/plane plate with an area of F (this means that $V_1=V_0$) (neg)

- entire/all shielded surface is moistened by water ($\xi_{в.п} = 1,0$).

Page 199.

With such assumptions the density of external heat flux average over surface under conditions of icing can be calculated from the formula, analogous (5.51a):

$$\tilde{q} = \tilde{\alpha}\,(\tilde{t}_{п.\,в.п} - t_0)\,X_0, \qquad (7.2)$$

where

$$X_0 = 1 + \frac{1550}{p_0} \cdot \frac{e_п - e_0}{t_{п.\,в.п} - t_0}.$$

Then the required flow rate of hot air is equal to

$$G = \frac{\tilde{q} \cdot F}{c_p (t'_{вх} - t'_{вых})} = \frac{\tilde{\alpha} (\tilde{t}_{п. вл} - t_0) X_0 F}{c_p (t'_{вх} - t'_{вых})}, \qquad (7.3)$$

or taking into account formula (7.1)

$$G = \frac{\tilde{\alpha} (\tilde{t}_{п. вл} - t_0) X_0 F}{c_p (t'_{вх} - \tilde{t}_{п. вл}) \eta_т}. \qquad (7.3а)$$

Being assigned by the temperature of hot air at the entry into deicer $t'_{вх}$ and the calculated temperature of moist surface $t_{п. вл}$ (they usually accept, that $t_{п. вл} = 0$), it is possible to rapidly rate/estimate the necessary air flow rate at this temperature of icing t_0.

The designing calculation method is based on the more precise representation of all processes which occur with the work of deicer.

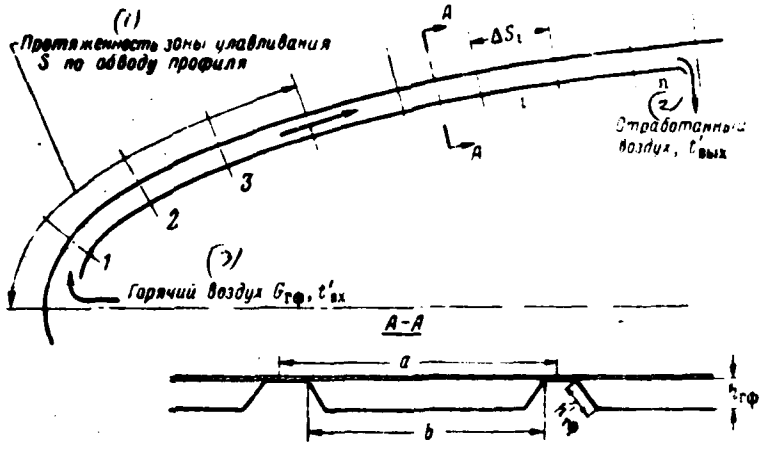

Fig. 7.1. Diagram for the calculation of the air-heat deicers with longitudinal-transverse channels.

Key: (1). Extent of the zone of catching S on the enclosure of profile/airfoil. (2). Exhaust air. (3). Hot air.

Page 200.

Let us examine the heat balance of moist surface during the course of hot air in transverse channels (Fig. 7.1), which are the accessory/affiliation of the majority of the most widely used types of air-heat POS. Let us break entire length of transverse channel into the series/row of the sections (segments) of small length ΔS and will comprise for the arbitrary i section of the outer covering of the equation of heat balance.

During course in transverse channel hot air gives up heat to

external and lower coverings. The first equation of heat balance which approximately describes the process of heat transfer in transverse channel, has the following form:

$$q_{ni}a\,\Delta S_i = \alpha_i'(t_i' - t_{ni})\,b\,\Delta S_i + \alpha_i'(t_i' - t_{r\phi i})(b + 2h_{r\phi}')\,\Delta S_i \quad (7.4)$$

or with $b \gg h_{r\phi}'$

$$q_{ni}a = [\alpha_i'(t_i' - t_{ni}) + \alpha_i'(t_i' - t_{r\phi i})]\,b, \quad (7.4a)$$

where α_i' - a local internal heat-transfer coefficient in W/m²deg;

$t_{r\phi i}$ - temperature of the wall of corrugation in the considered/examined cross section in °C;

t_i' - temperature of hot air in °C.

During the compilation of this equation disregarded/neglected the effect of thermal conductivity on skin/sheathing chord wise, since experimental data show that this leads to insignificant errors.

Since the external and lower coverings are contacted, then are theoretically possible two cases: 1) the heat, accumulated in the lower covering, is not transmitted to the outer covering; 2) entire heat from the lower covering passes via thermal conductivity to the outer covering. Virtually the first case can occur with usual riveted

joint of skins/sheathings, since it has very high thermal resistance [114]. The equation of heat balance for this case takes the form

$$q_{ni}a = \alpha_i' (t_i' - t_{n\ ani})\, b. \qquad (7.5a)$$

In the second case which can be during the seam welding (several to a lesser degree - with point), the outer covering obtains heat both directly from hot air and indirectly, via thermal conductivity from the lower covering through the connections between skins/sheathings. Therefore the equation of heat balance for the second case can be presented as follows (with b $h_{(.)}$):

$$q_{ni}a = \alpha_i' (t_i' - t_{n\ ani})\, 2b. \qquad (7.5б)$$

Consequently, in the case of the ideal thermal connection of skins/sheathings heat flux to the outer covering increases two times in comparison with heat flux for usual riveted joint.

Page 201.

In actuality the difference between the heat fluxes indicated will be somewhat less. However, the comparison of these versions shows that it is necessary to approach that so that the thermal connection/communication between skins/sheathings in transverse channel would be as more modern as possible.

During the heat transfer to outer skin the temperature of hot air is decreased as hot air moves over channel. Consequently, it is possible to write the second equation of heat balance for the i section of the corrugation:

$$q_{ni}a \cdot \Delta S_i = G_в c_i \Delta t_i', \qquad (7.6)$$

where $\Delta t_i'$ - a temperature drop in section ΔS_i (see below).

The density of external heat flux q_{ni} is determined from formula (5.51) for this section ΔS_i:

$$q_{ni} = \alpha_i (t_{п.вн i} - t_{1i}^*) X_i',$$

where

$$X_i' = 1 + \xi_{вн i} \frac{1550}{p_{1i}} \cdot \frac{e_п - e_1}{t_{п.вн i} - t_{1i}^*}.$$

In this case $\xi_{вн i} = 1{,}0$ in the zone of the catching of drops and then is gradually decreased (see Fig. 5.7). In order to satisfy the conditions of heat balance from hot air to the outer covering, equations (5.51), (7.5a) or (7.5b) and (7.6) must be solved together, the coefficients in these equations depending on unknown values. Therefore we will use the method of successive approximations (in this case flight conditions and the construction/design of the channels of deicer it is predicted known).

The first space consists in the selection of certain initial value of the flow rate of hot air $G_к$ in transverse channel, that it is possible to make on the basis of formula (7.2). Then are assigned by value temperature drops of hot air $\Delta t_i'$ in section ΔS_i in question and from equation (7.6) is determined value $q_n^{(1)}$ in the first approximation. In this case mean temperature of hot air in the i section can be approximately found from the formula

$$t_i' \approx t_{вхi}' - \frac{1}{2}\Delta t_i'. \qquad (7.7)$$

After substituting values $q_{ni}^{(1)}$ and t_i' in equation (7.5a) or in equation (7.5b), they calculate the temperature of moist surface $t_{п.вхi}$ in the i section, after which from equation (5.51) is found value $q_{ni}^{(2)}$ in the second approximation and it is compared with the first value $q_{ni}^{(1)}$ If these two values differ from each other, then they are assigned by the new value of a temperature drop of air $\Delta t_i'$ and calculation is repeated as long as the preceding/previous and subsequent solution will not be indentical with acceptable precision/accuracy.

Page 202.

With the selected air flow rate successive approximations are fulfilled for each section of transverse channel, beginning from the first and terminating with such section, on which either will occur

the complete evaporation of entire captured by the profile/airfoil of water or the temperature of surface will become equal to 0°C.

The quantity of water which evaporates in section ΔS_i per unit time, can be calculated on the basis of formulas (5.30) and (5.50):

$$G_{wi} = \alpha \xi_{\infty,i} \frac{c_{wi}}{p_{\infty} c_p} \Delta S. \quad (7.8)$$

Knowing a quantity of water, which flows to section ΔS_i, $G_{wi} = G_{\infty,i} + G_{w(i-1)}$ and a quantity of evaporating water G_{wi}, it is possible to calculate a quantity of water, which disappears back/ago from profile/airfoil beyond the limits ΔS_i:

$$\Delta G_{wi} = (G_{wi} - G_{wi}) a.$$

If the temperature of surface becomes equal to zero before entire absorbed by water will be vaporized, then in this case is formed barrier ice which will be greater, the more will run out water along profile/airfoil for the warmed zone. The procedure presented makes it possible to find the chordwise distance, which must be warmed in order to vaporize entire water, recovered by profile/airfoil, and also the minimum flow rate of hot air which is required for the complete evaporation of the absorbed by water, before the temperature of surface it will achieve 0°C. Such calculation is produced for the so-called de-icing systems of complete evaporation. For the systems of incomplete evaporation the

calculation is produced thus, but in this case it is necessary to estimate the possible value of barrier ice.

If deicer is carried out on diagram with the longitudinal channel (see Fig. 3.17a), then the calculated equations of heat balance will take somewhat another form. Diagram for the calculation of this deicer is given in Fig. 7.2. Principle of the compilation of the equations of the heat balance of the same as for transverse channels.

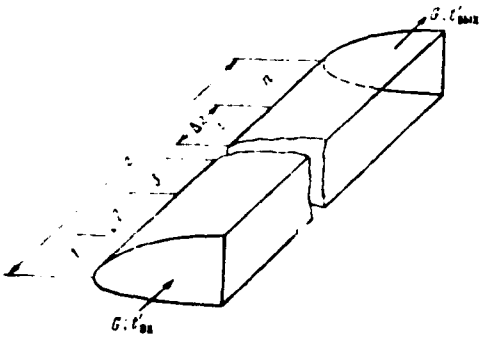

Fig. 7.2. Diagram for the calculation of the air-heat deicer with longitudinal channel.

Page 203.

Longitudinal channel with a length of z is divided/marked off into the series/row of the sections of small length Δz. The first equation of heat balance for the i section will take the following form:

$$q_{ni} = \alpha_i' (t_i' - t_{n\,ni}), \qquad (7.9)$$

where α_i' - a heat-transfer coefficient from hot air to the walls of longitudinal channel in W/m²·deg.

Analogously is composed the second equation of the heat balance

$$\tilde{q}_{ni} S_u \Delta z_i = G_i c_p \Delta t, \qquad (7.10)$$

in which S_u - size/dimension of zone heating for the external enclosure of profile/airfoil. To these two equations is connected the equation for external heat flux $\tilde{q}_{ni}$, averaged along the length S_u. The calculation of the required flow rate of hot air (and of the sizes/dimensions of channel) is produced also by the method of successive approximations. Thus can be produced the calculations of heat transfer in the diagrams of deicers with the longitudinal-transverse distribution of hot air.

7.2. Calculation of heat-transfer coefficients in internal ducts.

For the solutions of the equations of heat balance it is necessary to know the coefficients of internal heat emission α' from hot air to the walls of channel. Heat-transfer coefficients at the entry into transverse channel are greatest and further are decreased to constant value [11], [38], [64], [68].

For the calculation of heat-transfer coefficient in the transverse channel of that of most being adequate/approaching is the following formula:

$$\alpha' = \left(1 + 1{,}7\,\frac{d_r}{S}\right)\alpha'_0 \quad вт/м^2 \cdot град, \qquad (7.11)$$

(1)

Key: (1). Вт/м²·deg.

in which d_r is a hydraulic diameter of channel, S - distance from the beginning of channel, and α'_0 - heat-transfer coefficient during the stabilized course in channel. This coefficient is determined thus:

$$\alpha'_0 = 7{,}96 \left(\frac{T_{эф}}{d_r}\right)^{0,2} (\bar{G})^{0,8} \text{ вт/м}^2 \cdot \text{град}. \quad (1) \qquad (7.12)$$

Key: (1). W/m²•deg.

Heat-transfer coefficients from hot air in longitudinal channel with the fluted lower covering it is possible to find from the expression

$$\alpha' = 2{,}2 \left(\frac{T_{эф}}{d_r}\right)^{0,4} (\bar{G})^{0,6} \text{ вт/м}^2 \cdot \text{град}. \quad (1) \qquad (7.13)$$

Key: (1). W/m²•deg.

Page 204.

If in longitudinal channel is utilized flat dual skin/sheathing, and also when deicer does not have transverse channels, it is possible to use formula for the turbulent flow in the tubes

$$\alpha' = 6{,}37 \left(\frac{T_{эф}}{d_r}\right)^{0,2} (\bar{G})^{0,8} \text{ вт/м}^2 \cdot \text{град}. \quad (1) \qquad (7.14)$$

Key: (1). W/m²•deg.

For a clarity it should be pointed out that $\bar{G}$ is mass rate of

discharge (air flow rate, in reference to the cross-sectional area of channel), and value of so-called "effective" temperature $T_{эф}$ is defined as the mean arithmetic value of inlet temperature and at the output of channel or section of channel in question.

7.3. Calculation of the temperature of air in manifolds and longitudinal channels.

By another parameter which is required to know for solving the equations of heat balance, is temperature of air at the inlet into the channel of deicer. Before hitting the deicer of one or the other aircraft component, the hot air moves from source over inlet pipes, losing in this case certain quantity of heat. Further decrease of the temperature of hot air occurs in the longitudinal channels of deicer or in distributing pipes (tubes "piccolo").

For the calculation of a temperature drop in distribution network of the air-heat de-icing system let us examine the conduit/manifold of constant section with a length of $l_{тр}$, along which flows hot air with permanent flow rate/consumption $G_{тр}$ and variable temperature t'. Let us isolate on this conduit/manifold infinitesimal section $d\ell$ and let us compose for it the equation of heat balance during the trimmed/steady-state flow conditions:

$$-c_p G_{тр}\, dt' = K_{тр}(t' - t_{о.тр})\,\Pi\, dl, \qquad (7.15)$$

where $t_{o.тр}$ - ambient temperature out of the conduit/manifold;

P - perimeter of the conduit/manifold;

$K_{тр}$ - coefficient of heat transfer, determined in to the formula

$$K_{тр} = \frac{1}{\frac{1}{\alpha_{тр}} + \frac{\delta_{из}}{\lambda_{из}} + \frac{1}{\alpha_{о.тр}}} \text{ (1) } вт/м^2 \cdot град, \qquad (7.16)$$

Key: (1). W/m²•deg

where $\alpha_{тр}$ - heat-transfer coefficient to the internal wall of tube in W/m²deg;

$\alpha_{о.тр}$ - heat-transfer coefficient from the external wall of conduit/manifold into its ambient medium in W/m²deg;

$\lambda_{из}$ - coefficient of thermal conductivity of insulation/isolation in W/m•deg.

Page 205.

Integrating equation (7.15) (taking into account boundary condition $t = t_{вх}$ with $\ell = 0$, we will obtain the instantaneous value of

the temperature of air along the length of the tube

$$t' = (t'_{вх} - t_{о.тр}) \exp\left(-\frac{K_{тр}\Pi}{c_p G_{тр}} l\right) + t_{о.тр}. \qquad (7.17)$$

Consequently, the decrease of the temperature of hot air at output from this conduit/manifold will comprise

$$\Delta t' = t'_{вх} - t' = (t'_{вх} - t_{о.тр})\left[1 - \exp\left(-\frac{K_{тр}\Pi}{c_p G_{тр}} l\right)\right]. \qquad (7.18)$$

The air flow rate can be decreased in proportion to approximation/approach to deicer, which in turn, will produce change in the coefficient of heat transfer. Therefore the total decrease of the temperature of hot air $\Delta t'_{\Sigma}$ in distribution network from engine to the channel of deicer will be equal to the sum of temperature drops in each tube. Thus, temperature of air at the inlet into channel is determined by the relationship/ratio

$$t'_{вх.к} = t'_{отб} - \Delta t'_{\Sigma}. \qquad (7.19)$$

The temperature of selected/taken air $t'_{отб}$ is determined on the basis of the characteristics of heat source in this mode/conditions (for example, in accordance with the engine characteristics).

Thus is designed a temperature drop of hot air in longitudinal feeders and tubes "piccolo", moreover it is necessary to consider that the air flow rate is variable/alternating along the length of longitudinal channel, since in proportion to motion it is

abstracted/removed either into transverse channels or it escape/ensues from openings/apertures (tube "piccolo"). Therefore the calculation of a temperature drop in longitudinal channel at length l before the cross section of deicer in question can be produced on the basis of formula (7.17), accepting $\Delta l_i = a$ (see Fig. 7.1), and the air flow rate per the i section of channel it is located through the formula

$$G_i = G_{вх} - 2m_{кi}G_к. \qquad (7.21)$$

where $2m_{кi}$ - a quantity of transverse channels on upper and pressure side of profile before this cross section.

In this case the local coefficient of heat transfer is located through to the formula

$$K_i = \frac{1}{\frac{1}{\alpha_к} + \frac{1}{\alpha_0}} \text{ вт/м}^2\cdot\text{град}, \qquad (7.21a)$$

(1)

by Key: (1). W/m²·deg

where $\alpha_к$ - heat-transfer coefficient from hot air to the internal walls of longitudinal channel in W/m²·deg;

α_0 - heat-transfer coefficient from wall into the internal cavity of wing in W/m²·deg.

Page 206.

Analogously for tubes "piccolo" let us have

$$G_i = G_{вх} - m_{отв} G_{отв}, \qquad (7.22)$$

where $m_{отв}$ - quantity of openings/apertures before this cross section and

$$K_i = \frac{1}{\frac{1}{\alpha_{гр}} - \frac{1}{\alpha_{о.гр}}} \text{ (1) } вт/м^2 \cdot град. \qquad (7.21б)$$

Key: (1). W/m²·deg.

Let us note that value $\alpha_{о.гр}$ here and in formula (7.16) is determined in essence by the conditions for free convection and can be found from the formula, given in work [64]:

$$\alpha_{о.гр} = 11{,}0 + 0{,}010 t_{эф} \sqrt[3]{t_{эф}}, \qquad (7.23)$$

moreover it is possible to consider that

$$t_{эф} = \frac{t' + t_{о.гр}}{2}. \qquad (7.24)$$

Since the temperature of hot air in longitudinal channel is decreased, then the calculation of the required flow rate of air whose procedure is presented above, it is expedient to carry out for two cross sections of deicer, which correspond to maximum (for the evaluation of possible superheating) and minimum temperature of air

in this channel. Determining will be the cross section in which hot air has minimum temperature.

7.4. Hydraulic design of system.

For the satisfactory work of air-heat POS it is necessary to ensure the appropriate pressures of hot air in distributing pipes and at the entry into transverse and longitudinal channels.

In this case is performed hydraulic design. Losses of pressure in transverse channels are determined from the formula

$$\Delta p_к = \left(\zeta_{вх} + c_f \frac{l}{d_{гидр}}\right) \frac{\varrho v_к^2}{2} \text{ (1) } н/м^2. \qquad (7.25)$$

Key (1). N/m^2.

where $\zeta_{вх}$ - an intake loss coefficient;

c_f - coefficient of friction.

On the basis of experimental data it is known that $\zeta_{вх} = 0{,}5 \div 1{,}0$.

A pressure drop in longitudinal air duct along leading edge can be calculated by the analogous formula

$$\Delta p_к = c_f \frac{\varrho v_к^2}{2} \frac{l}{d_{гидр}} \text{ (1) } н/м^2. \qquad (7.26)$$

Key (1). N/m^2.

Page 207.

If the lower covering is carried out fluted, then the coefficient of friction c_f in this formula can be calculated approximately according to formula for the strongly rough tubes:

$$c_f = \frac{0.22}{\mathrm{Re}_k^{0.2}}, \text{ где } \mathrm{Re}_k = \frac{v_k d_{\text{экв}}}{\nu}. \qquad (7.27)$$

Key: (1). where

But if are utilized transverse channels in the form of dual skin/sheathing, then the value of the coefficient of friction is found through formula for the usual technical conduits/manifolds:

$$c_f = \frac{0.184}{\mathrm{Re}^{0.2}}. \qquad (7.28)$$

Losses of pressure in the straight/direct sections of the conduits/manifolds, which supply hot air from engine to the shielded surface, is designed from the formula

$$\Delta p_{\text{тр}} = \sum_{i=1}^{n} \left(\zeta_i + f_i \frac{l}{d_{\text{тр}}} \right) \frac{\rho_i v_i^2}{2}, \qquad (7.29)$$

in which number n it is a number of sections in distribution network, and the values of the local factors of loss ζ_i and local coefficient of friction C_{fi} in the i section of distribution network are taken on the basis of the experimental data given in the reference literature (see for example, [18]).

Hydraulic design of the air-heat deicers, carried out according to diagrams in Fig. 3.17d, e and f, differs from that given above some special features/peculiarities. In these versions hot air must escape/ensue from the openings/apertures of tubes "piccolo" with the transonic speed; therefore all over length of conduit/manifold static pressures must be not less than critical pressures at given flight altitude. It is obvious that in this case it is necessary to ensure the uniform distribution of the hot air through openings/apertures in distributive tube.

So that the static pressure along the length of conduit/manifold would be constant, it is necessary that in the beginning of conduit/manifold the air speed would be more than the air speed at the end of the conduit/manifold and a difference in the dynamic pressures, corresponding to the speeds of air circulation along the length of conduit/manifold, was equal to the total loss of pressure on main line. This it is possible to attain, if to accept the specific cross sections along the length of conduit/manifold. The change in the cross section can be carried out either smoothly (conical tube), or it is gradual (the flexible pipes of different diameter). It is desirable to provide minimum speeds along the length of conduit/manifold and maximum (sonic) discharge velocities from openings/apertures.

Page 208.

For the calculation of air pressure conduit/manifold can be considered as the chamber/camera of the constant static pressure, equal to critical. We consider that during the outflow of air from openings/apertures is lost one dynamic pressure alone, which corresponds to discharge velocity $V_{отв}$. Furthermore, as a result of the compression of jet upon the entry into opening/aperture $\zeta_{вх} = 0,5$, and exit losses are rated/estimated by value $\zeta_{вых} = 1,0$. These losses must be equal to static air pressure in conduit/manifold [19]

$$p = 1,5\frac{\rho V_{отв}^2}{2}.$$

Let us assume that in the beginning of conduit/manifold the speed is greater than at the end before the latter/last opening/aperture, i.e., $V_{нач} > V_{кон}$. For the constancy of static pressure all over length of main line it is necessary to observe the equality

$$\frac{\rho V_{нач}^2}{2} - \frac{\rho V_{кон}^2}{2} = \sum(\Delta p_{тр} + \Delta p_м), \qquad (7.30)$$

where $\Delta p_{тр}$ - total loss of pressure to friction along the length of distributing pipe in N/m²;

$\Delta p_м$ - loss of pressure in the local resistance of all openings/apertures in conduit/manifold in N/m².

For simplicity of calculation let us accept such values of the diameters of conduit/manifold so that the air speed after each opening/aperture would be decreased by one and the same value

$$\Delta V = \frac{V_{нач} - V_{кон}}{n}, \qquad (7.31)$$

where n- number of holes in conduit/manifold.

Loss of pressure between adjacent openings/apertures due to velocity change during the division of flow will be equal to

$$\Delta p_м = \frac{1}{3}\left(\frac{V_{нач} - V_{кон}}{n}\right)^2 \frac{\rho}{2} = \frac{1}{3}\rho\frac{(\Delta V)^2}{2}. \qquad (7.32)$$

Since along the length of conduit/manifold there are by n of openings/apertures, then total loss of pressure on local resistance will comprise

$$\sum \Delta p_м = \frac{1}{3n}(V_{нач} - V_{кон})^2 \frac{\rho}{2}. \qquad (7.33)$$

Adding to this value $\sum \Delta p_м$ loss of pressure on friction $\sum \Delta p_{тр}$, we will obtain the total loss of pressure in conduit/manifold, which must satisfy equation (7.30). Otherwise should be to accept other values of speed $V_{нач}$ and $V_{кон}$ and again fulfilled the calculation of losses.

Page 209.

After conducting of complete hydraulic design of air-heat de-icing system total losses of pressure must be compared with the available pressures of the source of hot air at given height/altitude. For the operation of system it is necessary that the available pressures would be more than calculations.

7.5. Calculation of the temperature of heating surface during the flow of its "dry" air.

Besides the flow rate of hot air it is frequently necessary to know the temperature of heating surface during the flow of its "dry" air. Let us determine the temperature of surface during the trimmed/steady-state mode/conditions. For this let us break transverse channels into the series/row of sections 1, 2, 3, ..., i, ..., n of small length ΔS_i and for each of them let us examine the system of equations (5.2), (7.6) and the equation, analogous (7.5a), but for a "dry" surface (for the welded joint of skins/sheathings):

$$\left.\begin{aligned} q_{ni} &= \alpha_i (t_{ni} - t_{1i}^*), \\ q_{ni}a &= \alpha_i' (t_i' - t_{ni})\, 2b, \\ q_{ni}a\,\Delta S_i &= c_p' G_x' \Delta t_i'. \end{aligned}\right\} \qquad (7.34)$$

In this case according to (7.7) we accept

$$t_i' = t_{\text{ex}i}' - \frac{1}{2}\Delta t_i'.$$

Then from system of equations (7.34) we are have

$$t_{ni} = \frac{t_{\text{ex}i}' + B_i t_{1i}^*}{1 + B_i}, \qquad (7.35)$$

where

$$t'_{\text{вх } i} = t'_{\text{вх } i-1} - \Delta t'_{i-1}, \qquad (7.36)$$

$$\Delta t'_{i-1} = C_{i-1}(t_{\text{п } i-1} - t^{\circ}_{1\,i-1}). \qquad (7.37)$$

In these formulas B_i and C_i are the dimensionless coefficients, which are the thermal characteristics of channel in this section ΔS_i:

$$C_i = \frac{a\,\Delta S_i}{c_p G}\,\alpha_i, \qquad (7.38)$$

$$B_i = \frac{1}{2}\left(C_i + \frac{a}{b}\,\frac{\alpha_i}{\alpha'_i}\right). \qquad (7.39a)$$

It is necessary to note that in the case of the riveted connection (more precisely saying, in the case of the heat-insulated corrugation) coefficient B_i will have other somewhat writing:

$$B_i = \frac{1}{2}\left(C_i + 2\,\frac{a}{b}\,\frac{\alpha_i}{\alpha'_i}\right). \qquad (7.39б)$$

Page 210.

All remaining calculation formulas remain without change.

On the basis of given formulas (7.35)-(7.39) it is possible to find the temperature of surface in the middle of each section ΔS_i, if is known inlet temperature into transverse channel. The analysis of

equations (7.35)-(7.39) shows that the temperature of external surface in the i section can be raised by three paths:

1) by an increase in the temperature of air at the inlet into transverse channel $t_{вх i}$;

2) by an increase in the flow rate of hot air, which leads to the decrease of a temperature drop of hot air in i section Δt_i and, therefore, to increase t_i;

3) with an increase in the heat-transfer coefficients.

For the prescribed/assigned flow rate of air of an increase in the heat-transfer coefficients α_i it is possible to attain by decreasing the cross section of channels, i.e., by decreasing the height/altitude of corrugations, as this follows from the examination of equations for heat-transfer coefficients.

An increase in the temperature of hot air at the entry into transverse channel has limitations from the point of view of the strength of the outer covering. For usual duralumin skins/sheathings is allowed/assumed the maximum temperature of heating on the order of 100°C. Calculations show that in that case the temperature of hot air at the entry into transverse channel must not exceed 200°C [1].

FOOTNOTE 1. If air supply with higher temperature in any flight conditions is not eliminated, then it is necessary to provide for the installation of the limiters of the temperatures which must disconnect the supply of hot air to overheated section POS.

With known extent zone heating on the enclosure of profile/airfoil it is possible to find the optimum relationship/ratio between the height/altitude of transverse channel, the flow rate of hot air and the temperature of hot air on the entry into this channel. The relationship/ratio indicated will be determined by such values: $h_{r\phi}$, $G_к$ and $t_{вх1}$, at which the value of the coefficient of heat efficiency $\eta_т$, determined according to formula (7.1), will be maximum for the given construction/design of deicer. In order to find the optimum values of the parameters indicated, it is necessary to fulfill calculations according to formulas (7.35)-(7.39) for different values $h_{r\phi}$, $G_к$ and $t_{вх1}$ and then according to formula (7.1) to find the coefficients of heat efficiency in each special case.

7.6. Conversion of the characteristics of the air-heat heaters of surface on flight conditions in "dry" air.

Let us derive the relationships/ratios between the characteristics of air-heat deicers in two arbitrary modes/conditions on height/altitude and speed for the case of flight in "dry" air.

Page 211.

The quantity of heat, which exits from heating surface of F per unit time, in flight in "dry" air can be found from the equation

$$Q = \tilde{\alpha}(\tilde{t}_n - \tilde{t}_0^*) F, \qquad (7.40)$$

where the average heat-transfer coefficient in external flow $\tilde{\alpha}$ is determined from formula (5.20), and value $\tilde{t}_0^*$ - according to formula (5.5) for case of $V_1 = V_0$.

Formula (5.20) corresponds to turbulent flow conditions in boundary layer on surface of body. Specifically, this flow conditions is of greatest interest during the calculation of the parameters POS, as was shown in chapter V. A difference in the temperatures in brackets can be represented as follows:

$$\tilde{t}_n - \tilde{t}_0^* = \Delta\tilde{t}_0 - \Delta\tilde{t}_0^*,$$

where, in this case, $\Delta\tilde{t}_0$ - average/mean temperature drop between the temperature of surface and the temperature of airflow. Consequently, finally let us have the following equation for the heat flux:

$$Q = C \frac{F}{S^{0,2}} (\rho_0 V_0)^{0,8} (\Delta\tilde{t}_0 - \Delta\tilde{t}_0^*). \qquad (7.41)$$

As follows from formulas (7.3) and (7.20), the total air flow rate, necessary for protection from the icing of surface with an area of F, it will be equal to

$$G_{\Sigma} = \frac{Q}{c_p(\Delta t'_{отб} - \Delta t'_{\Sigma} - \tilde{\Delta t}_0)\eta}.$$

Let us present this dependence into somewhat other form

$$Q = c_p G_{\Sigma}(\Delta t'_{отб} - \Delta t'_{\Sigma} - \tilde{\Delta t}_0)\eta. \qquad (7.42)$$

In this formula $\Delta t_{отб}$ is the temperature drop between the temperature of the air, selected/taken from engine $t_{отб}$, and the temperature of surrounding air t_0.

Substituting equation (7.42) in equation (7.41), we will obtain

$$c_p G(\Delta t'_{отб} - \Delta t'_{\Sigma} - \tilde{\Delta t}_0)\eta = C\frac{F}{S^{0,2}}(\rho_0 V_0)^{0,8}(\tilde{\Delta t}_0 - \tilde{\Delta t}_0^{\circ}). \qquad (7.43)$$

From the comparison of two different flight conditions escape/ensues the following general/common/total equation for the combined effect of height/altitude and speed:

$$\frac{G_{\Sigma 1}(\Delta t'_{отб\,1} - \Delta t'_{\Sigma 1} - \tilde{\Delta t}_{01})}{G_{\Sigma 2}(\Delta t'_{отб\,2} - \Delta t'_{\Sigma 2} - \tilde{\Delta t}_{02})} = \left(\frac{\rho_{01}V_{01}}{\rho_{02}V_{02}}\right)^{0,8}\frac{\tilde{\Delta t}_{01} - \tilde{\Delta t}_{01}^{\circ}}{\tilde{\Delta t}_{02} - \tilde{\Delta t}_{02}^{\circ}}. \qquad (7.44)$$

During the compilation of equation (7.44) was produced the contraction of the coefficients of the heat efficiency of systes in two different modes/conditions. Generally speaking, this coefficient has different values in flight conditions, but these differences are small.

Let us examine several calculated cases.

1) In flight at the permanent height/altitude $p_{01}=p_{02}$, consequently:

$$\frac{G_{\Sigma 1}\left(\Delta t'_{\text{отб}}-\Delta t'_{\Sigma 1}-\Delta\tilde{t}_{01}\right)}{G_{\Sigma 2}\left(\Delta t'_{\text{отб}\,2}-\Delta t'_{\Sigma 2}-\Delta\tilde{t}_{02}\right)}=\left(\frac{V_{01}}{V_{02}}\right)^{0,8}\frac{\Delta\tilde{t}_{01}-\Delta\tilde{t}^{\bullet}_{01}}{\Delta\tilde{t}_{02}-\Delta\tilde{t}^{\bullet}_{02}}. \quad (7.44a)$$

2) at permanent true airspeed $V_{01}=V_{02}$ and $\Delta t^{\bullet}_{01}=\Delta t^{\bullet}_{02}$, therefore

$$\frac{G_{\Sigma 1}\left(\Delta t'_{\text{отб}\,1}-\Delta t'-\Delta\tilde{t}_{01}\right)}{G_{\Sigma 2}\left(\Delta t'_{\text{отб}\,2}-\Delta t'-\Delta\tilde{t}_{02}\right)}=\left(\frac{p_{01}}{p_{02}}\right)^{0,8}\frac{\Delta\tilde{t}_{01}-\Delta\tilde{t}^{\bullet}_{01}}{\Delta\tilde{t}_{02}-\Delta\tilde{t}^{\bullet}_{01}}. \quad (7.44b)$$

3) at permanent indicated airspeed will occur the following relationship/ratio:

$$\varrho_1 V_{01}^2=\varrho_2 V_{02}^2$$

or

$$\frac{V_{01}}{V_{02}}=\sqrt{\frac{\varrho_2}{\varrho_1}}=\sqrt{\frac{p_{02}}{p_{01}}\cdot\frac{T_{01}}{T_{02}}}.$$

Substituting this dependence in equation (7.44), we will obtain

$$\frac{G_1\left(\Delta t'_{\text{отб}1}-\Delta t'_{\Sigma 1}-\tilde{\Delta t}_{01}\right)}{G_2\left(\Delta t'_{\text{отб}2}-\Delta t'_{\Sigma 2}-\tilde{\Delta t}_{02}\right)}=$$

$$=\left(\frac{T_{01}p_{01}}{T_{02}p_{02}}\right)^{0,4}\frac{\tilde{\Delta t}_{01}-\tilde{\Delta t}^{*}_{01}}{\tilde{\Delta t}_{02}-\tilde{\Delta t}^{*}_{02}\left(\frac{p_{01}T_{02}}{p_{02}T_{01}}\right)}. \qquad (7.44б)$$

The given equations make it possible to design the characteristics of the air-heat deicers for any mode/conditions, if are known the characteristics of this deicer to some mode/conditions. Obvious also that for such conversions must be known the engine characteristics on height/altitude and speeds, available flow rates of air and temperature of the selected/taken air.

7.7. The approximate computation of the flow rate of hot air for jet-edge protection from icing.

Let us examine the approximation method of the calculation of the flow rate of hot air, necessary for the jet-edge method of protection from the icing (see Section 3.2 and 5.5).

Page 213.

In mixing zone the air, which escape/ensues from the nozzle (see Fig. 3.21b), behaves as the jet near the wall whose temperature can be determined approximately from (5.60) or from relationship/ratio,

which is given in work [139]:

$$\frac{T_c - T_0}{T'_{вых} - T_0} = 3{,}5\left(\frac{S}{h}\right)^{-0{,}5}, \qquad (7.45)$$

where h - width of the slot of two-dimensional nozzle m;

S - distance along surface from nozzle edge m;

T_c - temperature of the surface of glass at a distance of S from nozzle in °K;

$T'_{вых}$ - temperature of hot air at the nozzle outlet in °K.

Latter/last equation is correct for the case when discharge velocity behind the nozzle is close to sonic (during this mode/conditions jet-edge protection is most effective). The air flow rate during sonic outflow behind two-dimensional nozzle by length l is determined from the formula

$$G = 4{,}08 \cdot 10^{-3} \frac{p^*_{вх} l}{\sqrt{T'_{вых}}} = 4{,}08 \cdot 10^{-3} \frac{p^*_{вх}}{\sqrt{T'_{вых}}} hl \ \text{kg/s} \qquad (7.46)$$

where $p^*_{вх}$ - the total pressure in front of the nozzle in N/m².

Solving together equalities (7.45) and (7.46), we will obtain

$$G_{(1)} = \frac{G}{l} = 3{,}33 \cdot 10^{-3} \frac{p^*_{вх}}{\sqrt{T'_{вых}}} \left(\frac{T_c - T_0}{T'_{вых} - T_0}\right)^2 S. \qquad (7.47)$$

According to this formula it is possible to determine the matching flow rate of hot air per 1 m of the length of slot, necessary for protection from the icing of surface at a distance of S from nozzle edge. Thus, for instance, when $\Delta T = T_г - T_в = 30°$ C, $p_{max} = 2 \cdot 10^5$ N/m^2, $t_{max} = 200°$ C and $t_в$=-20°C is required the flow rate of hot air $G_в$ =0.285 kg/s·m, in order to ensure protection from the icing of the surface with a length of S=0.5 m of nozzle. This several times more than it is required for protection from the icing of one linear meter of the wing whose deicer is carried out on the usual diagrams (see Fig. 3.17). Therefore jet-edge protection it is expedient to utilize for protection from the icing only of those aircraft components (helicopter), which have small area and for which it is not possible to use the more economical methods of heating.

Page 214.

Chapter VIII.

FLIGHT SAFETY UNDER CONDITIONS OF ICING[1].

FOOTNOTE [1]. Written by R. Kh. Tenishev. ENDFOOTNOTE.

Each flight can be examined from the point of view of providing its safety and from the point of view of the normal accomplishing of flight mission. Flight safety is provided, even if in the case of the failure of any system aircraft can be planted at least on the nearest airfield. However, the normal accomplishing of flight mission, obviously, can be guaranteed only if all vital systems will act during flight smoothly. With respect to these tasks must be distinguished requirements and to systems.

8.1. Evaluation of the probability of safe flight.

Questions of the circuit reliability of systems are presented in the appropriate literature, for example [14], [15]; therefore we will be restricted to the evaluation of the probability of safe flight under conditions of icing.

Let us examine different situations, during which is provided (or it is not provided) flight safety under conditions of icing, for example for standard thermoelectric POS, described in chapter III.

Let us record these situations in the form of the events, united into products and sums with the aid of Boolean algebra, so that it would be possible to compose the equation of the probability of safe flight in the case in question. From Boolean algebra it is known [for 24] that to union corresponds the product of events, to union or - a sum, etc. Thus, flight safety will be be provided:

a) if there is a reliable signaling of the beginning of the icing

- and pilot in proper time included/connected POS,

- and the temperature of icing in the case not lower than that in question, for which was designed the system,

- and operably works POS,

- and the signaling of soundness of POS correctly signals about

the operable operation of system[2];

FOOTNOTE [2]. On many aircraft for a control/check of the work of deicers is applied not the signaling of failure, but the signaling of operable work, i.e., with the operable operation of system burns green bulb, in the case of failure it must go out. ENDFOOTNOTE.

or

b) if is reliable the signaling of the beginning of the icing

- and pilot in proper time included/connected POS,

- and the temperature of the icing not lower than calculation,

- and operably works POS.

Page 215.

- and in this case refused the signaling of soundness of POS (spurious signal of failure), and pilot takes measures for aircraft handling as with "refused POS" (although actually POS works, since the signal of the soundness of work went out, pilot was forced to consider that refused the system, if he does not have other means of

control/check of its work);

or

c) if is reliable the signaling of the beginning of the icing

- and the temperature of the icing not lower than calculation,

- refused POS,

- and in this case correctly are signalled about failure systems,

- and pilot, knowing about failure of POS, in proper time takes measures and correctly pilots the iced over aircraft; or finally

d) if is reliable the signaling of the beginning of the icing

- and aircraft (helicopter) hit under conditions of the icing lower than calculations with which the deicer cannot remove ice.

- pilot knows that he hit under the conditions of icing indicated and in proper time took measures for piloting of the iced over aircraft (helicopter).

Similar situations can be examined, also, for the case when flight safety under conditions of icing is not provided.

On the basis of the enumerated conditions, utilizing algebra of logic [24], it is possible to record (after the appropriate conversions) the equation of the probability of the safe flight:

$$P_{б.п} = P_{с.обл}[P_t(P_{пос}P_{н.р} + Q_{пос}P_{н.р}P_{пил} + Q_{н.р}P_{пос}P_{пил}) + Q_tP_{пил}], \quad (8.1)$$

where $P_{с.обл}$ - probability of the reliable signaling of the beginning of icing and timely reaction of pilot to the signal;

P_t - probability of flight under conditions of icing, which do not come out beyond the limits of the calculations;

$P_{пос}$ - probability of safe work of POS;

$P_{н.р}$ - probability of the trouble-free operation of the signaling system of the soundness of work of POS;

$Q_{пос}$ - failure probability of POS;

$Q_{н.р}$ - failure probability of the signaling system of the soundness of

work of POS;

Q_i - hit probability under the off-design conditions of the icing;

$P_{пов}$ - probability of correct aircraft handling in the case of failure of POS.

The conditions of providing flight safety despite all the examined situations can be clearly presented in the form of logical diagram (Fig. 8.1).

Page 216.

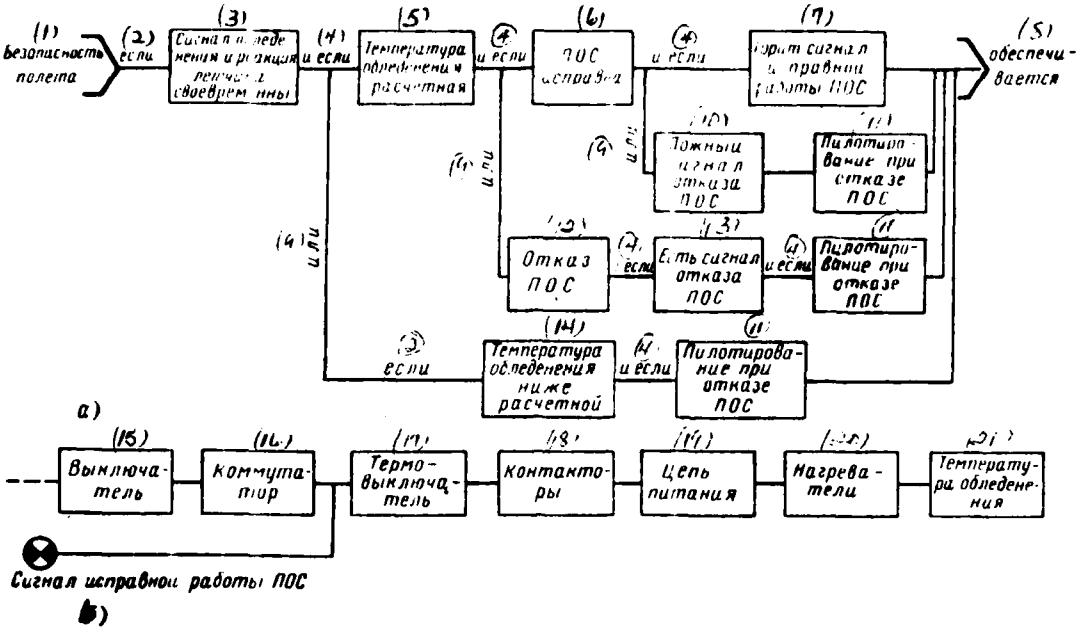

Fig. 8.1. Logical diagram of probability of guaranteeing safe flight under conditions of icing (a) and structural diagram of signaling of work of deicer (b).

Key: (1). flight safety. (2). if. (3). Signal of icing and reaction of pilot are timely. (4). and if. (5). Temperature of icing calculation. (6). POS is operable. (7). Burns signal of operable work of POS. (8). it is provided. (9). or. (10). Spurious signal of failure of POS. (11). Piloting in the case of failure of POS. (12). Failure. (13). There is signal of failure. (14). Temperature of icing lower than calculation. (15). Switch. (16). Switchboard. (17).

Thermoswitch. (18). Contactors. (19). Feed circuit. (20). Heaters. (21). Temperature of icing. (22). Signal of operable work of POS.

Page 217.

In these all cases it is assumed that the probability of the reliable and timely signaling of the beginning of icing is high. Otherwise flight safety, as can be seen from the given above equations, it is not provided. Unfortunately, not all existing ice-indicating equipment satisfy the necessary requirements. Therefore pilots frequently determine the beginning of icing, for example, on the icing of glasses, and also according to some indirect signs/criteria (behavior of aircraft or helicopter with icing, appearance of vibrations, etc.). However, such signs/criteria are always not reliable, especially during night flights, but for some parts as on engines or helicopter rotors, to await their appearances is hardly admissible. Furthermore, the presence of reliable signal indicators is the necessary conditions of applying automatic turn-on of de-icing systems.

As far as signaling is concerned of operable work of POS, then it also always is not successful. As an example Fig. 8.1b gives the structural diagram of the signaling system of the soundness of the work of deicers, which is applied on some aircraft. From diagram it

is evident that this system actually signals only about the operable work of switchboard and cannot react to the failure of the remaining elements of system (contactors, heating elements, thermoswitches, supply leads) and, therefore, has the sufficiently large probability of the spurious signal of operable work with which can arise dangerous situation.

If we examine not only the task of providing flight safety, but also the requirement of the successful accomplishing of target, then it is obvious that the latter can be fulfilled only in the first of the examined above cases (see page 214), since in the case of any failures of POS flight with icing can be carried out only from by more or less considerable flight limitations. Thus, the probability of the successful accomplishing of target under conditions of icing can be sufficiently great only with the very high probability of failure-free operation of POS.

8.2. Means of the signaling of icing.

With the need for the reliable signaling of icing, besides the aforesaid in the preceding/previous section, is connected still the fact that the system is completely operational under normal conditions for operation, upon overdue inclusion/connection during prolonged time it proves to be ineffective. First of all this is

related to the systems of permanent action and the "thermal knives" of the deicers of cyclic action. In this case ice built-up edge thaws, but is not thrown off, pressed by the flow (see Fig. 3.5a).

Page 218.

The signaling of icing is accomplished/realized with the aid of the signal indicators which are fulfilled usually in the form of the independent self-contained devices (although there are such, which enter into construction/design of POS).

Are at present known (yearly it is proposed) many signal indicators of different types and constructions/designs. Everything it is possible to conditionally divide them into two basic groups [115]:

1) the signal indicators of direct action,

2) the signal indicators of indirect action.

The signal indicators of the first group react to the presence of ice on sensor. Their fundamental shortcoming in the fact that they give signal only after certain time after the beginning of icing and, furthermore, many of them do not react to the "horn-shaped" forms of

ice which is obtained during the specific combination of the conditions of icing and flight conditions (see Chapter II).

To the sensitivity of the signal indicators of this group to a considerable degree affect the form, sizes/dimensions and site of installation of sensor on aircraft and helicopter. From chapter IV follows that their sensitivity the higher, the less the diameter of the sensor (if it cylindrical) or is pointed its end connections (if it shaped) (Fig. 8.2). The decrease of the thickness of sensor is limited to its mechanical strength and need of positioning/arranging in it the heater.

The site of installation of sensor on aircraft must be selected so that air flow on the way to sensor would be overshaded in no way, on that already turned the attention in Section 4.4. Vital importance has also a selection of the distance of the sensitive part of the sensor of skin/sheathing (i.e. the operating altitude of sensor). The speed of ice formation in proportion to removal from the surface changes: at first it usually grows/rises, at certain distance it reaches maximum T_{max}, then again somewhat is decreased and it reaches value I_∞. This occurs in accordance with the change in the concentration of water content near the streamlined body, which "adjusts" the trajectories of drops.

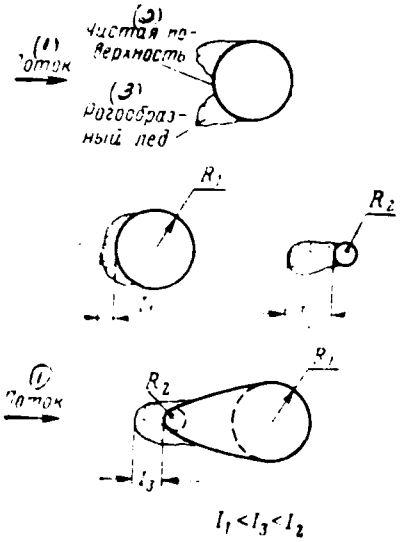

Fig. 8.2. Ice formation on the sensors of different size/dimension and form.

Key: (1). Flow. (2). Clean surface. (3). Horn-shaped ice.

Page 219.

Consequently, the speed of ice formation on sensor l_A differs from the same on aircraft components as a result of two reasons: the large difference between the size/dimension of sensor and the sizes/dimensions of the icing up aircraft components and change in the concentration of water content near body surface. This concentration near body can be both the increased and reduced relative to the water content of the undisturbed flow, in the latter

case $l_{max} = l_{\infty}$ (Fig. 8.3). Distance $h_{l\,max}$ of region with the maximum concentration of water content depends on many factors and can be in limits from centimeters to several ten centimeters.

From the aforesaid it follows that most successful place for setting up of the sensor of signal indicator is the front/leading lower part of the fuselage or wing. A question about the setting up of signal indicator in engine requires special examination.

The signal indicators of the second group react to the presence in the atmosphere of the drops of water. They are based on the principle of the measurement of the indirect values: heat emission, electrical conductivity, resistance, etc. The sensitivity of them is considerably above - they give signal virtually simultaneously since the beginning of the icing, and in certain cases even for several seconds prior to beginning (because of an improvement in the humidity and a change in the temperature near cloud). Form, sizes/dimensions and site of installation of sensor little affect the sensitivity of these signal indicators. However, their essential shortcoming is the fact that they can be used only in combination with the device/equipment (diagram), which reacts to the temperature of surrounding air, which must separate/liberate the spurious signals, which appear from water drops at temperature higher than 0°C, and in certain cases - from crystal water. In view of instability and

insufficient reliability of such devices/equipment the signal indicators of indirect action did not thus far obtain proper use/application as series instruments.

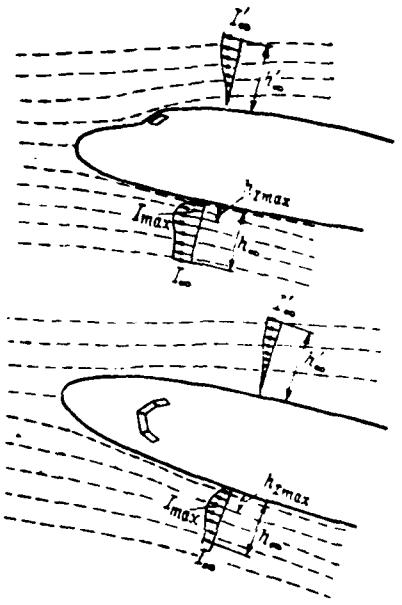

Fig. 8.3. Intensity of ice formation on sensor depending on its location.

Page 220.

To the ice-indicating equipment of indirect action can be attributed also the remote methods of the detection of drop water in the atmosphere: the existing radar and in principle possible (in the future) ultrasonic and infrared or other methods which would make it possible to signal about the presence of icing previously, prior to the entry into cloudiness, but they, naturally, will also require the reliable devices/equipment which would separate/liberate real signals

about the presence of icing from false ones.

Given below table shows the fundamental forms of the signal indicators of the first and second groups.

Table 8.1. Fundamental forms of signal indicators.

(1) Сигнализаторы	(2) Принцип получения сигнала	(3) На что реагирует
(4) Пневматические	4 а) Изменение динамического давления или разрежения в приборе при обледенении отверстий датчика воздействует на мембрану, замыкающую электрические контакты	(5) На лед
	4б) Разность давлений в обледеневшем и постоянно обогреваемом датчиках воздействует на мембрану	(6) То же
(7) Механические	7 а) Момент от вращающегося цилиндра при появлении на нем льда передается рычагу (скребку), замыкающему контакты	» »
	7б) Разность центробежных сил обледеневшей и постоянно обогреваемой вращающихся лопастей прибора передается рычажному контактному устройству, чувствительному к разбалансу	» »
	7в) Изменение частоты или амплитуды вибраций датчика при нарастании на нем льда регистрируется в виде сигнала	» »
(8) Радиоизотопные	(9) Изменение потока радиоактивного излучения при обледенении датчика с помощью счетчика частиц и усилителя преобразуется в сигнал	» »
(10) Электростатические	(11) Изменение электростатического поля при образовании льда на датчике преобразуется в сигнал	» »
(12) Оптические	13 Изменение интенсивности прямого или отраженного луча при наличии льда на датчике с помощью фотоэлемента и усилителя преобразуется в сигнал	» »

(1) Сигнализаторы	(2) Принцип получения сигнала	(3) На что реагирует
Электрокондуктивные (4)	(4) а) Электропроводность льда на датчике вызывает срабатывание чувствительного реле (4б) Электропроводность пористого слоя, пропитанного составом, взаимодействующим со льдом, вызывает срабатывание реле	(5) На лед и на капли воды [1] (6) На лед, на капли воды [1], а также на кристаллы льда [2]
Термические (7)	(8) Разность температур смоченной (при обледенении) передней и несмоченной задней поверхностей датчика с помощью чувствительного моста или усилителя преобразуется в сигнал	(9) На капли воды [1], на кристаллы льда [2]
Дистанционные (10)	(11) Отражение луча локатора от облаков	(12) На наличие в воздухе капель воды [1] или кристаллов льда

Key: (1). Signal indicators. (2). Principle of obtaining signal. (3). To what it reacts. (4). Pneumatic. (4a). A change of the dynamic pressure or rarefaction/evacuation in instrument with the icing of pickup holes acts on the membrane/diaphragm, which closes electrical contacts. (4b). Pressure difference in iced over and constantly warmed sensors acts on the membrane/diaphragm. (5). To ice. (6). Then. (7). Mechanical. (7a). Moment/torque from the rotating cylinder upon the appearance on it of ice is transmitted to the lever (scraper), circuit closing contacts. (7b). A difference in the centrifugal forces of that iced over and constantly warmed of the rotating blades/vanes of instrument it is transmitted to the lever/crank contact device, sensitive to unbalancing. (7c). A change in frequency or amplitude of the vibrations of sensor during the increase on it of ice is recorded in the form of signal. (8). Radioisotope. (9). Change in flow of radioactive radiation with icing

of sensor with the aid of particle counter and amplifier is converted into signal. (10). Electrostatic. (11). Change in electrostatic field with ice formation on sensor is converted into signal. (12). Optical. (13). Change in intensity of straight/direct or reflected beam /in presence of ice on sensor with the aid of photocell and amplifier is converted into signal. (14). Electroconductive. (14a). Electrical conductivity of ice on sensor activates sensing relay. (14b). Electrical conductivity of the porous layer, saturated with the composition, which interacts with ice, activates of relay. (15). To ice and to drops of water[1].

(16). To ice, to drops of water[1], and also to crystals of ice[2].

FOOTNOTES [1]. It requires blockings of signal at positive temperature.

[2]. With very low t_0 can not react. ENDFOOTNOTES.

(17). Thermal. (18). Difference in temperatures of moistened (with icing) front/leading and unwetted rear of surfaces of sensor with the aid of sensitive bridge or amplifier is converted into signal. (19). To drops of water [1], to crystals of ice [2]. (20). Remote. (21). Reflection of ray/beam of locator from clouds. (22). To presence in air of drops of water [1] or crystals of ice.

Page 221.

The description several types of signal indicators (pneumatic, mechanical with scraper, radioisotope and electroconductive) can be found in work [58].

Especially one should speak about the signaling of the icing of the helicopter for which, naturally, it is most important to have a signal about the presence of ice directly on propeller blades. However, in this case we encounter with the contradictory requirement: with temperature of air on the order of -10°C and lower than blade/vane they ice up all over length, moreover the maximum thickness of ice is formed at the end/lead (see Chapter II), whereas at higher temperatures blade tip not at all ices up, therefore, to there establish/install the signal indicator of the beginning of icing is impossible. However, in root part is very low the intensity of ice formation; therefore the established/installed here signal indicator of direct action proves to be considerably less sensitive, i.e., signal appears only if at blade tip at average/mean and low temperatures of air the thickness of ice already reaches the significant magnitude. From the aforesaid it follows that for the reliable signaling of the beginning of the icing of helicopter it is necessary to establish/install in the root part of the blade/vane the extremely sensitive signal indicator of direct action or to apply the

signal indicator of indirect action which can be established/installed aboard. But it is more expediently in all cases when it is possible, to establish/install sensors in the valve port of engine.

Page 222.

One should mention about one more variety of ice-indicating equipment which can successfully be used for pilot's warning about failure of POS or the incidence/impingement of aircraft under off-design conditions of icing. These are the signal indicators of the presence of ice on the shielded surface, including barrier ice. The use/application of such instruments can considerably raise flight safety under conditions of icing. They can act on the same principles as the described above signal indicators of the beginning of icing, but they must be established/installed directly on the icing up parts of the flight vehicle.

Page 223.

Part Two.

METHODS FOR TESTING DE-ICING SYSTEMS.

The tests of de-icing systems are subdivided into the tests which are conducted before the creation of flight vehicle, and to the tests of experimental aircraft or helicopter according to the evaluation of characteristics and effectiveness of its POS.

During the design of aircraft or helicopter are conducted model tests and separate elements/cells of their shielded of icing parts on laboratory installations, then - tests of experimental mock-ups or sections on stands or flying laboratories. In tests are more precisely formulated calculated coefficients, thermal characteristics and other data, necessary for designing full-scale POS. Furthermore, if previously it is not represented possibly of theoretical analysis or from experiment of the investigations of the preceding/previous constructions/designs to design the optimum construction/design of experimental deicer, then this can be made as a result of comparative tests of several experimental mock-ups (sections).

The tests of experimental deicers in flight can be carried out both in the artificial ones and in the natural conditions of icing on the specially equipped aircraft or helicopters, but preference in this stage should be returned artificial icing. In this case in the stage of the tests of experimental aircraft or helicopter is produced the evaluation of the work of deicers and their aggregates/units, development/detection and elimination of possible shortcomings, but in the stage official tests of aircraft or helicopter - a general/common/total evaluation of the effectiveness of all de-icing systems.

According to methods the evaluations of characteristics and effectiveness of testing systems are subdivided into the following forms:

- testing out of the conditions of icing (in "dry" air);

- testing under conditions of the artificial icing;

- testing in the natural icing;

- testing according to the evaluation of the effect of icing on flight aircraft characteristics and its power plants.

Page 224.

Tests in "dry" air are necessary mainly for determining of the thermal characteristics of systems and their comparison with calculations. The available methods of the conversion of the external thermal characteristics of the systems of heating as this is obvious from V, VI, VII chapters, make it possible to sufficiently accurately rate/estimate the effectiveness of thermal deicers with point the views of the necessary power of heating. But the sufficiency of the sizes/dimensions of the shielded zones can be checked only under conditions of icing, moreover these conditions about parameters of drops and to ambient temperature must be not below calculations, otherwise the results of tests will not be convincing. Conducting such natural condition tests proves to be extremely difficult, it requires a very large number of flights and due to the seasonality of the conditions of icing usually is involved/tightened for a prolonged time, especially if it is necessary to test several experimental versions of deicers.

Tests with artificial icing do not depend on meteorological conditions and season, since the conditions of artificial icing are established at experimenter's discretion. This makes it possible to carry out the tests of prototype systems within considerably shorter periods and under the prescribed/assigned, standardized/normalized

conditions. In this case in the portion of natural condition tests remains only a small number of check flights, necessary for the evaluation of efficiency of an entire system as a whole, including the signaling of icing, and also for checking the effect of icing on the behavior of flight vehicle in failure of POS.

However and for the last goal in many instances more expediently to resort to the artificial imitators of the icing which make it possible to rate/estimate the effect of icing more rapid and it is more precise than under natural conditions, since as a result of the great variety of the forms of ice and their variability in of tests, periodic destruction of built-up edges (especially on propellers) it is to difficult compare the results of investigations, obtained even during one flight.

Tests according to the evaluation of the reliability of de-icing systems encompass tests regarding their functional characteristics and special tests for obtaining the quantitative indices of reliability.

For the decrease of time and space of tests should be applied the accelerated methods for testing, without which, apparently, to fulfill the quantitative evaluation of reliability of POS under flight conditions is represented by hardly possible. As is known,

there are two fundamental methods for accelerated tests. 1) Testings at the increased intensity of the factors, which affect the article (loads, number of inclusions/connections, duration of the operating modes, temperatures, vibrations, pressures, etc.).

Page 225.

For the possibility of the evaluation of the results of tests according to this method it is necessary to have previously definite dependence of the mean time of the failure-free operation of aggregates/units on the intensity of the factors indicated. Such dependences must be determined as a result of special laboratory or bench tests of separate experimental articles or elements of systems. 2) Investigation of the parameters and indices, which are determining the reliability of articles and systems during the reduced time intervals, and the subsequent extrapolation of the obtained results for determining the mean time of failure-free operation.

In this book are examined mainly the methods for testing regarding functional characteristics of POS.

Chapter IX.

TESTINGS REGARDING THE THERMAL CHARACTERISTICS OF DEICERS[1].

FOOTNOTE [1]. Section 9.1-9.5 and 9.7 are written by V. K. Kordinov, Section 9.6 - by V. N. Leont'yev, Section 9.8 - by V. S. Savin, Section 9.9 - by R. Kh. Tenishev. ENDFOOTNOTE.

9.1. Methods of measuring the temperature of surrounding air.

Before testing/experiencing aircraft or helicopter under conditions of icing, should be defined the thermal characteristics of their de-icing systems in "dry" air, i.e., during flights out of the conditions of the icing (in this case, as it was already said above, by "dry" air is understood the air, which does not contain drop water or crystals of ice).

For the evaluation of system it is necessary to determine the fundamental external parameters: the temperature of heating surfaces, the temperature of surrounding air, speed and flight altitude and series/row of the internal characteristics which depend on type of POS.

So, for thermoelectric systems should be determined current strength and voltage of supply of sections, in the necessary cases - loss in wires/conductors, etc.

In the air-heat systems, as a rule, they are measured:

- the mass flow rate of hot air,

- temperature of air at the inlet and at output from the warmed noses/leading edges of the parts of the flight vehicle, shielded from icing,

- the characteristics, which are determining engine power rating (if hot air is selected/taken from compressor), etc. The methods of determining of height/altitude and flight speed are sufficiently well known [8] and do not require special examination.

Page 226.

The temperature of surrounding air is one of the fundamental parameters; therefore on the methods of its measurement one should stop in more detail.

During determining of the thermal characteristics of deicers the

measurement of the temperature of surrounding air should be produced special thermometers, since the precision/accuracy of on-board instruments for this purpose is insufficient.

Frequently is utilized in flight tests the so-called electrical resistance thermometer (ETS) with the chamber/camera of total stagnation or its prototype P-69. This sensor is shown in Fig. 9.1, has the heat-sensitive element/cell, made from the nickel wire with a diameter of 0.05 mm, by rolled into ribbon thickness of 0.02 mm and wound around special framework/body out of hardened paper. Sensor has four outlets, the relation to total area of which to intake area is equal to 0.3-0.4. As is known, the temperature, received by the thermometer of braking, $T_{\text{терм}}$ is determined by the expression

$$T_{\text{терм}} = T_0 + r^*_{\text{терм}} \frac{k-1}{2kR} V_0^2 = T_0 + r^*_{\text{терм}} \frac{V_0^2}{2c_p} = T_0(1 + 0{,}2r^*_{\text{терм}}M^2), \quad (9.1)$$

where $r^*_{\text{терм}}$ - a coefficient of braking the thermometer which depends on the ratio of the sum of discharge areas to intake area.

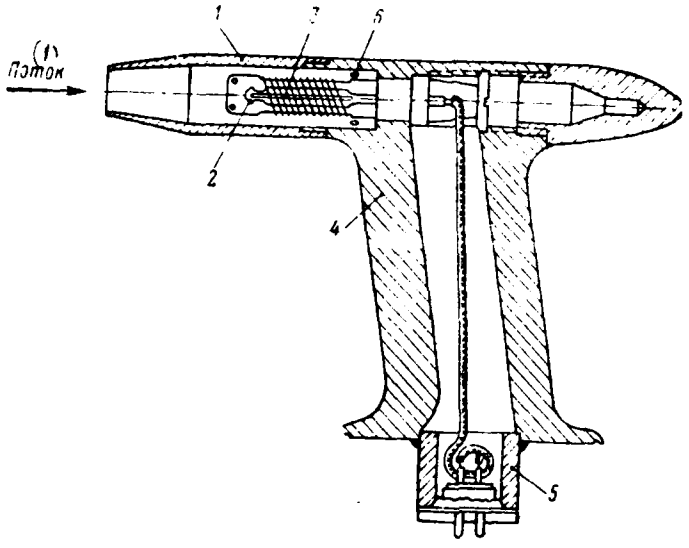

Fig. 9.1. The construction/design of sensor P-69: 1 - nozzle; 2 - framework/body of the heat-sensitive element/cell; 3 - wire-wound resistor of the element/cell; 4 - strut of sensor 5 - plug-type connector; 6 - outlet.

Key: (1). Flow.

Page 227.

The less this relation, the nearer value $\dot{r}_{терм}$ to unity and the less the error from incomplete braking in chamber/camera sensor; however, too low a relationship/ratio of areas leads to the increase of the inertness of sensor. The method of determining the coefficient

of braking is described, in particular, in work [8].

For sensors of the type ETS instead of the coefficient of braking is utilized also the quality coefficient

$$N = \frac{T_{\text{терм}}}{T^*} = \frac{1 + 0.2r^*_{\text{терм}}M^2}{1 + 0.2M^2}, \qquad (9.2)$$

where T* - temperature, which corresponds $r^*_{\text{терм}} = 1$. For sensors ETS-2 N=0.999, while for sensors P-69 N=0.996.

In this case the actual temperature of air is determined from expressions (9.1) and (9.2) according to the formula

$$T_* = \frac{T_{\text{терм}}}{N(1 + 0.2M^2)}. \qquad (9.3)$$

In the practice of flight tests for measurement the temperatures of surrounding air utilize also a sensor P-5 from the assembly of the thermometer TNV-15, which is at present established/installed almost in all aircraft types. A sensor of the type P-5 according to operating principle can be named the sensor of "critical" temperature. The heat-sensitive element/cell of this sensor, depicted in Fig. 9.2, is located in the narrow cross section of the specially shaped tube.

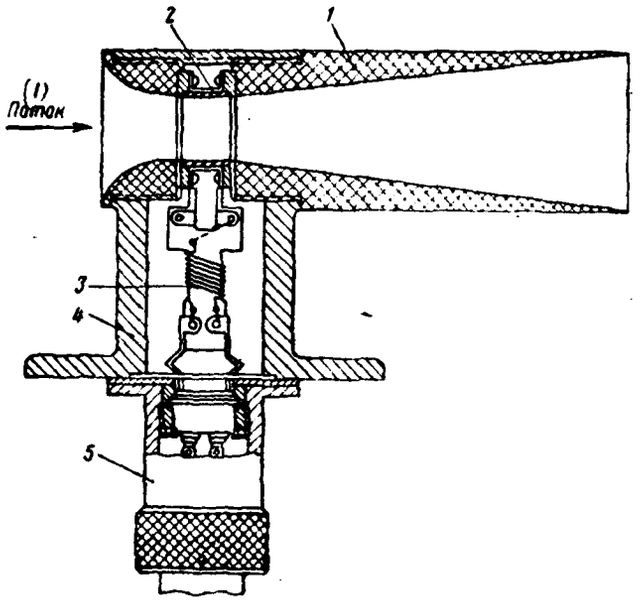

Fig. 9.2. The construction/design of the sensor of critical temperature P-5: 1 - nozzle; 2 - wire-wound resistor of the heat-sensitive element/cell: 3 - supplementary resistance; 4 - upright strut with the collar; 5 - plug-type connector.

Key: (1). Flow.

Page 228.

With the specific relationship of intake $F_{вх}$ and narrow F_{min} of cross sections $\left(\frac{F_{вх}}{F_{min}} \geq 3\right)$ upon reaching M≥0.45 in the narrow cross section of sensor is established/installed critical speed ($M_{кр} = 1$)

The value of the coefficient of braking sensor $\dot{r}_{\text{repm}}$ from flight speed is variable, especially with small Mach numbers, when coefficient can be even negative, i.e., the temperature, received by the heat-sensitive element/cell of sensor, can be even lower temperature of the undisturbed flow, since a sensor of the type P-5 in principle differs from the sensor of total stagnation. It respectively has another value of quality coefficient N. Investigations established/installed, that the quality coefficient for a sensor P-5 with $M \geqslant 0.45$ is constant and numerically equal to 0.978 ± 0.001. For $M<0.45$ its value is changed, as shown in Fig. 9.3. The true value of temperature during the use/application of a sensor P-5 is determined from formula (9.1). Furthermore, for determining the actual temperature of surrounding air at flight speeds from M=0.5 to M=1.5 it is possible to use the nomogram, given in Fig. 8 application/appendix. On scale I are plotted/applied the marks, which correspond to the values of flight mach number; on scale II are plotted/applied the marks, which correspond to the values, obtained by sensor P-5, and on scale III are plotted/applied the marks, which correspond to the actual temperature of surrounding air.

For determining the actual temperature of surrounding air at the low speeds of flight (to M=0.5) can be used another nomogram, given

on Fig. 9 application/appendix. On scale I are plotted/applied the marks, which correspond to Mach numbers of the flight; scale II is the auxiliary scale; on scale III are plotted/applied the marks of the values of quality coefficient N; on scale IV are plotted/applied the marks, which correspond to the temperature, put out by sensor, and on scale V are plotted/applied the marks, which correspond to the actual temperature of surrounding air.

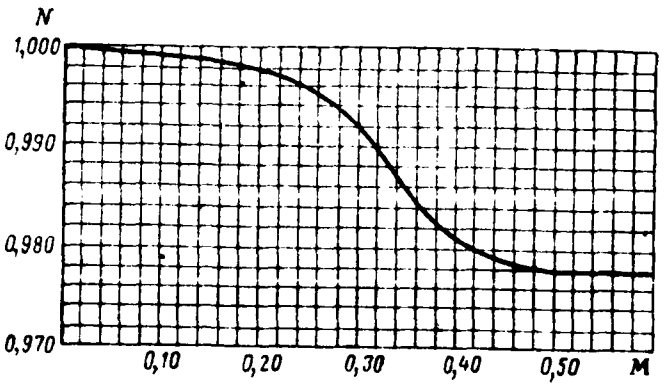

Fig. 9.3. Dependence of quality coefficient on flight mach number for a sensor P-5.

Page 229.

For determining the actual temperature at the low speeds of flight the obtained value Mach numbers plot/deposit on scale I and by curve is determined the quality coefficient N, which corresponds to the value of Mach number. The obtained value will deposit on scale III.

marks on scales M and N (I and III) connect by straight line to to rule. On scale IV plot/deposit the value of the temperature, determined by sensor.

Mark on scale II, obtained as a result of the intersection

straight/direct, carried out through marks M and M, connect by straight line with mark on scale IV. Intersection with this straight line with scale V gives the value of the actual temperature of surrounding air in °C. An example is given on nomogram itself.

It must be noted that in practice are encountered sometimes the cases of erroneous use/application for sensors P-5 of the values of coefficients of N or even $r_{терм.}$ obtained for the thermometers of total stagnation. In this case the error in determination of t_0 can be very considerable.

9.2. Methods of measuring the temperature of surface.

The measurement of the temperature of surface can be fulfilled by different methods with the aid of thermocouples, tape/film thermosensitive elements of resistance, thermistors, thermocolors, pyrometers of infrared radiation, etc. Is most common both and outside boundary the method of measurement of temperature with the aid of thermocouples. Somewhat more rarely are applied film gauges.

Measurement of the temperature of surface with the aid of thermocouples.

As is known, the value of thermo-emf (TEMF) depends on a

difference in the temperatures of the junctions of thermocouple and material of its thermoelectrodes (conductors). Table 2 of application/appendix gives value of TEMF of some materials relative to platinum with a difference in the temperatures of their joints in 100°C and some other physical characteristics of different metals and alloys. From the table indicated it is evident that the materials, produced in the form of wire (for example, copper, constantan, chromel, etc.), have in the which interests us temperature range of heating surfaces of POS small value of TEMF; therefore during the use of thermocouples from materials indicated is required sufficiently sensitive registering apparatus. Table 9.1 gives value of TEMF for the most widely used thermocouples in the range of temperatures to 500°C.

Page 230.

For recording of TEMF during flight tests are applied the potentiometers of direct current and optical chart recorders (oscillographs), and in certain cases galvanometers.

The major advantage of potentiometers is the fact that the readings does not depend on the resistance of the circuit of thermocouple, since measurement is accomplished/realized by a compensation method.

In practice in essence are applied the movable potentiometers of a direct current of the type PP, which have the range of measurements from 0 to 71 mV. A fundamental reading error of this potentiometer does not exceed ±0.1 mV at temperature of +20 ±2°C and relative air humidity not more than 80o/o. The supplementary reading error of potentiometer, caused by the deviation of temperature of the surrounding instrument of air from normal, does not exceed 0.1o/o on ±10°C.

The schematic of the connection of instrument - galvanometer, tail of chart recorder and the like - to thermocouple is shown in Fig. 9.4. Into metering circuit of diagram enters the resistance of the framework of instrument (galvanometer) R_r, the resistance of coupling or compensating leads $R_{пв}$ and the resistance of thermocouple $R_{тп}$.

If TEMF of thermocouple is equal $E_{тп}$, then current in metering circuit will be equal to $i = \frac{E_{тп}}{R_r + R_{пв} + R_{тп}}$, whence voltage across terminals of galvanometer will be equal

$$U = iR_r = E_{тп} - i(R_{пв} + R_{тп}), \tag{9.4}$$

or

$$U = \frac{E_{тп}R_r}{R_r + R_{пв} + R_{тп}},$$

whence

$$E_{тп} = -\frac{U(R_г + R_{пв} + R_{тп})}{R_г} = U + U\frac{R_{пв} + R_{тп}}{R_г}. \qquad (9.5)$$

Table 9.1. Thermo-emf of thermocouples in mV at temperature of cold-soldered joint of 0°C.

(1) Тип термопар	(2) Температура рабочего спая термопары в °С															
	10	20	30	40	50	60	70	80	90	100	150	200	250	300	400	500
(3) Хромель-копель	0,65	1,31	1,97	2,65	3,34	4,03	4,73	5,45	6,17	6,95	10,68	14,66	18,88	22,91	31,49	40,16
(4) Железо-копель	0,54	1,09	1,65	2,21	2,78	3,36	3,95	4,55	5,15	5,75	8,85	12,01	15,15	18,11	24,56	30,91
(5) Железо-константан [1]	0,5	1,0	1,5	2,02	2,53	3,04	3,56	4,08	4,60	5,15	7,83	10,60	13,36	16,25	21,90	27,60
(6) Медь-копель	0,41	0,83	1,35	1,81	2,28	2,76	3,21	3,74	4,24	1,75	7,42	10,21	13,18	16,49	23,11	30,16
(7) Медь-константан [1]	0,4	0,8	1,21	1,63	2,05	2,48	2,92	3,35	3,79	1,25	6,48	8,87	11,37	14,13	20,04	26,10
(8) Хромель-алюмель	0,40	0,80	1,20	1,61	2,02	2,43	2,85	3,26	3,68	4,10	6,13	8,13	10,15	12,21	16,41	20,65

Key: (1). Type of thermocouples. (2). Temperature of working junction in °C. (3). Chromel-Copel. (4). iron- Copel. (5). iron- constantan[1].

FOOTNOTE [1]. These types of thermocouples are not standardized, but frequently they are applied during the flight tests of POS. The value of their TEMF can differ from the given in table values by ±0.3 mV for different samples/specimens of iron or constantan. During the use of the thermocouples indicated should be carried out their individual calibration. ENDFOOTNOTE.

Thus, voltage across terminals of galvanometer is always less than thermo-emf of thermocouple to value $U \frac{R_{вн}}{R_г} \frac{R_{гр}}{R_г}$. Consequently, the greater the resistance of framework $R_г$ in comparison with external resistance, the less the allowance which differs the value of thermo-emf of thermocouple from voltage across terminals of galvanometer.

In practice in order to avoid this correction and also some other errors, thermocouples usually they calibrate together with the instrument used, taking into account the resistance of entire metering circuit. Calibration it is best to produce in the special thermostat where into the well agitated medium (liquid) are placed standard thermometer (thermocouple) and working junction of the calibrated thermocouple. The cold-soldered joint of the calibrated thermocouple should be placed into thermos with melting ice, moreover the temperature of this ice mixture at the point of the determination of joint must be checked by standard thermometer, since during the insufficiently good mixing of mixture its temperature at depth can differ from 0°C (as is known, the greatest water density with +4°C). In such cases is introduced the correction for the temperature of a cold layer.

When selecting of the type of the tail of chart recorder it is necessary previously to rate/estimate, how many degrees of the measured temperature it is necessary on 1 mm of the ordinate of recording, or how many millimeters of the ordinate of recording will fall to one degree of the measured temperature.

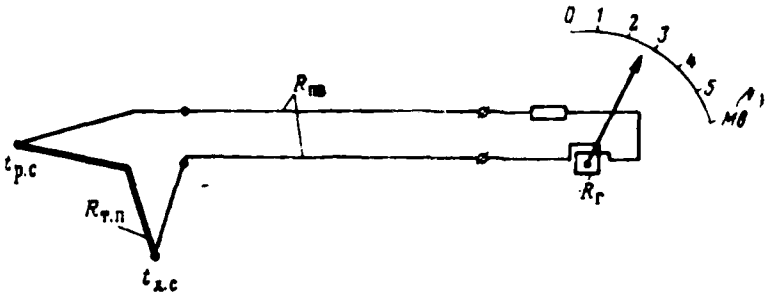

Fig. 9.4. Schematic of the connection of thermocouple to galvanometer.

Key: (1). MV.

Page 232.

The ordinate of recording h of the selected type of tail is defined as the product of current strength in metering circuit to the sensitivity of the tail:

$$h = iA = \frac{E_{тп}A}{R_г + R_{тп} + R_{пр}}, \qquad (9.6)$$

where A - the sensitivity of tail into mm/mA which is indicated in log book or description of instrument.

If one measuring meter it is necessary to fix/record readings from several thermocouples, then their connection is produced through the switch (Fig. 9.5).

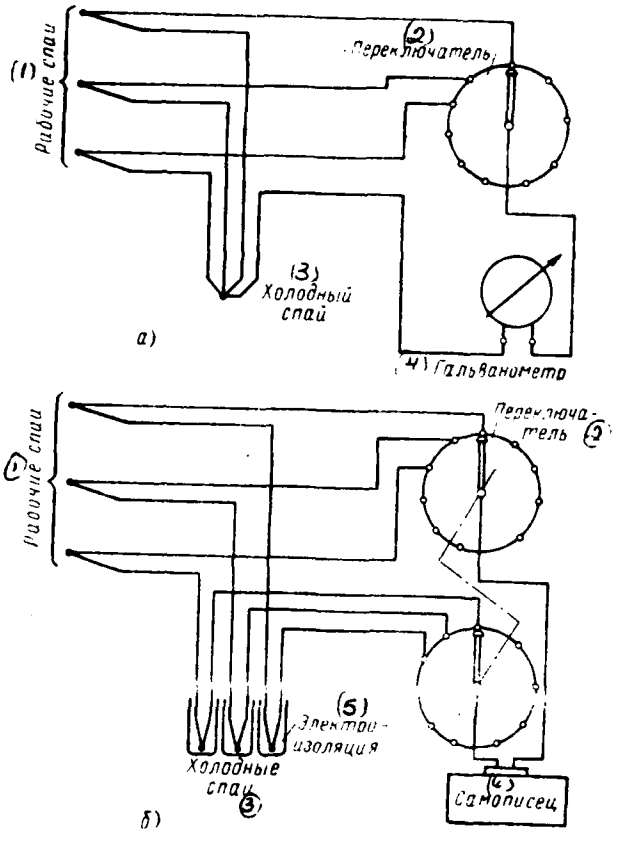

Fig. 9.5. The schematic of the connection of thermocouples to the instrument through the switch: a) is single-wire; b) twin-lead.

Key: (1). Working joints. (2). Switch. (3). Cold-soldered joint. (4). Galvanometer. (5). Electro-insulation. (6). Chart recorder.

Page 233.

Switching can be accomplished/realized either by hand or it is automatic, for example with the aid of programmer.

For recording a large number of points are applied the switches of consecutive and group interrogation. The latter are utilized in essence for the de-icing systems of the cyclic action (since in this case is provided the simultaneous recording of the group of thermocouples). A number of thermocouples in group is usually selected equal to a number of tails in chart recorder.

During the installation of thermocouples on aircraft a complicated question is the thermostatic control of cold ends. The best version is the arrangement/position of cold ends in thermos with melting ice. This is the simplest and reliable method, which ensures the temperature constancy of the cold-soldered joints. But the setting up of thermos near the surface being investigated is not always structurally/constructurally possible. Furthermore, before each flight it is necessary to follow servicing of thermos with ice. Therefore in certain cases it fits other methods of thermostatic control of the cold-soldered joints. Thus, for instance, thermos can be replaced with the well thermo-insulated box, temperature within which is known and virtually it remains constant/invariable during experiment.

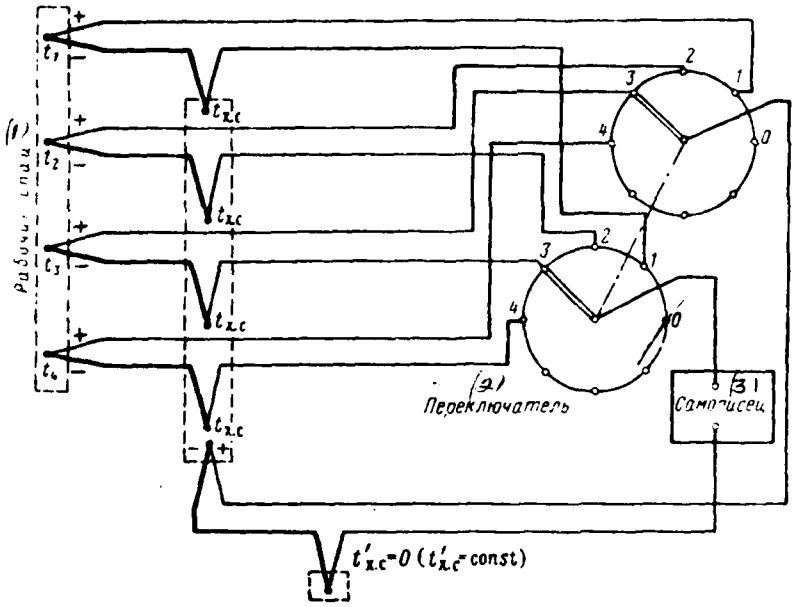

Fig. 9.6. Circuit diagram into the circuit of the measuring thermocouples of compensating thermocouple.

Key: (1). Working junctions. (2). Switch. (3). Chart recorder.

Page 234.

During the use of a diagram with the switch of the thermocouples of consecutive interrogation it is possible in the circuit of each thermocouple to consecutively/serially include the compensating thermocouple which must compensate change in TEMP with a change in the temperature of the cold-soldered joints of measuring

thermocouples. As shown in Fig. 9.6, the cold-soldered joint of compensating thermocouple can be carried out into any place, convenient for the installation of thermos. So that the total resistance of this metering circuit would not be considerable, the wire/conductor of compensating thermocouple it is possible to select larger diameter than the wires/conductors of measuring thermocouple, but materials of the wires/conductors both of the measuring and compensating of thermocouples they must be identical.

As one additional example of the use/application of similar diagrams can serve the diagram in Fig. 9.7, in which the cold-soldered joint of compensating thermocouple instead of the thermos is derived into cavity of total stagnation type sensor ETS-2 or P-69 or into the special nozzle, equipped with thermometer.

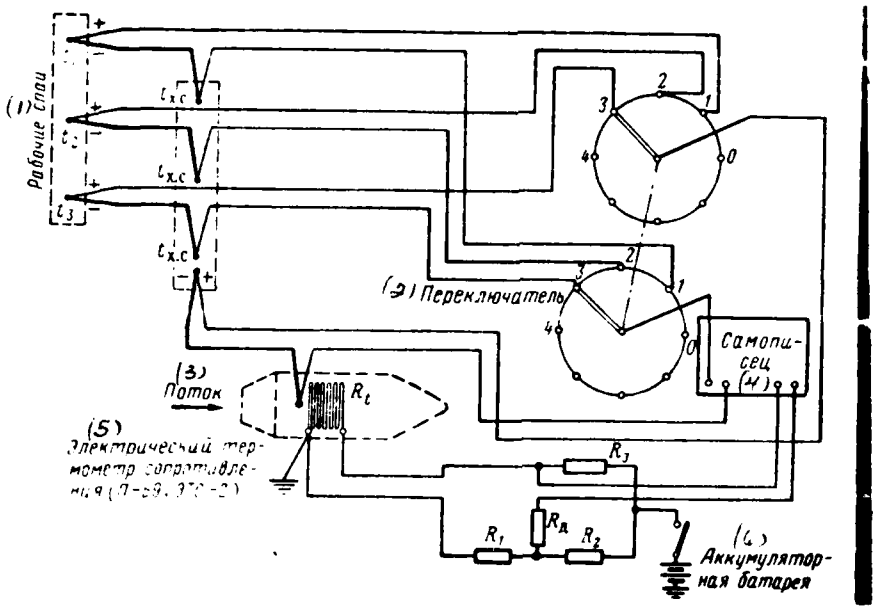

Fig. 9.7. The location of the cold-soldered joint of compensating thermocouple in the sensor of thermometer of the braking: R_1, R_2, R_3 - ratio arms; $R_д$ - additional resistance.

Key: (1). Working junctions. (2). Switch. (3). Flow. (4). Chart recorder. (5). Electrical resistance thermometer. (6). Storage battery.

Page 235.

Is applied also the automatic introduction of correction for the temperature of the cold-soldered joints with the use of compensating

resistance as this shown, for example, in Fig. 9.8. Specially matched impedance R_1, connected into one of ratio arms, is sensing element, which reacts to a change in the temperature of cold end. With a change in the temperature of the cold-soldered joint changes and the value of resistance R_1 in connection with which bridge it leaves equilibrium and the appearing voltage on measuring diagonal compensates a change in TEMF in the thermocouple. Shortcomings in this diagram are: the decrease of the sensitivity of measuring thermocouple and, consequently, also the accuracies of measurement due to the inclusion into the circuit of the thermocouple of supplementary resistance, the difficulty of agreeing the change in the voltage on the measuring diagonal of bridge with a change in TEMF in the thermocouple, the need for strictly stable supply voltage of bridge.

It must be noted that the wires/conductors, identical using material to thermoelectrodes, used for the elongation of thermocouples, frequently call compensating leads. However, it is necessary to bear in mind, that they do not compensate the temperature of the cold-soldered joint, as sometimes erroneously they assume/set, but they only transfer it of one place into another. This erroneous opinion, obviously, is connected with the fact that the series/row of the measuring meters, frequently used for the measurements of temperature, has internal temperature compensation

and account of the temperature of the cold-soldered joints in them it is fulfilled by automatically mechanical or electrical methods.

If thermostatic control is fulfilled it is not impossible, then it is necessary to ensure the permanent measurement of the temperature of cold ends. For this can be used the resistance strain gages (tape/film or of the type P-1), thermistors, etc.

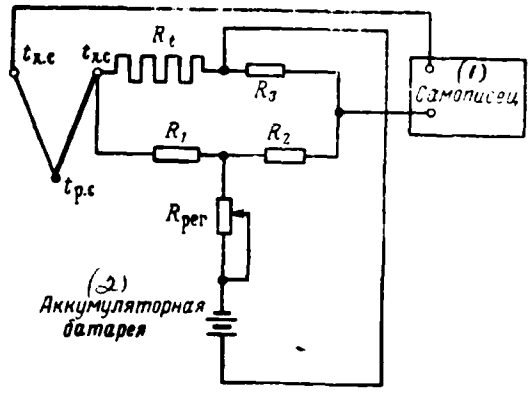

Fig. 9.8. Diagram of automatic correction for the temperature of cold end.

Key: (1). Chart recorder. (2). Storage battery.

Page 236.

If the temperature of the cold-soldered joints is known, then the introduction of the corresponding correction (by calculation or with the aid of calibration curve) does not represent work [47], [59].

Before instaling on aircraft or helicopter all thermocouples it is expedient to break into groups with identical resistance for decreasing a number of calibration curves.

Sealing of the working junctions.

The sealing of the working (called also "hot") thermocouple junctions at the selected points of surface can be realized with the aid of soldering, calking, welding or their attachment to surface. For the soldering of working joint to Duralumin the surface in the place of soldering (Fig. 9.9) is cleaned, are degreased and are tinned by the solder "Avia" or by the alloy, which consists by weight of 50o/o of zinc and 50o/o of tin. This used for soldering iron must have sufficiently large heat output or skin/sheathing must be heated by any other heater. It is necessary to keep in mind that the soldering iron bit must be pure/clean from colophony. The presence even of an insignificant quantity of colophony does not make it possible to produce tinning, since liquid solder in this case is assembled into drop and does not adhere to surface.

For increasing the precision/accuracy of measurments in skin/sheathing are done the deepenings (grooves), in which working joints seal in themselves or are calked. The depth of groove is selected from strength condition of skin/sheathing. The width of groove must be 1.5-2 times greater than the thickness of two thermoelectrodes of thermocouple. The length of groove must not exceed 15-20 mm.

The ends/leads of the conductors for their soldering to surface are cleaned to the length of 5-8 mm and are tinned by usual solders. If tinning was produced with the aid of colophony, then its remainders/residues must be removed by the tampon, moistened in alcohol. The soldering of the working junctions to the tinned places is produced by usual soft solder also without colophony.

The quality of the preparation of the working junction on surface in many respects determines the precision/accuracy of measurment. If working joint proves to be out of the surface (see Fig. 9.9a) or will not be provided the insulation/isolation of thermoelectrodes out of the surface (see Fig. 9.9b), then in measurement will be allowed large error. So that this it would not occur, necessary after soldering to breed by tweezers thermoelectrodes, to thoroughly cover with their cement or varnish, and only after cement (varnish) will dry, to lie/fall/lay them in place and then to stick on the surface (see Fig. 9.9c). Usually wires/conductors are glued round from above by the cloth tape width of 30-50 mm, in this case the places of the soldering of working joints remain free.

Page 237.

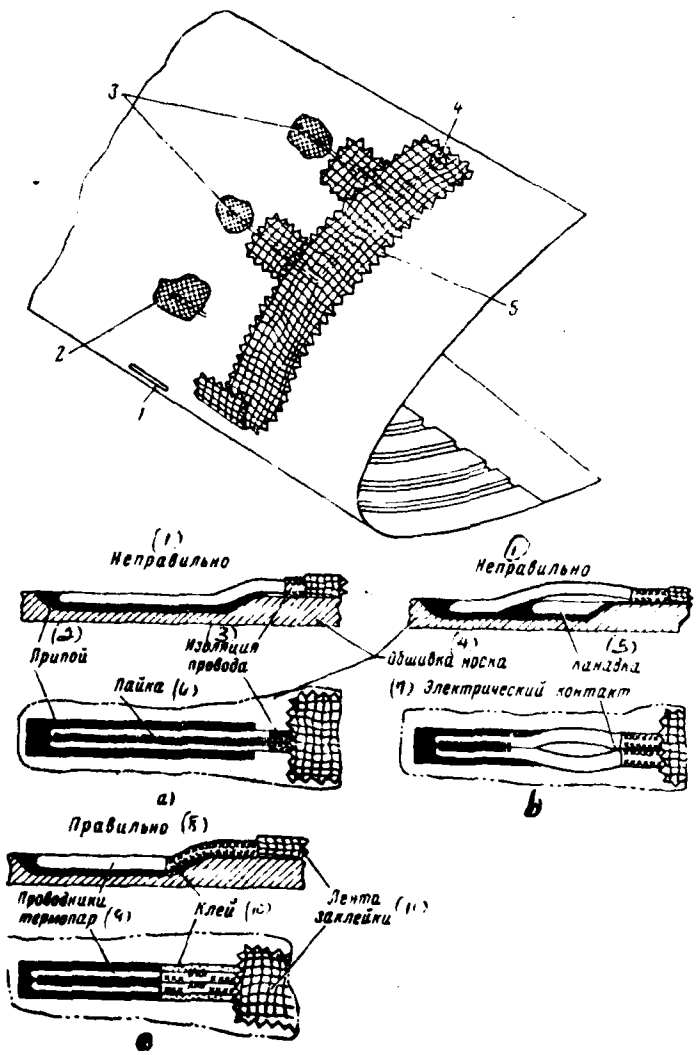

Fig. 9.9. Preparation of working junctions on heating surface: 1 - groove for working junctions; 2 - tinned section; 3 - soldered working junctions; 4 - conclusion/output of thermocouples; 5 -

shielding belt.

Key: (1). It is incorrect. (2). Solder. (3). Wire insulation. (4). Skin of nose/leading edge. (5). Groove. (6). Soldering. (7). Electrical contact. (8). It is correct. (9). Conductors of thermocouples. (10). Cement. (11). Belt of stopping up.

Page 238.

Measurement of the temperature of surface with the aid of resistance thermometers.

Besides thermocouples, for measurement the temperatures of surface utilize wire resistance thermometers. Most frequently during flight tests are applied tape/film resistance thermometers from copper wire (d=0.02-0.05 mm). In this case the dependence of the resistance of sensor on temperature is expressed by the formula

$$R_д(t) = R_{д(0)}(1 + 0{,}00428t), \qquad (9.7)$$

where $R_{д(0)}$ — a resistance of sensor with 0°C;

t- the temperature in °C.

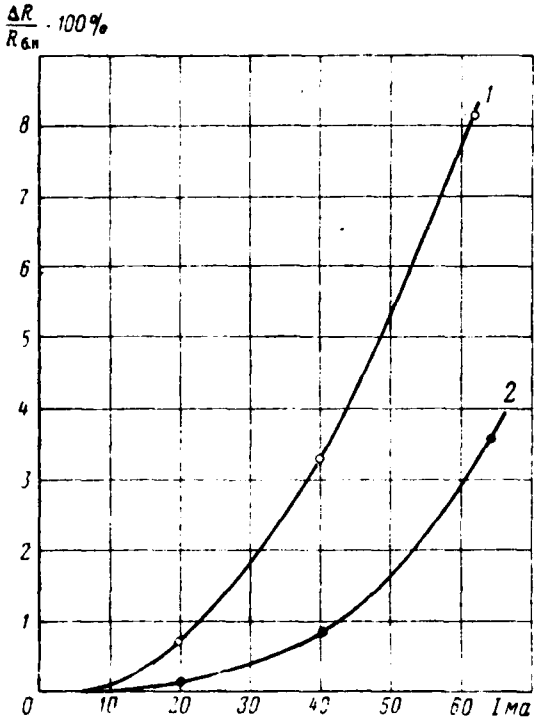

Fig. 9.10. A relative change of resisting the sensor from the strength of passing through it current under the varied conditions of the heat removal: 1 - sensor in the vacuum; 2 - sensor between two layers of sponge rubber.

Page 239.

To materials, from which are made the sensors, are presented the following fundamental requirements: stable and the largest possible temperature coefficient of electrical resistance, the largest

possible resistivity, sufficient thermal and chemical stability.

The electrical resistance thermometers usually enter the schematic of the balanced Wheatstone bridge, in diagonal of whom is included measuring meter or tail of oscillograph. The parameters of bridge circuit are selected so that the taking place through the current-sensing device would not heat by its and thereby would not distort the results of measurement. If sensor is found under conditions of low convective heat removal, then the value of the operating current through the sensor must not exceed 10 mA. With the increased heat removal the value of operating current and, consequently, also instrument sensitivity can be somewhat increased. Fig. 9.10 shows a relative change of resisting the sensor in dependence on the value of its operating current. As is evident, for a sensor, which is located between two layers of sponge rubber, the value of operating current can be allowed almost two times more than for a sensor, which is located in the vacuum (i.e. heat removal even through sponge rubber makes it possible to considerably increase operating current). However, the value of the operating current through the sensor, glued to metallic surface, with its blowout by air can several times exceed value (10 mA) indicated.

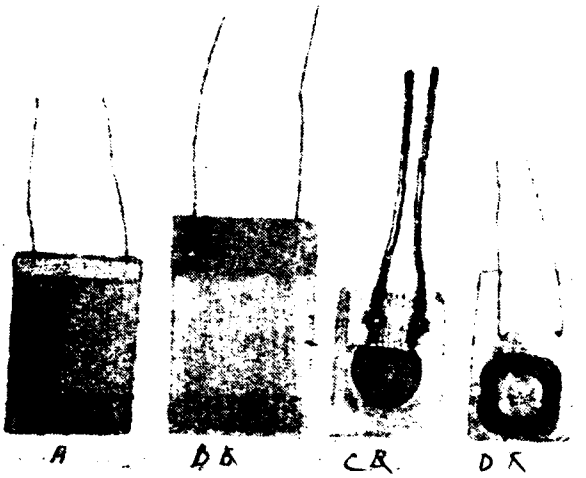

Fig. 9.11. Different types of electrical resistance strain gages.

Page 240.

An error of measurement of temperature as a result of heating of sensor by electric current can be evaluated according to the formula

$$\Delta T = \frac{i^2 R_д}{\alpha_д F_д}, \qquad (9.8)$$

where i - the operating current, which takes place through the sensor;

$R_д$ — resistance of the sensor;

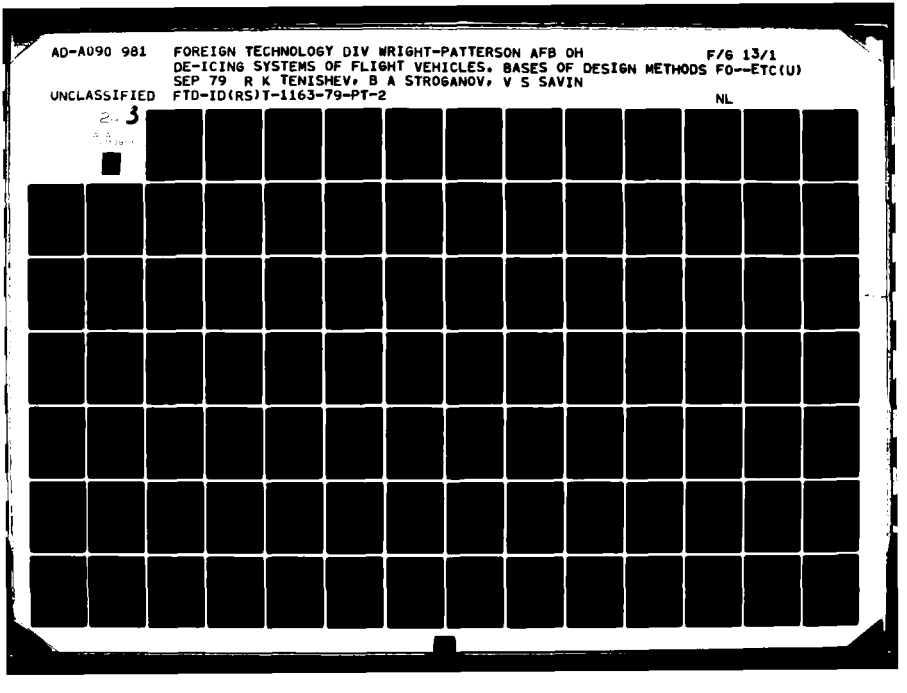
AD-A090 981
FOREIGN TECHNOLOGY DIV WRIGHT-PATTERSON AFB OH
F/G 13/1
DE-ICING SYSTEMS OF FLIGHT VEHICLES. BASES OF DESIGN METHODS FO--ETC(U)
SEP 79 R K TENISHEV, B A STROGANOV, V S SAVIN
UNCLASSIFIED
FTD-ID(RS)T-1163-79-PT-2
NL
2 3

$\alpha_л$ — heat-transfer coefficient from the surface of the sensor;

$F_л$ — surface of sensor.

For measurement the temperatures of surface apply the tape/film resistance thermometers of different types, some of them are shown in Fig. 9.11. They are made from copper wire with a diameter of 0.02-0.03 mm, packed on a thin base with thickness of 0.08-0.05 mm. Sizes/dimensions of the sensors; the type A - approximately/exemplarily 20x30 mm, the type B - 25x35-40 mm, the type C - about 10 mm, the type D - about 15 mm.

The initial resistance of such sensors is usually 80-100 ohms, but recently were adopted more low-resistance sensors (on the order of 30 ohms). On surface the resistance strain gages usually stick with the aid of cements BF-2, BF-4, AK-20, etc.

One of main disadvantages in the film gauges is their very low mechanical strength, due to what applied them for measuring the temperature of surface should be only when it is not the possible to utilize for this purpose of thermocouple.

9.3. Errors of measurement of temperature drops on heating surfaces.

During the determination of temperature drops on heating surfaces of POS of aircraft or helicopter of relatively surrounding air an error of measurement will be composed of an error of measurement of the temperature of surface and error of measurement of the temperature of surrounding air.

Error in the measurement of the temperature of surface depends on:

- type and sensitivity of thermosensitive element (thermocouple or resistance thermometer);

- method of the sealing of sensor on surface (quality of the thermal contact between the sensor and the surface);

- change of resisting the elements/cells of metering circuit with a change in the temperature of the surrounding air;

- sensitivity of measuring meter or tail of the oscillograph;

- accuracy of reading of the readings or interpretation of the oscillograms;

- zero drift instruments or tail.

Page 241.

During the use of thermocouples additionally appear specific errors as a result of inconstancy or inaccuracy of measurement of the temperature of the cold-soldered joints. in certain cases appear parasitic emf from electrostatic or magnetic fields.

During the use of resistance thermometers there can be supplementary errors due to the inconstancy of voltage level, supplied to Wheatstone bridges, deformations of sensor with his gluing, heating of sensor by current passing through it.

The greatest error in the measurement of the temperature of surface is connected with the sealing of the resistance strain gage or thermocouple on surface. So, the gluing of the resistance strain gage or thermocouple can give the error in measurement to 30o/o and more. The soldering of thermocouples substantially decreases this error and is the best method of sealing, since in this case is provided the direct thermal contact of hot junction of thermocouple with the surface whose temperature is measured. The sealing of hot ends into surface by the method of calking or victuals also gives smaller magnitude of error, than gluing. For decreasing the heat

removal from measuring point on thermoelectrodes and lengthening wires/conductors the latter it is desirable to lay at certain distance (not less than 50 mm) from heating surface in that direction, where the gradients of the temperature are minimum.

With the sealing of the working junctions into the skin/sheathing by the method of soldering, calking or victuals cold ends should be thoroughly insulated from each other, since the presence of the electrical contact between them will lead to the onset of eddy currents and the supplementary error in measurements. Cold ends, placed into thermos, are usually insulated from each other by vinyl chloride small-diameter tubes (2-3 mm). For decreasing the thermistor, exerted by tubes, it is expedient to fill with their light-grade oil or kerosene and to place into thermos after 20-30 min to measurement, otherwise the delay of such isolated/insulated joints in thermos prior to the beginning of experiment must be increased to 40-60 min. On the graph of Fig. 9.12 is shown the relative change in the voltage, developed with thermocouples after the location of their cold-soldered joints with different insulation/isolation into the ice medium (working joints were located at certain constant temperature, different from 0°C).

Magnitude of error, connected with a change of resisting the wires/conductors of thermocouple from temperature, virtually can be

disregarded, since this change with respect to the resistance of entire metering circuit is usually very insignificant.

Page 242.

In order to exclude possible error from the onset of idle thermocurrents, electrostatic and magnetic fields, it is necessary thermoelectrodes and jumpers to thoroughly electrically insulate and to follow so that with the wiring it would not be loops ("wing nuts"), but in the presence of powerful/thick magnetic fields should be applied the shadowing of wires/conductors. In a number of cases in the measurement of the temperature of the surface, warmed by alternating current when cannot be avoided focusings/inductions, should be in the circuit of thermocouple included the capacitor filter, which extinguishes variable/alternating focusings/inductions.

Besides in addition to this, the error in measurement can be caused by the onset of parasitic thermal emf in the contact connections of measuring meters or in the joints of the circuit of thermocouple.

The inclusion/connection of measuring meter or tail of chart recorder into the circuit of thermocouple can be carried out on two diagrams (Fig. 9.13). In the first case measuring meter is included

in the explosion of the cold-soldered joint, in the second case in explosion of one of the thermoelectrodes.

As is known, the thermoelectromotive force of thermocouple upon the inclusion into its circuit of the supplementary conductor, distinct in material from thermoelectrodes (in our case of measuring meter or tail), will not change, if the temperature of its both ends/leads will be identical. Otherwise appears supplementary parasitic thermal emf. This fact should be considered upon the start of measuring meter or during the use/application of plug-type connectors in the circuit of thermocouple, since it can cause the error in measurement.

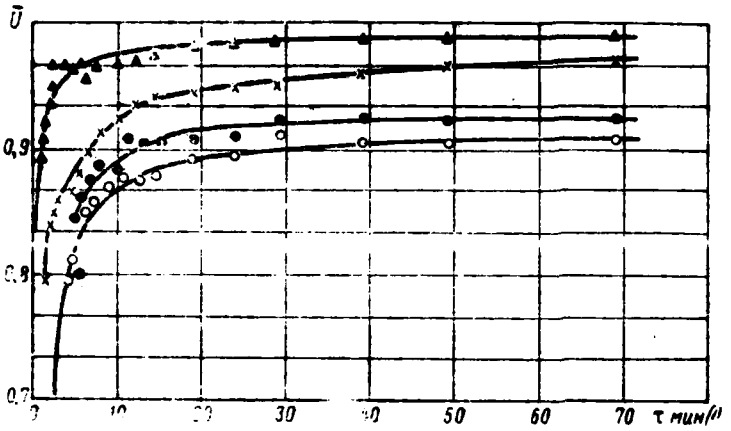

Fig. 9.12. Relative change in voltage of thermocouples in time from moment/torque of location of cold-soldered joints into ice medium: O - vinyl chloride tube, filled with kerosene; X - vinyl chloride tube, filled with oil; O - vinyl chloride tube without filler; Δ - cold end, coated by cement BF-4.

Key: (1). min.

Page 243.

From this point of view is very convenient the use/application of thermocouples with copper thermoelectrode. In this case upon the inclusion of measuring meter or joints into the circuit of copper electrode the temperature of contact points is not important. Therefore in practice wide distribution received copper-constantan

thermocouples. Are frequently utilized also Chromel-Copel thermocouples. More rarely are applied the thermocouples, comprised of other materials: alumel, iron, etc., indicated in Table 9.1.

The value of an instrument/tool meter error or tail usually is indicated in service record or log book the instrument. Thus, for instance, in the chart recorders of series K12 and K20 tails of III-V types give the limit of error to 1.0o/o, and tails of VI-VII types to ±1.5o/o. In order to exclude error in measurement from the drift (zero drift) of tails, in experiment it is necessary to periodically prescribe "mechanical" zero and, if is detected their displacement, then during working/treatment of materials of experiment it is necessary to introduce correction for this displacement.

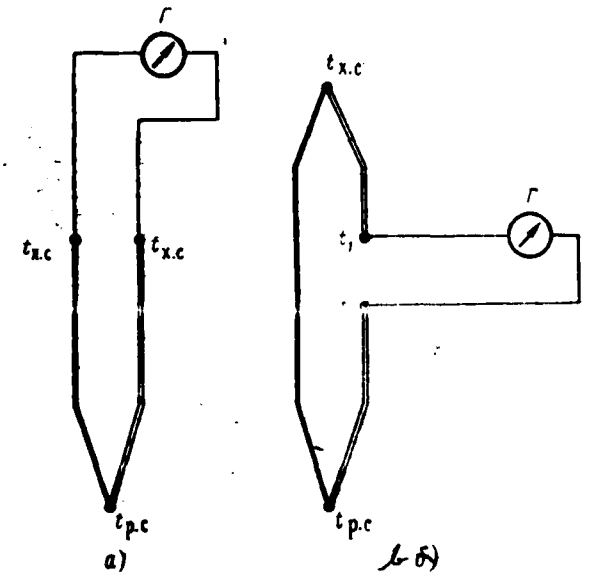

Fig. 9.13. Inclusion of measuring meter into the circuit of the thermocouple: a) the inclusion of instrument into the explosion of cold end; b) the inclusion of instrument into the explosion of thermoelectrode.

Page 244.

Magnitude of error in the measurement of the temperature of surface from inaccuracy with the interpretation of oscillograms in essence is determined by the skill of decoder. It is established/installed, that with the careful interpretation of oscillograms the value of the error in determination of ordinate of

recording can comprise not more than ±0.15 mm. Thus, for example, with the sensitivity of tail 0.3-0.35 mm/°C the error with interpretation will compose ±0.5°C, and with sensitivity 0.8-1.20 of approximately ±0.15°C, which in the majority of cases is satisfactory.

In the measurement of the temperature of surface by electrical resistance thermometers which usually are stuck on surface, fundamental error depends on the method of gluing. For determining the errors, that depend on the method of the preparation of resistance thermometers, the author carried out investigations with the aid of the installation, which is the tube with a diameter of 100 mm and with a length of 1.5 m, equipped with the outer side with electrical heating, within which was created the airflow in speed to 140 m/s. From inside of tube at a distance of 1 m from entry to surface were stuck different sensors. The resistance thermometers of the type A, B, C, and D (see Fig. 9.11) adhered on the internal surface of tube by cement BF-4 or by cement K-88. In one case the sensors had shielding gluing (by percale tape), while in other case they were without it. In the same cross section of tube were sealed in as control three copper-constantan thermocouples. For the "true" value of the temperature of surface was accepted the average/mean reading of these three thermocouples. A difference in their readings did not exceed 1-1.5°C. For the comparison several thermocouples were

also stuck.

Experiments were conducted in the range of the temperatures of surface of 25-80°C, velocities of the airflow 40-140 m/s and specific power from 0.37 to 0.7 W/cm². The results of experiments showed that the sensors, stuck on surface by cement BF-4, understated the temperature of surface from 7 to 30o/o, gluing of sensors by percale strip on top decreasing this understating of temperature (to value 13o/o), and in some cases it led even to the overestimate of temperature (to 37o/o). With the gluing of sensors cement K-88 the error in the direction of understating was still more and it composed 12-60o/o. Even with gluing of these sensors percale band the measured temperatures proved to be in all cases of below (on 11-35pp) "true" temperature.

From the investigated sensors the smallest errors in "pure" mind (without gluing) kept sensors of the type A and B, stuck BF-4, greatest - a sensor of the type C (see Fig. 9.11).

It should be noted that all stuck thermocouples also showed the understated temperatures: on cement K-88 - to 36o/o without gluing and to 20o/o with gluing and on cement BF-4 - to 12o/o. Large spread in the measurements of the temperature of surface with the aid of resistance thermometers is explained by difference in the thickness

of the layer of cement, in thickness and material of the backing of sensor, in their sizes/dimensions and in the method of gluing.

Page 245.

In such a way as to decrease the error in the measurement of the temperature of surface desirable to utilize sensors, analogous types A or B, their patch one should produce with the smallest thickness of tack coat and without stopping up their fabric. However, one should consider that in this case will occur certain understating of the measured temperature of surface.

The practice of flight tests shows also that the error in the measurement of the temperature of surface by film gauges frequently depends on flight altitude, especially if sensor has porous backing, that it is possible to explain by the effect of a change in the heat-conducting properties of backing and skin of fabric with a change in the air density.

To the accuracy of the measurement of temperature with the aid of resistance thermometers significantly affects a change of resisting the jumpers, which go to sensor, from temperature [23] in the case of the two-wire circuit of the connection of sensor, Fig. 9.14a. This effect can be rated/estimated according to the formula

$$\Delta t' = \frac{\alpha_{RA}}{\alpha_{R\,\text{пр}}} \frac{2R_{\text{пр}}}{R_A} \Delta t_{\text{пр}}, \qquad (9.9)$$

where $2R_{пв}(t)$ — a resistance of two jumpers at temperature t°C;

α_{R_A} — temperature drag coefficient of the sensor;

$R_A(t)$ — resistance of sensor at temperature t°C;

$\alpha_{R\,пв}$ — temperature drag coefficient of the wires/conductors;

$\Delta t_{пв}$ — change in the temperature of wires/conductors.

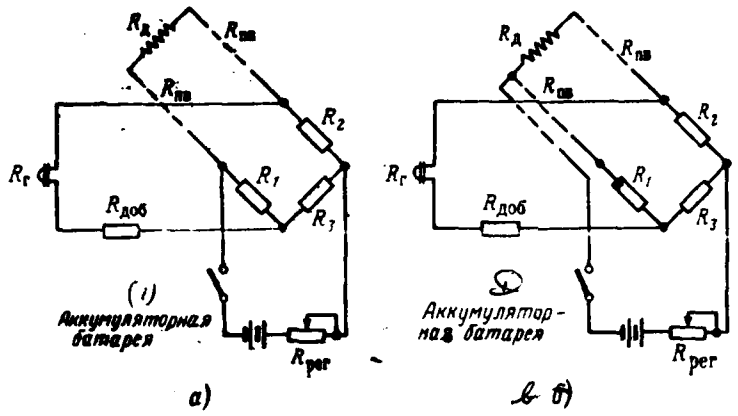

Fig. 9.14. Two- and the three-wire schematics of the connection of sensors to wheatstone bridge.

Key: (1). Storage battery.

Page 246.

Or, if sensor and jumpers are made from one material, then

$$\Delta t' = \frac{2R_{пв}}{R_д}\Delta t_{пв}. \qquad (9.9а)$$

Thus, the higher the resistance of sensor in comparison with the resistance of jumpers, the less their effect.

For decreasing the temperature error should be applied the so-called three-wire schematic of the connection of sensor. In this

diagram the voltage on the third wire/conductor is supplied directly to the sensor (see Fig. 9.14b), thanks to which the jumpers prove to be in different ratio arms of Wheatstone and is not introduced error in measurements. In this case also is eliminated the effect of a change of resisting the wires/conductors from temperature. However, for this diagram it is necessary, in order to $R_2=R_3$.

An error of measurement from a change in the stress level,

applied to Wheatstone bridge, is directly proportional to this change. In fact, the current strength through the tail of chart recorder, connected into the measuring diagonal of the bridge (see Fig. 9.14a), is determined by the expression

$$i_r = U\left[(R_{д0}+2R_{пв})R_3 - R_1R_2\right]\frac{1}{R'}, \qquad (9.10)$$

where

$$R' = [(R_r + R_{доб})(R_д + 2R_{пв} + R_2)(R_1 + R_3) + R_2(R_д + 2R_{пв})\times (R_1 + R_3) + R_1R_3(R_д + 2R_{пв} + R_2).$$

So that this error would be minimum, it is necessary to stabilize the voltage applied to bridge. For this purpose into diagram is introduced control resistor $R_{рег}$ or feed/supply of bridge is accomplished/realized from sufficiently stable source (usually the low-voltage storage battery/accumulator) voltage which continuously is checked, recording with chart recorder. Knowing this voltage, it is

not difficult to introduce the appropriate correction. Then the corrected ordinate of recording is defined as

$$h_{\text{испр}} = h_{\text{изм}} \frac{U_{\text{тар}}}{U_{\text{изм}}},$$

where $h_{\text{изм}}$ — the measured ordinate of the recording of the parameter;

$U_{\text{тар}}$ — voltage during the calibration;

$U_{\text{изм}}$ — measured voltage during recording of the parameter.

Of entire aforesaid it above follows that the methods of measurement of the temperature of surface with the aid of thermocouples (soldered or welded to skin/sheathing) have advantage before the methods, which use tape/film resistance strain gages. Therefore in all cases when this is possible, first should be given preference.

Page 247.

9.4. Measurement of the flow rate of hot air.

For measuring the flow rate of hot air, which enters the de-icing systems, are utilized different measuring devices (Venturi tube, diaphragm, nozzle, etc.) of both of that normalized and not

normalized of types.

Without stopping on the theory of the measurement of expenditure/consumption, which is sufficiently fully presented in the literature [42], [47], etc., let us note that all normalized tapered devices/equipment must satisfy the requirements of the rules of 27-54 committees of standards, measures and measuring meters with the Council of Ministers of the USSR, Mashgiz [State Scientific and Technical Publishing House of Literature on Machinery Manufacture], 1955, but not normalized they must be thoroughly calibrated before the installation to aircraft.

In the practice of flight tests for determining the air flow rate frequently utilize the nozzles L-, T-shaped forms (Fig. 9.15), combs and tubes with the series/row of the openings/apertures, directed against the airflow (Fig. 9.16), etc. During the use/application of such nozzles it is necessary that they would be calibrated together with the section of the conduit/manifold where they are established/installed. This requirement is connected with the fact that the straight portions of the conduits/manifolds where is produced measurement, it is usually small, in consequence of which the diagram/curve of the distribution of velocity vectors in conduit/manifold it can considerably differ from theoretical.

The flow rate of hot air is determined from the formula

$$G_г = 1{,}1 D_{тр}^2 \varphi \sqrt{\rho(\tilde{p}_{пп} - p_{ст})} \text{ kg/m}_\text{.} \qquad (9.11)$$

where

$\tilde{p}_{пп}$ — the complete (it is more average/more mean over cross section) pressure of hot air in N/m²;

$p_{ст}$ — the static pressure of hot air in N/m²;

$D_{тр}$ — inner diameter of the conduit/manifold;

φ - coefficient, which considers the nonuniformity of air flow in conduit/manifold and determined experimentally during the calibration of nozzles with the section of the conduit/manifold in which they are established/installed.

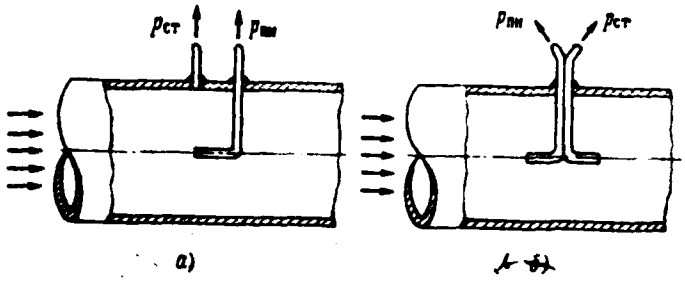

Fig. 9.15. Nozzles for measuring the air speed: a) L-shaped; b) T-shaped.

Page 248.

Air density ρ is determined from equation of state

$$\rho = \frac{p_{ст}}{RT} \text{ kg/m}^3.$$

For decreasing the error in the measurement of the static pressure of opening/aperture in the walls of conduit/manifold must be not more than 1.0 mm and not have projecting edges on edges.

For converting the value of velocity head (in the measurement of the air flow rate) into the electrical signal which is further recorded by chart recorder, it is possible to apply the potentiometric pressure-ratio sensing elements, for example, of the type EDPD, while for converting the value of static pressures - manometric pressure sensors of potentiometric type (MDD, etc.).

For measuring the temperature of hot air in conduits/manifolds are applied the thermocouples or resistance thermometers [10], [42]. From thermocouples most frequently are utilized Chromel-Copel both for the visual observation (for example, TTsT-1, TTsT-2) and for trace.

From resistance thermometers usually are utilized the sensors (for example, type P-1, from the assembly of on-board thermometer TUB-48).

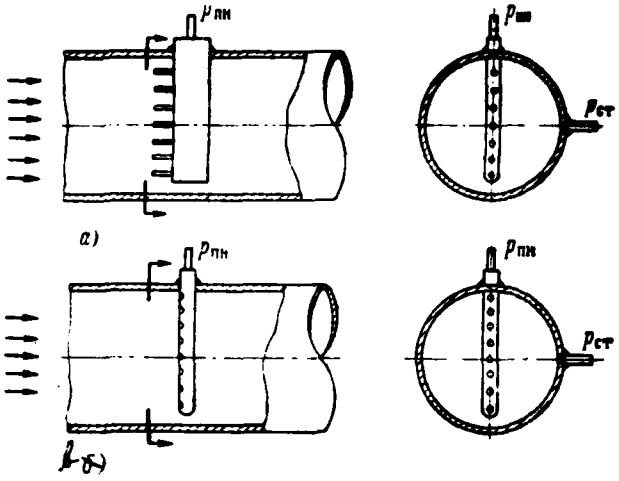

Fig. 9.16. Nozzles for measuring of the velocity fields in the conduit/manifold: a) in the form of the comb; b) tube with openings/apertures.

Page 249.

9.5. Selection of registering apparatus.

At present there is a large quantity of registering apparatus, used for investigations in different areas of technology. Therefore it is expedient to indicate the fundamental types of chart recorders and sensors, which most satisfy the purposes of the tests of de-icing systems, which will simplify preparation for such tests and processing the results of measurements. It goes without saying that

all of a similar kind of recommendation can bear only the character of an example, since metrology continuously is improved.

In particular, in recent years for flight tests ever more wide application finds the method of recording the measured parameters multichannel magnetic accumulators/storage with post-flight automatic interpretation and processing of the results of measurements. Method begins to be utilized, also, during the tests of POS, however, here, especially in the part of the measurement of the temperature of surface by thermocouples, are encountered difficulties, since for this are required very sensitive and stable amplifiers - converters of the weak signals of thermocouples, which complicates equipment used.

From optical chart recorders at present widely are applied the chart recorders of the type K12 and K20, which make it possible to simultaneously record respectively 12 or 20 parameters. They are convenient in operation and have a series/row of advantages before other types of chart recorders. The tails used in them are interchanged and possess large sensitivity (for example, the VII-X types of tails), which makes it possible to directly connect to them thermocouples in the measurement of the small temperatures of surface. This fact is very substantial for the tests of POS.

During the use of thermosensitive elements of resistance it is possible to apply less sensitive tails (for example, the V type), each chart recorder if necessary can be completed by several groups of tails with different sensitivity. Furthermore, tails in tests can be replaced.

Fundamental data of chart recorders are given in table 9.2. The types of the sensors, utilized for measuring different parameters in assembly with chart recorders indicated above, are given in table 9.3.

9.6. Testings of the de-icing system of engine V "dry" air.

Tests for determining of the characteristics of POS of engine in "dry" air are fulfilled in essence employing the same procedure, that also for another POS, but it is possible to note some specific moments/torques.

Page 250.

Table 9.2. Oscillographs, used for the tests of POS.

(1) Типы осциллографов	(2) Число шлейфов	(3) Типы шлейфов	(4) Чувствительность мм/ма	(5) Общее сопротивление шлейфа	(6) Скорость протяжки бумаги мм/сек	(7) Ширина бумаги мм	(8) Длина бумаги м
К20-22	20	V	300÷450	24	1; 2,5; 10; 25		
К20-21	20	VI	600÷850	50	100 ± 5%	190	30
К20-23	20	VII	1200÷1650	50			
К21-21	20	X	6000÷10 000	60			
К12-21	12	V—VII	250÷1650	24÷50	3; 12,5; 60; 250	100	20
К12-22	12						
К10-51 (9) (Вариант I)	10	V—VII VIIIM	250÷1650 1000	40÷50 70	0,2; 0,5; 2,5; 12,5; 2; 5	100	18
К10-52	10	V—VII	250÷1650	40÷50	25; 125 ± 10%	100	18

Notes: 1. In oscillographs K10-51 and K-10-52 two tails they are intended only for the recording of velocity and flight altitude. 2. Tail X of type is produced by experimental series. 3. In oscillograph K20-23 is possible daytime recording of parameters on special-photographic paper. 4. In oscillograph K21-21 are applied small/miniature tails.

Key: (1). Types of oscillographs. (2). Number of tails. (3). Types of tails. (4). sensitivity mm/mA. (5). Total resistance of tail. (6). Rate of broach of paper mm/s. (7). Width of paper mm. (8). Length of paper m. (9). Version.

Table 9.3. Sensors for measuring the parameters at the tests of POS.

Измеряемые параметры (1)	Диапазон измерения (2)	Типы датчиков (3)	Схема или способ соединения (4)	Примечание (5)
$V_{пр}$ — скорость полета (6)	0—900 км/час (7) 0—250 км/час (8) 0—200 км/час (8)	МДД-0-1, МДД ± 0,3, МДД ± 0,4 ЭДПД-1 ЭДПД-2	Мостовая (8)	Возможно использование датчика МРД (9)
H — высота полета (10)	0—10 000 м	МДД-760 ÷ 220; МДД-1-760	Мостовая (8)	Возможно использование датчика МРД (9)
$t_в$ — температура наружного воздуха (11)	± 50° С	П-69; ЭТС-2; П-5, спиртовой термометр с насадком полного торможения (12)	»	
$t_п$ — температура поверхности (13)	От —20 до +80° С	Термопары медь-константановые. Хромель-копелевые и др. (14)	Непосредственно к шлейфу (15)	
I — потребляемый ток (постоянный) (16)	10 ÷ 500 а (17)	Шунты типа ШС, ША и др. на 75 мв	Последовательно в цепи питания, с шунта — на шлейф (18)	
I — потребляемый ток (переменный) (19)	1—10 а 10—50 а	Термопреобразователи Т-1; Т-2 (20)	Последовательно, в цепи питания, с преобразователя на шлейф (21)	
ΔU — падение напряжения (22)	0—200 в 36—220 в	Мостик выпрямительный (23)	Мостовая (8)	
Температура воздуха в каналах ПОС (24)	0—300° С	Медь-константановые, хромель-копелевые и др. (25)	Непосредственно к шлейфу (26)	
УПРТ — режим работы ТВД (27)	0—105° угловой шкалы (28)	МУ-611; МУ-62; МУ-68; ДЛП	Мостовая или потенциометрическая (29)	
Режим работы ТРД (обороты n) (30)	0—12 000 об/мин (31)	ДТЭ-2	Один канал датчика на СО-51 (32)	СО-51 — самописец (33)
G — расход воздуха (34) Δp (Δh) — перепад (35)	От —100 до +200 мм вод. ст (36) От —200 до +400 мм вод. ст. (37) 0 ÷ 1500 мм вод. ст. (38)	ЭДПД-2 ЭДПД-1 ЭДД-31	Мостовая или потенциометрическая (39)	
$p_{ст}$ — статическое давление (40)	0 ÷ 12 атм (41)	МДД-0-1; МДД-0-2; МДД-0-3; МДД-0-4; МДД-0-6; МДД-0-12		
$t_г$ — температура газа за турбиной (42)	До 700° С	ТВГ-11; ТВГ-61 и др. (43)	Параллельно указателю ТВГ на шлейф (44)	Кроме термопары Т-80 (45)

Key: (1). Measured parameters. (2). Range of measurement. (3). Types of sensors. (4). OR gate method of joining. (5) note. (6). flight speed. (7). km/h. (8). Bridge. (9). Is possible use of sensor MRD. (10). flight altitude. (11). temperature of surrounding air. (12). spirit thermometer with nozzle of total stagnation. (13). temperature of surface. (14). Thermocouples copper (constantan. Chromel-Copel, etc. (15). It is direct to tail. (16). consumed current (constant). (17). Shunts of type ShS, ShA, etc. to 75 mV. (18). Consecutively/serially in feed circuit, from shunt - to tail. (19). consumed current (variable/alternating). (20). Thermal converters. (21). Consecutively/serially in feed circuit, from converter to tail. (22). voltage drop. (23). Bridge (rectifying. (24). Temperature of air in channels POS. (25). Copper constantan, Chromel-Copel, etc. (26). It is direct to tail. (27). mode of operation TVD. (28). angular scale. (29). Bridge or potentiometric. (30). Mode of operation of TRD (revolutions n). (31). r/min. (32). One channel of sensor on CO-51. (33). chart recorder. (34). flow rate of air $\Delta p(\Delta h)$ - drop/jump. (35). From. (36). to. (37). water column. (38). Bridge or potentiometric. (39). mm H_2O. (40). static pressure. (41). atm. (42). temperature of gas behind turbine. (43). etc. (44). In parallel to indicator TVG to tail. (45). Besides thermocouple T-80.

Page 252.

The tests of POS of engine on temperature drop it is desirable to begin in bench tests, simultaneously with performance testing and calibration of engine. Preparatory works to conducting of such tests usually are considerably less labor-consuming, than flight ones, furthermore, they make it possible to utilize different laboratory measuring equipment, not applied in flight.

A quantity of measuring points of the temperature of heating surfaces (cook, cone, struts, air intake of blades of VNA, etc.) must be sufficient for the construction of temperature field on heating surface. Thus, for instance, on cook or cone the quantity of measuring points must be not less than 3, on struts or blades of VNA - not less than 4-5. Moreover thermocouples are established/installed not on all struts or blades, but only on 2-3 characteristic ones on heating or clearly having the lowered/reduced heating. The exemplary/approximate locations of thermocouples on engine are shown in Fig. 3.23. The measurements of temperature drops for the elements/cells of inlet duct and engine should be conducted both under conditions, which correspond to real cruise flight envelopes, and in the special modes/conditions, characteristic according to operating conditions of engine.

The tests of the devices/equipment of the heating of the elements/cells of inlet duct and VNA in "dry" air can be accomplished/realized also simultaneously with the flight tests of experimental engine on the special aircraft, utilized as flying laboratories. Especially thoroughly air-heat POS of the engine it must be checked under conditions, close to idling, since in these modes/conditions the selection of hot air and its temperature is usually minimum.

It should be noted that the tests of POS of engine on temperature drop make it possible to rate/estimate its effectiveness usually with smaller confidence than, for example, for lifting surfaces, since for the parts of inlet duct, which have the most diverse layout and complicated flow pattern, process of icing it does not yield to sufficiently precise calculation. Therefore determining the temperature characteristics of deicers in this case is the especially preliminary stage, necessary, for example, for solving a question about the possibility of conducting the tests of engine under conditions of icing. On the other hand, the data on temperature drops occur necessary, also, during the final evaluation of effectiveness of POS.

9.7. Conversion of the values of the temperature drops with electrical heating.

Let us assume that during the tests of POS in "dry" air in certain flight conditions were measured the temperature drops at different points of the shielded surface. Is placed the task of determining by calculation temperature drop on surface for any other flight conditions. This problem easily is solved for the temperature drops in thermoelectric POS, averaged over the shielded surface. After using the method, presented in Section 7.6, in this case it is possible to obtain the following dependence for temperature drops in the relatively equilibrium temperature of the boundary layer:

$$\Delta\tilde{t}_{n2} = \Delta\tilde{t}_{n1}\left(\frac{\rho_{01}V_{01}}{\rho_{02}V_{02}}\right)^{0.8}\left(\frac{q_2}{q_1}\right). \qquad (9.12)$$

In this equation the indices "1" and "2" are related to two different flight conditions, moreover it is assumed that for the 1st mode/conditions are experimental data.

The specific power of thermoelectric POS in the majority of the cases virtually does not depend on flight conditions (with exception of systems with the adjustable specific power), i.e., $q_1=q_2=\text{const}$. Therefore equality in this case somewhat is simplified

$$\Delta\tilde{t}_{n2} = \Delta\tilde{t}_{n}\left(\frac{\rho_{01}V_{01}}{\rho_{02}V_{02}}\right)^{0.8}. \qquad (9.12a)$$

Furthermore, in flight at permanent height/altitude ($p_{01}=p_{02}$)

$$\Delta\tilde{t}_{m2}=\Delta\tilde{t}_{m1}\left(\frac{V_{01}}{V_{02}}\right)^{0.8}. \qquad (9.12б)$$

In the case of permanent true airspeed $V_{01}=V_{02}$

$$\Delta t_{m2}=\Delta\tilde{t}_{m1}\left(\frac{p_{01}}{p_{02}}\right)^{0.8}. \qquad (9.12в)$$

But if in two flight conditions is maintained/withstood permanent indicated airspeed, then let us have

$$\Delta\tilde{t}_{m2}=\Delta\tilde{t}_{m1}\left(\frac{T_1p_{01}}{T_2p_{02}}\right)^{0.4}. \qquad (9.13)$$

The temperature drop relative to the temperature of surrounding air Δt_0 will be in accordance with Section 5.2 with $V_t=V_0$ equal to

$$\Delta\tilde{t}_{02}=\Delta\tilde{t}_{m2}-r^*\frac{V_{02}^2}{2c_p}. \qquad (9.14)$$

The given formulas of conversion make it possible to considerably simplify the flight tests of thermoelectric POS, since by having the measured temperature drops/jumps at any speed and height/altitude, it is possible by calculation to lead these drops/jumps to standard level and to compare them with the prescribed/assigned requirements.

Page 254.

9.8. Experimental methods of determining the heat-transfer

coefficients.

During calculation and especially during the investigation of the thermal characteristics of the newly developed/processed deicers in a number of cases it is necessary to have more precise (actual) values of local heat-transfer coefficients, since the calculations usually are fulfilled at the extreme or averaged values of the entering the formula values. Furthermore, these same values are not always sufficiently accurately known (for example, the local velocities of flow, position of the transition points of boundary layer, heat-transfer coefficient at the critical point of profile/airfoil, etc.).

In such cases it is necessary to resort to the experimental methods of determining the heat-transfer coefficients. These methods can be based on the use both of stationary and nonstationary thermal processes [27], [46], [118], [119], [125].

Is described below the procedure of the measurement of external local heat-transfer coefficients analogously it can be comprised the procedure of the measurement of heat-transfer coefficients in the internal ducts of the air-heat deicers.

The principle of the stationary method consists in the use of

equation of convective heat exchange (5.2), from which it follows

$$\alpha = \frac{q_n}{(t_n - t_1^*)}.$$

During transient processes for the experimental determination of heat-transfer coefficient is utilized another equation of the heat exchange

$$q = \frac{1}{F} \cdot \frac{dQ}{d\tau}, \qquad (9.15)$$

where F - the exothermal surface of meter.

At first glance, the simplest version of use/application of both methods is the direct use of a heating element of deicer. However, as it was shown in chapter VI, large leakages of heat along skin/sheathing they make wrong assumption about the unidimensionality of heat flux, and this leads to considerable errors in the measurement of the local importance of the temperatures of surface.

Sensors for determining the coefficients of convective heat emission can be fulfilled in the form of calorimetric "plugs" and in the form of the strip/tape or film gauges of the most diverse constructions/designs. In this case most adequate/approaching is, apparently, the method of the electrically heated tapes (see [99], [100], [102], [134] [135]), that makes it possible to combine the stationary and transient methods of determining the coefficients.

With comparative simplicity of the method used a total error of measurement does not exceed 10o/o.

Page 255.

The principle of the operation of sensor consists of the following. To the body being investigated, usually prepared from thermal insulation material, is stuck thin metallic tape (made of Nichrome or stainless steel), on which is passed the electric current of the specific value.

If we isolate the segment element of tape (Fig. 9.17a) and to compose for it the equation of heat balance, in reference to the unit of surface, then we will obtain the following formula for a local heat-transfer coefficient:

$$\alpha = \frac{q_{эл} - q_{изл} + q_{пр} - q_{ал} - q_{бок}}{t_п - t_ж^*}. \qquad (9.16)$$

Heat-flux density, which appears in the tape as a result of the passage on it of electric current, is determined from the formula

$$q_{эл} = \frac{I^2 R}{b}, \qquad (9.17)$$

in which I - the current strength, R - electrical resistance on 1 m of the length of belt, and b - the width of belt.

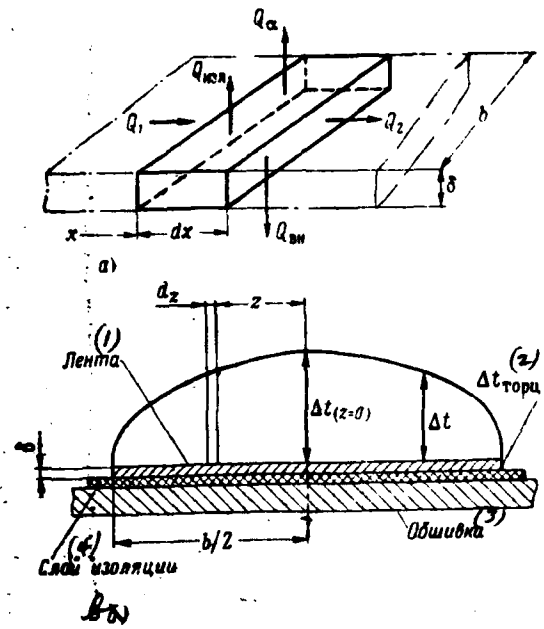

Fig. 9.17. Schematic of the heat exchange of the strip/tape sensor: a) the heat fluxes of the segment element; b) temperature field in the transverse plane of belt.

Key: (1). Belt. (2). face. (3). Skin/sheathing. (4). Layers of insulation/isolation.

Page 256.

Radiation/emission from the heated surface of belt can be considered with the aid of the known relationship/ratio

$$q_{изл} = \varepsilon\sigma\left(\frac{T_п}{100}\right)^4, \qquad (9.18)$$

where ε — emissivity factor of the belt; σ - Stefan-Boltzmann's constant (σ=5.77 Вт/м²·°К⁴) .

It is easy to show that heat-flux density via thermal conductivity lengthwise directly the measuring belt it is possible to represent as follows:

$$q_{пр} = q_2 - q_1 = \lambda\delta \frac{d^2t_п}{dx^2}, \qquad (9.19)$$

where λ and δ - respectively the coefficient of thermal conductivity and the thickness of belt. Value $\frac{d^2t_п}{dx^2}$ is located by the graphic differentiation the distribution curve of temperature on the belt which is measured in experiment.

One of the possible methods of determining the density of internal heat flow is based on the use of the formula

$$q_{вн} = \frac{\lambda_{из}}{\delta_{из}}(t_п - t_{вн}). \qquad (9.20)$$

in which $\lambda_{из}$ and $\delta_{из}$ — coefficient of thermal conductivity and thickness of thermal insulation, and $t_{вн}$ — temperature of the surface of skin/sheathing under insulation/isolation at the point in question. For determination $q_{вн}$ this temperature must be measured, i.e., is required supplementary thermocouple.

The effect of the lateral leakages of heat can be rated/estimated by approximate solution of the equation of heat balance for the element/cell of belt dz (see Fig. 9.17b). In this case let us have

$$q_{бок} = \frac{\lambda}{b/2}(t'_п - t_п), \qquad (9.21)$$

where $t_п$ and $t'_п$ the temperature in the middle of belt in the absence and in the presence of lateral leakages. In this case the temperature differential is determined from the following relationship:

$$t'_п - t_п = \frac{\frac{q_{зл}}{\alpha} - (t_п - t_1^*)_{z=b/2}}{ch\frac{b}{2}\sqrt{\frac{\alpha}{\lambda\delta}}}. \qquad (9.22)$$

It is obvious that independent determination $q_{бок}$ from formula (9.21) is impossible, since into formula (9.22) enters the measured value α. In order to decrease the lateral leakages of heat, are introduced supplementary belts from both sides from the master tape, heated to the same temperature.

Page 257.

As it follows from formula (9.22), in this case heat flux through the lateral sides of belt can be significantly reduced. Furthermore, for decreasing of all thermal leakages (via radiation/emission and

thermal conductivity) and simplification in the experiment the temperature of the heated surface must be supported at minimum level. Virtually it proves to be that the temperature differential of the heated and "cold" belt must not exceed 20-30°C.

Thus, for obtaining the local values of heat-transfer coefficients it is necessary to measure the strength of current I, which passes on belt, the temperature of the surface of belt t_n and the equilibrium temperature of boundary layer t_l^*. The last they accept the surface of belt equal to temperature in the absence of heating. For the introduction of method-of-operation corrections in measurement α should be used formulas (9.18)-(9.22).

The described above electrically heated belts make it possible to produce the determination of local heat-transfer coefficients, also, in transient method. Solving together equations (5.2) and (9.15), we will obtain

$$\alpha = \frac{\rho c \delta}{\Delta \tau} \ln \frac{t_{n1} - t_l^*}{t_{n2} - t_l^*}, \qquad (9.23)$$

where ρ and c - density and the specific heat of material of belt, and $\Delta\tau$ - time interval for which proceeds a change in the local temperature of belt from t_{n1} to t_{n2}.

It should be noted that the measuring belts can introduce

noticeable distortions during the flow of air about the body being investigated and cause premature transition/transfer to turbulent flow. Therefore usually are utilized the belts, which have the thickness not more than 0.05-0.1 mm. Certainly, in this case the obtained inequalities I will create turbulence boundary layer on body surface; however, the effect of measuring belts to flow conditions will be insignificant in comparison with the effect of ice, which is formed on body surface with icing.

The method described above was used for measuring the local heat-transfer coefficients in the experimental section of wing, established/installed on flying laboratory for the investigation of the protection from icing whose photo is given in chapter XI. To the surface of the removable nose/leading edge of section, prepared from fiberglass laminate VPT, in three cross sections were stuck according to three belts from stainless steel OKh18N9 with thickness 0.1 mm and width of 25 mm, series-connected between themselves. Feed/supply to measuring belts was fed/conducted from the source of direct current. For measuring the temperature of the surface of belts were applied the copper-constantan thermocouples with a diameter of 0.2 mm.

Page 258.

To hot ends was soldered the copper foil (in diameter approximately 5

mm and thickness of 0.06 mm). The electrical insulation of thermocouples from the current-conducting belt was accomplished/realized by a layer of the tracing paper. The wires/conductors of thermocouples at the length of 20-30 mm were packed under belt in special grooves and then they were derived/concluded into the internal part of the section. In each measuring cross section in two lateral belts (with respect to central belt) were drilled the openings/apertures with a diameter of 0.8 mm for measuring the local static pressures on the surface of the leading edge of an airfoil profile. the location of these openings/apertures corresponded to the location of thermocouples on central belt. To the openings/apertures of from within section were conducted/supplied copper tubes in inner diameter 2 mm.

In tests flight altitude varied from 900 to 10000 m, true flight speed - from 92 to 174 m/s and the angle of setting section - from -10 to +10°. The sweep angle of section on leading edge comprised 39°30'.

Fig. 9.18 depicts the data, obtained after criterial processing of the results of the measurements of local heat-transfer coefficients on the surface of the nose/leading edge of the investigated section at zero angle of attack. For a comparison on graph is plotted/applied the dependence of local heat-transfer

coefficients for a flat/plane plate during turbulent flow conditions, calculated by formula (5.8). A good coincidence of theoretical and experimental data is confirmation of the sufficiently high precision/accuracy of the procedure of calculation of heat-transfer coefficients for aerodynamic profiles/airfoils, presented in chapter V.

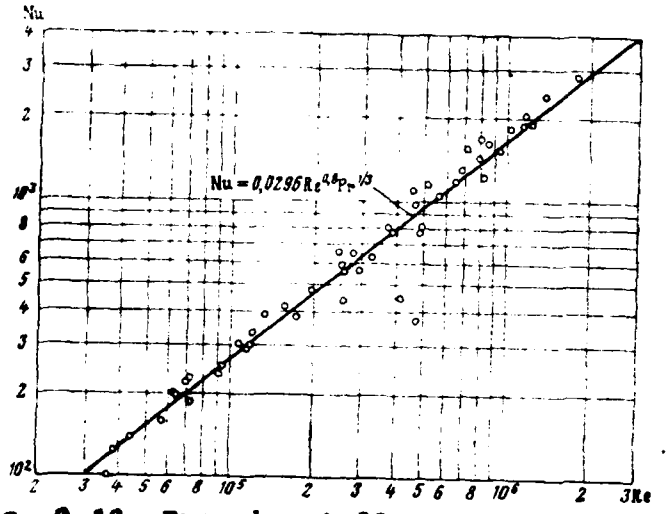

Fig. 9.18. Experimentally obtained and designed heat-transfer coefficients in the profile/airfoil of the nose/leading edge of the sweptback wing.

Page 259.

9.9. Determination of the rate of heating surface from separate experimental points.

If during processing of the results of experiment it is necessary to obtain entire curve of the heating of any heater, and there is only segment of curve or its separate points, then it can be obtained by the method of extrapolation.

From chapter VI it is known that temperature heating curve of thin-walled construction/design is sufficiently accurately described by exponential curve. Moreover, practice shows that heating curves of many other constructions/designs in the majority of the cases with virtually acceptable precision/accuracy can be approximated by exponential curve (with exception of initial section [26], [27]). Therefore are obtained very simple formulas for extrapolation.

For the plotting of curves of heating, described by exponential curve, it is necessary and it suffices to have value of steady temperature and rate of the heating (see Section 6.2).

The steady temperature drop (relative to equilibrium temperature) can be determined, if is known the value of temperature $t(\tau_0)$ and $t(\tau_1)$ into two arbitrary ones of the moment/torque of time τ_0 and τ_1:

$$\Delta t_{уст} = \frac{t(\tau_0) - t(\tau_1)}{e^{-m\tau_0} - e^{-m\tau_1}}. \qquad (9.24)$$

The rate of heating can be determined, having temperature at three moment of time $t(\tau_0)$, $t(\tau_1)$ and $t(\tau_2)$:

$$m = \frac{2}{\tau_2 - \tau_0} \ln \frac{t(\tau_1) - t(\tau_0)}{t(\tau_2) - t(\tau_1)} \quad 1/\text{м}, \qquad (9.25)$$

moreover the corresponding intervals of time must be connected with

the relationship/ratio

$$\frac{\tau_2-\tau_1}{\tau_1-\tau_0}=1 \qquad (9.26)$$

(or otherwise $\tau_2-\tau_1=\tau_1-\tau_0$).

Zero time τ_0 always can be to accept $\tau_0=0$ moreover, for any segment of curve, but not only for the beginning of heating (Fig. 9.19). I.e.,, if the section of curve in the beginning of heating, as so often is the case, does not clearly correspond to exponential curve, then it must not be allowed and as point τ_0 should be selected such, where heating becomes sufficient to regular ones [1].

FOOTNOTE [1]. The methods of the quantitative determination of regular thermal condition are in detail described in G. N. Kondratyev's works [26], [27]. ENDFOOTNOTE.

As it follows from (9.26), must be fulfilled the condition

$$\tau_2=2\tau_1.$$

Page 260.

Cooling curve can be obtained according to formula (6.8), if is known the temperature at any moment of time (taken in calculation for zero) and rate of heating, determined according to formula (9.25). Having two points of the curve of cooling, it is possible to determine also the temperature of body prior to the beginning of heating, in particular the equilibrium temperature of the surface:

$$t_1^* = \frac{t(\tau_1') - t(\tau_2')e^{-m(\tau_1'-\tau_2')}}{1-e^{-m(\tau_1'-\tau_2')}}, \qquad (9.27)$$

where the moments of time, designated by prime τ', are related to cooling curve.

The values of the rate of heating m, obtained by the manner indicated above, make it possible to immediately rate/estimate the character of curve and the value of temperature at any moment of time, without deciphering an entire recording. For this it is possible to use Fig. 5 application/appendix, in which are represented the curves of dimensionless temperature for different values of m. The product of this function on $\Delta t_{уст}$ gives the value of temperature

drop of the relatively equilibrium temperature at any required moment of the time

$$\Delta t(\tau) = \vartheta(\tau) \cdot \Delta t_{y\text{cr}}.$$

For increasing the precision/accuracy of extrapolation it is desirable to fulfill calculation for several points of heating curve or cooling.

In formulas (9.24) and (9.25) it is possible to use the value of both temperatures and their drops/jumps (since enter their differences). Moreover, if readings are removed/taken with recorder tape whose calibration is close to the the linear t=kt, then in formula (9.25) it is possible to directly utilize ordinates of recording h in mm, not changing them into temperatures.

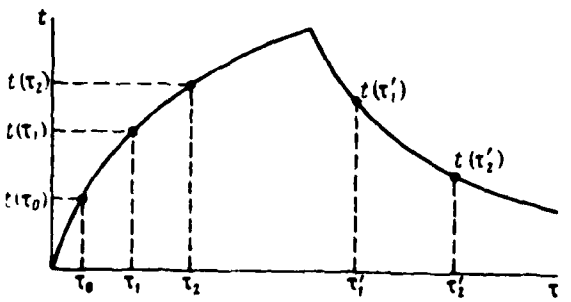

Fig. 9.19. Selection of calculation points in heating curve and cooling.

Chapter X.

Methods of measuring the parameters, characterizing the conditions of icing, and the testing of POS under conditions of icing [1].

FOOTNOTE [1]. It is written by B. A. Stroganov, R. Kh. Tenishev and V. K. Kordinov. ENDFOOTNOTE.

10.1. Methods of recording of parameters, characterizing the conditions of icing.

The results of tests of flight vehicles under conditions of icing can be qualitative only in such a case, when is sufficiently accurately known the parameters, which characterize these conditions, i.e., the temperature of surrounding air, water content, size/dimension of drops, in a number of cases - air humidity.

In the measurement of these parameters in flight, especially on modern aircraft with the pressurized cabins (on which is required the use/application of instruments of remote action), we encounter with considerable difficulties. In particular, the temperature of air

under conditions of icing cannot be measured with the aid of usual on-board thermometers, since they are covered with ice and, naturally, change their calibration coefficients. To this fact frequently is not given proper attention, and during the tests are used readings of on-board thermometers, which leads to considerable errors during the determination of the temperature of surrounding air under conditions of icing.

Measurement of the temperature of air under conditions of icing.

Fundamental requirements for the thermometer, used for measuring the temperatures of surrounding air under conditions of icing, consist in the fact that, in the first place, on gauge element must not fall the moisture, in the second place, the recovery factor of thermometer must not noticeably change with the formation on it of ice (or they must be provided for the measures, which do not allow/assume the formation on it of ice).

For measuring the temperature of air in flight in clouds is applied the aircraft shielded thermometer SET (Fig. 10.1). It is the hollow cylindrical tube, within which is placed the temperature-sensing device (resistance thermometer) 1. In tube in area of the location of sensor are cut the openings/apertures for the duct of air 3. In tube face has conical or another easily streamlined

form tip, while in tail section is established/installed diffuser 4 for guaranteeing suction of air within tube.

Page 262.

The sensor of thermometer is made from copper, nickel or platinum wire in diameter from 50 to 100 μ, the resistance of sensor depending on bridge circuit and sensitivity of the tail of oscillograph is selected from 40 to 100 ohms. For decreasing the measuring errors due to radiation the sensor is closed by shield 2 in the form of thin-walled metal tube with the polished nickle-plated or chrome-plated surface.

As a result of the fact that the air, which blows out/blows off sensor, is sucked through narrow slots in the housing of thermometer, drop of water under the effect of the inertial forces they do not fall inside small tube and they do not settle on sensor. Therefore the readings of SET are little sensitive to the presence of cloudiness or rain.

According to the data of investigations of V. A. Zaytsev [17], the quality coefficient M of the shielded thermometers 1 investigated by him is equal to 0.83+-0.01.

FOOTNOTE [1]. Quality coefficient to a certain extent depends on the form of the tip of sensor; therefore for the concrete/specific/actual form of sensor this coefficient should be more precisely formulated. ENDFOOTNOTE.

However, SET is sufficiently sensitive to downwash, since this substantially changes the suction of air within tube, that it is necessary to keep in mind during its use in experiments.

Furthermore, considerable ice formation on nose/leading edge of SET changes the value of its recovery factor, which can be the reason for the appearance of considerable errors in the determination of actual temperature of air.

In the practice of the flight tests of latter/last years finds wide application the method of determining the actual temperature of surrounding air with the aid of two thermometers of braking. This method consists of the following. One of the thermometers (ETS-2, P-69) is placed normally (directly) along flow, and another they will expand/scan by 180° (conversely).

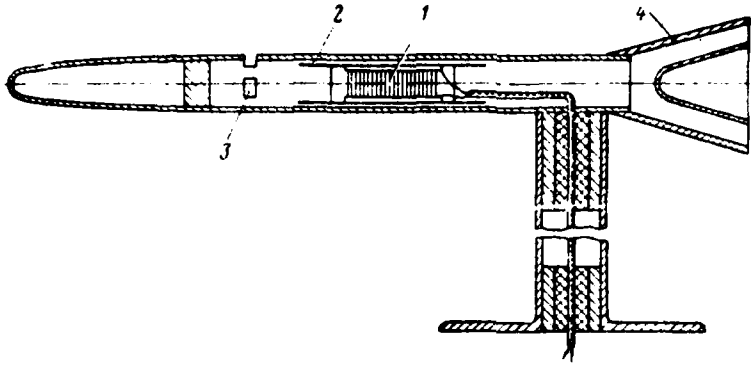

Fig. 10.1. Aircraft shielded thermometer.

Page 263.

It is preliminary, during flights in "dry" air with different heights/altitudes and at speeds are recorded their readings, from which is constructed graph $t_{пр} = f(t_{обр})$. The typical form of this graph is depicted in Fig. 10.2. During flights under conditions the icing determine the values of the turned thermometer (relative to its normal position) and find through graph/curve $t_{пр} = f(t_{обр})$ value $t_{пр}$. Then according to formula (9.3) or by the expression

$$t_0 = t_{пр} - \frac{r^*_{терм} V_0^2}{2c_p} \quad (10.1)$$

is determined the true value of the temperature of surrounding air.

While conducting of tests with artificial icing the temperature

of surrounding air usually is measured out of the conditions of icing (in "dry" air), assuming that the same temperature is retained in area of icing. When it is necessary to measure the temperature directly in the zone of icing (for example, during use of vapor for the condensation of drops or ejection of water), can be utilized the same methods, as with natural icing.

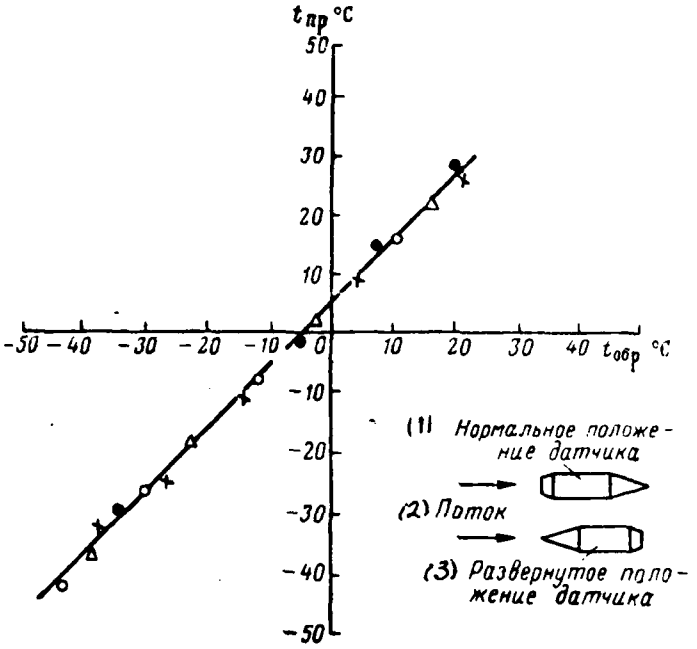

Fig. 10.2. The graph of the interdependence of readings of temperature-sensing devices one of which they will expand/scan by 180° relative to the incident flow.

Key: (1). Normal position of sensor. (2). Flow. (3). Expanded/scanned position of sensor.

Page 264.

Measurement of water content and size/dimension of drops in flight.

Methods of measuring the water content of the supercooled drops in flight most frequently are based on dependence (4.1), solved relative to w:

$$\omega = \frac{G_B \cdot 10^{-3}}{EV_0 C_M} \quad \text{кг/м}^3. \qquad (10.2)$$

To recover for this purpose water is possible, for example, by the air intake warmed all over length, on which the water drains into the graduated vessel where occurs the measurement of an increase in the space of water for the specific time interval. Fig. 10.3 shows construction/design of one of such air intakes [83]. Difficulty during the use of this method is connected with the fact that interception coefficient E as is known (see Chapter IV), it depends on the size/dimension of drops and flight conditions; therefore for the precise measurement of water content it is necessary to simultaneously measure the sizes/dimensions of drops, and to calibrate instrument under varied conditions for flight.

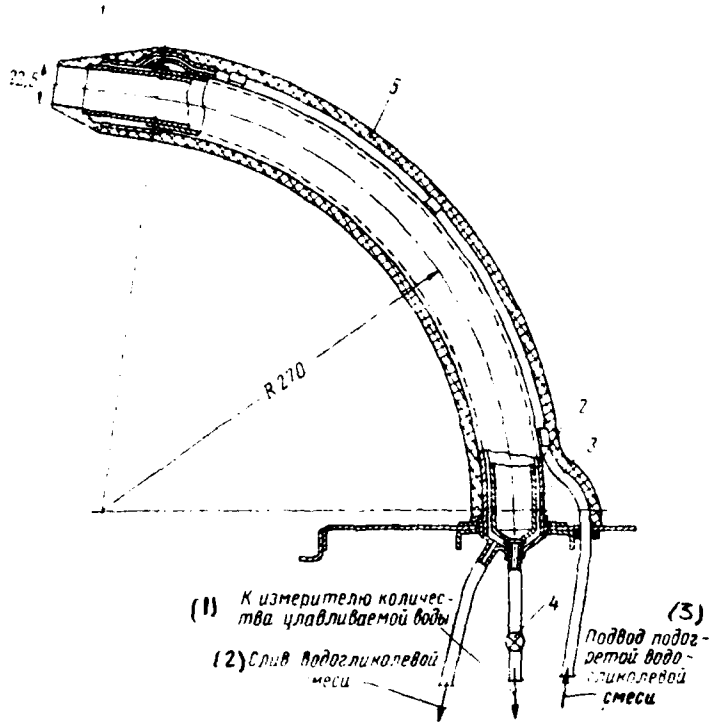

Fig. 10.3. Instrument for measuring the water content by the direct method: 1 - nose/leading edge, soldered to core tube; 2 - core tube; 3 - external tube; 4 - tap/crane; 5 - fiberglass laminate housing.

Key: (1). To the meter of the quantity of the absorbed by water. (2). Drain of water-glycol mixture. (3). Supply of heated water-glycol mixture.

Furthermore, such air intakes recover both drop water and crystals of ice.

On aircraft with the unpressurized compartment for determining a quantity of absorbed by water was utilized its freezing on the control cylinder with which ice periodically was removed/taken and was weighed. For pressurized cabins this method is very hindered/hampered and on contemporary aircraft barely is applied.

There are also methods, based on mass not measurement of water, but directly the space of the generatrix of ice. For this purpose are applied rotating cylinders [1] and other devices/equipment.

FOOTNOTE [1]. On the rotating cylinder, for example, is based the aircraft ice detector (SIO) of the plant Gidrometeopribor. The thickness of ice on it is measured with the aid of the carrier, deflected by ice increased on cylinder. Carrier is connected with the potentiometric pickup, signal from which is supplied to dial instrument and to chart recorder. A shortcoming in the instrument in the fact that it does not make it possible to throw off ice in flight and on the achievement of its thickness about 10 mm stop. Furthermore, instrument is designed only for flight speeds to 200-300 km/h. ENDFOOTNOTE.

The precision/accuracy of these methods depends (besides interception coefficient E) from the value of the specific density of ice, entered into calculation, and from the value of the coefficient of freezing ice $\varepsilon_{л}$, which can change sufficiently over wide limits. Therefore their precision/accuracy is small.

From similar methods the most simple and available is the method of determining the water content from the speed of ice formation on the frontal edge of control cylinder or profile with the aid of the measuring rule available on it.

Since the thickness of ice is fixed/recorded on the frontal edge of the profile/airfoil (or cylinder), which has small sizes/dimensions, then into calculation should be accepted no longer general/common/total interception coefficient E, but local ε, whose value for the face grinding of this profile/airfoil is close to unity and little it depends on flight speed [2] (see Section 4.1).

FOOTNOTE [2]. One should, however, consider that in proportion to the growth of ice the form of profile/airfoil can completely be distorted and, therefore, value ε will change. Therefore in the profiles/airfoils, utilized for determining the water content, must be provided the possibility of jettisoning ice upon reaching of the thickness of its more several millimeters. ENDFOOTNOTE.

In this case the water content is determined from the expression

$$w = \frac{h_л(\tau)\,\rho_л}{\varepsilon\xi_л V_0 \tau_л} = \frac{h_л(\tau)\,\rho_л}{\varepsilon\xi_л V_0 60\tau_{л\,(мин)}}\ г/м^3, \qquad (10.3)$$

where $\tau_л$ - a time of the growth of ice in s, and $\tau_{л\,(мин)}$ - in min;

$h_л$ - thickness of ice for the time of growth in mm;

$\rho_л$ - ice density in kg/m³.

For example, with $h_л = 10$ mm for $\tau_л = 3$ min, when $\rho_л = 700$ kg/m³, $V_0 = 150$ m/s, $\varepsilon = 0{,}9$, $\xi_л = 0{,}8$ we obtain w=0.36 g/m³.

Page 266.

The precision/accuracy of method, besides other factors, to a considerable degree depends on the accuracy of reading of the thickness of ice which during visual observation is not especially high and usually connected with subjective errors.

Majority of the enumerated instruments does not provide the continuous recording of readings and requires supplementary conversions, which in flight is inconvenient.

More the "high speed" methods from to continuous recording of readings are based, analogously with the ice-indicating equipment of indirect action, during the measurement of different indirect parameters, which depend on the value of water content. Most widely used of them is the method, based on the measurement of the quantity of heat, expended for the evaporation of the absorbed by water. Structurally/constructurally it can be accomplished/realized in the diverse variants. For example, V. A. Zaytsev's known instrument [17] is based on the comparison of the temperatures of two warmed surfaces, one of which recovers drop, and another is shielded from them. The greater the temperature difference between them, the greater the water content of air. A difference in temperatures is determined with the aid of thermocouples and is fixed/recorded with oscillograph or visual instrument, calibrated on water content. Dial face is broken into two ranges: 0-0.3 g/m^3 with scale value 0.005 g/m^3 and 0-3 g/m^3 with scale value 0.05 g/m^3.

The general requirement for such instruments lies in the fact that entire absorbed by water would evaporate in the limits of the warmed zone, having thermosensitive elements (thermocouples), otherwise the part of the water, draining beyond the limits of this zone, will not be considered in measurements.

From the instruments, based on other methods, is interesting V. I. Skatskiy's instrument [52], which effects during the measurement of electrical conductivity of sensing element during the incidence/impingement to it of water. For drainage is utilized high-frequency heating, and sensing element is connected into the circuit of the tube, which controls/guides high-frequency oscillator. Thus, in the absence of moisture the output power of generator is minimum, and during moistening of sensing element output power increases proportional to a quantity of absorbed by water.

Recording output power on oscillograph, it is possible to rate/estimate a quantity of grasped water and water content of clouds in any moment of time.

The great advantage of this instrument is its high response according to output power, which makes it possible to fix/record water content to 5 g/m^3 into very short time intervals. Fault of measurement of water content (according to V. I. Skatskiy's data) does not exceed 20o/o.

There exist also the instruments, based on the measurement of the electrostatic charge of drops, for which they preliminarily are

charged, for example, passing through the framework, established/installed on the path of drops and which has large potential.

Page 267.

Under the artificial conditions of icing let us use also the indirect method of determining the water content, based on the measurement of the flow rate of the water through the injectors:

$$w = \frac{G_в}{VF_ф} \quad кг/м^3, \qquad (10.4)$$

where $G_в$ - a flow rate of the water through injectors in the kg/s;

$F_ф$ - area of injector grid (collector/receptacle) in the $м^2$;

V - a speed of the flow through the collector/receptacle in m/s.

The measurement of the sizes/dimensions of drops is produced with the aid of photomicrography. The essence of this method lies in the fact that the drops are captured to microscope slide, and then photographed under microscope [105]. The measurement of the sizes/dimensions of drops is produced on the projection of negative on shield either on photograph, then is produced conversion in accordance with magnifying power or, which is more conveniently, on

the image of drops it is placed by the photo of the microgrid as which it is possible to utilize, for example, a microgrid, used during microbiological investigations.

So that the drops deposited to glass would retain the initial form (would not spread), the surface of glass they cover/coat with the mixture of petroleum jelly and transformer oil. The composition of the mixture of petroleum jelly and transformer oil depending on the temperature of surrounding air is given below, in Table 10.1.

The use/application of a mixture of oil and petroleum jelly usefully even and fact that it contributes to the slower evaporation of drops. According to V. A. Zaytsev's data, rate of change in the diameter of drop, which is located in the mixture indicated, on the average is 0.07 μ per minute, but error from the decrease of drop during photography does not exceed usually 0.2 μ. However, if the time between the sampling of test/sample and photography is great, then, in order to decrease the error in measurement due to evaporation, is expedient the glass plates with the grasped drops to photography to hold in special thermostat at temperature of approximately 0°C (but it is not below, since this can lead to the crystallization of drop).

Table 10.1.

(1) Температура воздуха в °С	0÷—5	—5÷—10	—10÷—15	15 и ниже (2)
(3) Доля вазелина в частях от состава	1	1	1	0
(4) Доля трансформаторного масла в частях от состава	4	6	10	1

Key: (1). Temperature of air in °C. (2). and it is below. (3). Portion of petroleum jelly in parts of composition. (4). Portion of transformer oil in parts of composition.

Page 268.

Since a quantity of grasped drops depends on the time of the exposure of plate in flow, then for the taking of samples from air flow in Central aerological observatory (TsAO (ЦАО) - Central Aerological Observatory]) is developed special air intake, in which the exposure of plate is limited (about 0.2 s).

For flight tests on aircraft with pressurized cabin, and is also on flying laboratories necessary the automatic or semiautomatic instrument with remote control, which ensures photographing the drops in the specific time.

The available at present experimental developments of such

instruments possess, unfortunately, the number of the structural/design shortcomings which do not make it possible to thus far recommend them for wide use during the tests of de-icing systems.

Although photomicrography does not make it possible to check cloud microstructure in flight (due to the need of treating photographic film), not it gives the possibility to fix/record the sizes/dimensions of drops, which occurred during tests. Therefore it is desirable to apply it in all cases.

During the creation of the artificial conditions of icing can be utilized also the indirect method of control/check or assignment of the sizes/dimensions of drops. For this preliminarily determine the dependence of the diameter of drops on pressure water $d_к = f(p_в)$ — for the swirl jets or on the relation of the flow rates of water and air $d_к = \varphi\left(\frac{\dot{G}_в}{\dot{G}_{зж}}\right)$ - for ejector injectors.

If during calibrations it was provided the blowing through of air with speeds, close to the modes/conditions of tests, and measurment was produced at a distance, corresponding to distance from collector/receptacle to test object, then it is possible to consider that this calibration makes it possible with sufficient precision/accuracy to rate/estimate during tests the size/dimension of drops.

The measurement of air humidity during bench tests can be performed by ordinary psychrometers. With flight tests under conditions of icing or on flying laboratories the humidity can be measured with the aid of on-board condensation psychrometers with liquid or semiconductor cooling [17].

However, in the majority of the cases the measurment of humidity by tests is not produced, but the necessary data are taken on the atmospheric sounding of the atmosphere in flying area.

10.2. Checking of the state of the shielded surface under conditions of icing.

By the fundamental method of recording surface condition, shielded from the icing (besides visual observation, which as far as possible must be provided in all cases), is photography. For this purpose is applied different photo- and film equipment.

Page 269.

The latter is applied usually if necessary for remote control, especially for photographing of the parts whose visual

survey/coverage is hindered/hampered or impossible. The start of motion-picture cameras can be accomplished/realized by hand or automatically through the prescribed/assigned time intervals with the aid of programmer.

During the setting up of apparatuses in flow they must be closed by fairings, moreover it is necessary to attempt to arrange objective so that for it would not fall the moisture. If for some reason this location of objective is impossible, then it should be shielded by the jets of warm air (air barrage) directed against flow (Fig. 10.4a) or used the warmed protective glass (in this case for guaranteeing the visibility it is desirable to cover the glass outside with hydrophobic lubrication). During the location of the apparatus higher than photographed surface it is possible to establish/install shielding visor, which screens the flow (see Fig. 10.4b).

Photographing the rotating parts can be used high-speed/velocity movie cameras, operating speed and time of exposure of which must be selected in dependence on the angular speed of rotation of object relative to objective.

Photographing helicopter screws/propellers in flight can also be fulfilled with the aid of the usual small/miniature movie cameras, adjusted above propeller hub, to dampers or it is direct to the root part of the blades/vanes. Are used for this purpose apparatuses they must possess sufficient mechanical strength and vibration stability.

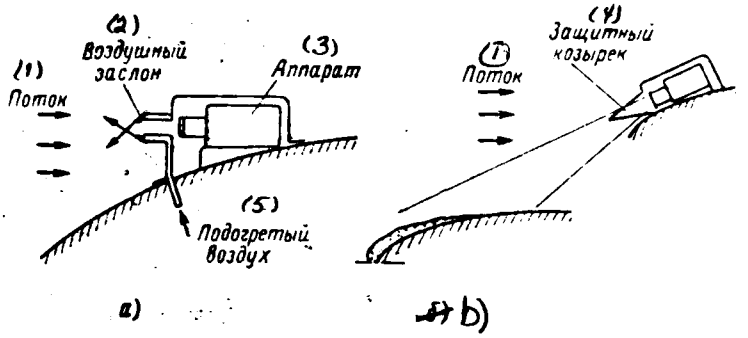

Fig. 10.4. Mounting methods of motion-picture camera against airflow: a) the use of air barrage; b) the use/application of a deflector.

Key: (1). Flow. (2). Air covering detachment. (3). Apparatus. (4). Shielding deflector. (5). Heated air.

Page 270.

Special requirements are imposed on the setting up of equipment in the inlet ducts of the engines: first, one should approach that so that it would not be the parts protruding into the flow; but if this is not performed, then protruded parts must be warmed. In the second place, it is necessary to ensure sufficiently intense illumination of the photographed parts. The cavities in which are established/installed the apparatuses and lighting headlights, must be separate/liberated from air duct by the transparent illuminators

(in this case must be accepted measures against misting of glasses) or these cavities they must be from outer side sufficiently hermetically sealed for preventing the duct of air which can attract after itself to the objective of the drop of water from the channel of engine (Fig. 10.5). For decreasing the interferences from scattering light which originates from the drops of water in air, headlight it is desirable to have available after the device or in places different with it along circumference.

For direct observation in tests of the icing of unavailable ones for the visual inspection of parts are used television equipment and different periscopes. In this respect promising can be the instruments with fiber optics. The objectives of the receivers of these installations must be arranged/located analogously with movie and photo cameras.

For the remote recording of the zone of catching and spreading of water can be used the instruments with the film gauges, based on the measurement of the electrical conductivity of ice or film of water on surface. But if it is required to measure the thickness of ice on the icing up surface, then for this it is possible to utilize the small/miniature radioisotope sensors, based on the same principle, as the radioactive signal indicator, described, for example, in work [58].

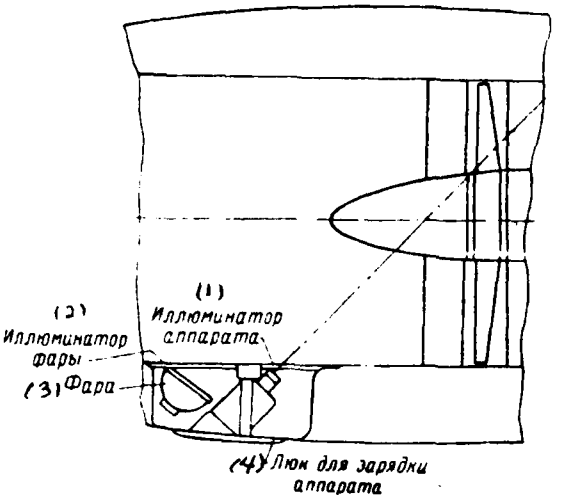

Fig. 10.5. Setting up of motion-picture camera and lighting headlight in the inlet duct of engine.

Key: (1). Illuminator of apparatus. (2). Illuminator of headlight. (3). Headlight. (4). Hatch for charging of apparatus.

Page 271.

For the one-shot measurment of the region of catching or spreading there can be used also different coatings and lubricants, washing off or changing color with wetting.

10.3. Evaluation criteria of the conditions of icing in flight.

The conditions of icing necessary for tests would be characterized sufficiently fully in the presence of the instruments which in flight would directly show the value of the fundamental parameters: water content, humidity, size/dimension of drops and temperature of air in cloudiness. But, as has already been spoken, the satisfactory methods of determining these all parameters in flight at present there is not. Therefore it is necessary to resort to some conditional criteria which do not provide the quantitative determination of the required parameters, but allow in tests themselves to totally rate/estimate conditions icing.

By simplest and available evaluation criteria of conditions, as for the definition of water content, is the speed of ice formation on control cylinder or profile/airfoil (as, for example, standard indicator GOSNII GA [58]) (Fig. 10.6).

Besides the speed of ice formation, on this profile/airfoil it is possible to observe the form of ice built-up edge and its extent over surface, which is also of interest. This evaluation is useful not only for test flights, but also for scheduled ones, since it gives the possibility to pilot approximately to judge about the intensity of ice formation and the forms of ice on all aircraft

components.

It is frequently necessary to determine the icing intensity of one or the other part of the flight vehicle. For this directly on the surface of interest there is captured the in parallel to flow measuring rule (or pin), on which periodic with the aid of motion-picture camera or visually is fixed/recorded the speed of the increase of ice.

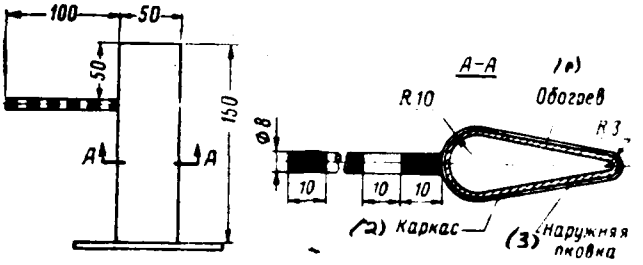

Fig. 10.6. Diagram of the standard indicator of the icing State NII ГОС НИИ ГА - Scientific Research Institute] GA.

Key: (1). Heating. (2). Framework/body. (3). External tipping.

Page 272.

During test flights it is to important rate/estimate not only icing intensity of individual parts, but also condition of icing in cloudiness (not depending on the type of flight vehicle and its flight conditions). In this connection deserves attention the criterion, proposed by O. K. Trunov [58] and representing the relative intensity of icing which does not depend on flight speed:

$$\bar{I} = \frac{60 I_{yk}}{V_0} \text{ mm/km}, \qquad (10.5)$$

where I_{yk} - a speed of ice formation on sight indicator in the mm/min (V_0 - in km/h).

It is logical that the required (final) for tests speed of ice formation does not remain constant, but it changes according to the temperature of the ambient air in accordance with the dependence of water content $w=f(t_0)$ (see Section 1.2). In this case it is necessary to bear in mind, that to fulfill tests under conditions of the icing which would be not lower than prescribed/assigned calculation, although it would be desirably, it is virtually hardly possibly, since for the searches of such conditions would be required hundreds of flights. Therefore during the assignment of final speed of ice formation it is necessary to select only probabilistic curve of the water content, the minimally necessary for the evaluation of system (see Chapter I), with which the volume of tests under conditions of icing would be acceptable. O. K. Trunov, for example, proposes for this to be restricted to 90-95o/o quantile, what is completely permissible (that corresponding to 90o/o of quantile of the speed of ice formation is given in Table 10.2).

Nevertheless, if one considers that the tests must be carried out at different temperatures of surrounding air, then for searches even of conditions indicated above is required the also very considerable space of flight time. Therefore in many instances, apparently, it is possible to allow an even lower quantile of water

content, on the basis of the fact that in proportion to decrease in the quantile of the amount of water content is decreased entire to a lesser degree (for example, upon transfer from 99o/o of quantile to 90o/o water content is decreased on the average approximately/exemplarily by 0.3 g/m^3, and from 90o/o to 60o/o - in all to 0.2 g/m^3), probability whereas of the rendezvous of latter/last conditions considerably grows/rises.

Table 10.2.

(1) Температура окружающего воздуха t_0 °С	(2) Относительная интенсивность льдообразования на указателе $\bar{I}$ мм/км	(3) Интенсивность льдообразования на указателе (V_0 = 500 км/час) $I^1_{y\kappa}$ мм/мин*
—5	0,7	5,9
—10	0,4	3,4
—15	0,25	2,2
—20	0,15	1,3

Key: (1). Temperature of surrounding air t_0 °C. (2). Relative intensity of ice formation on indicator $\bar{I}$ mm/km. (3). Intensity of ice formation on indicator (V_0=500 km/h) $I^1_{y\kappa}$ mm/min [1].

FOOTNOTE [1]. Intensity is designed for $\rho_л = 800$ kg/m³ and $\varepsilon = 0,8$.

Page 273.

However, need in endurance tests in natural icing generally is eliminated, if deicers are preliminarily treated in artificial conditions when without difficulties can be established/installed the required calculated value of water content. In this case, as has already been mentioned above, natural condition test it is possible to restrict by a minimum number of flights which can be fulfilled at temperatures, corresponding to the greatest probability of icing.

From other criteria should be noted relative evaluation criteria

of the conditions of icing in flight according to heat removal, proposed by A. M. Men'shchikov. Its sense consists in the fact that for the warmed profile/airfoil (or cylinder) they are determined experimentally or calculated of the conditions under which heat removal with heating surface maximum. Criterion $\bar{K}_{об.м}$ corresponding to these conditions is accepted for 1 (or 100o/o). Then all actual conditions will be expressed in the portions of unity. According to the scale proposed by A. M. Men'shchikov to the weak conditions of icing corresponds $\bar{K}_{об.м}$ to 0.45, to the averages from 0.45 to 0.7, the strong from 0.7 to 0.85 and very strong more than 0.85. Criterion $\bar{K}_{об.м}$ can exceed unity under conditions more severe than calculation.

Chapter XI.

Testings under conditions of artificial icing [1].

FOOTNOTE [1]. It is written by B. A. Stroganov, R. Kh. Tenishev, V. N. Leont'yev. ENDFOOTNOTE.

The creation of the conditions of artificial icing consists in artificial formation/education or spreading in air flow of the water drops which must have the same sizes/dimensions and shape and the same temperature as drop under natural conditions, but a quantity of water in flow must correspond to natural conditions.

11.1. Methods of creation of conditions of artificial icing.

Creation of the conditions of artificial icing in air flow by several possible methods:

a) by direct condensation of vapor;

b) with the aid of the spattering of water due to the

centrifugal forces;

c) with the aid of injectors (vortex/eddy or ejector).

Condensation of vapor gives drops in practice identical according to sizes/dimensions to natural ones, however, since the creation of the necessary water content requires a large quantity of vapor and, furthermore, its condensation produces preheating air flow, which in a number of cases is extremely undesirable, this method in "pure" form did not find use. In some installations, which will be discussed lower, vapor is utilized as the ejection gas and its condensation in this case it gives positive effect, forming additionally the drops of small/fine diameters.

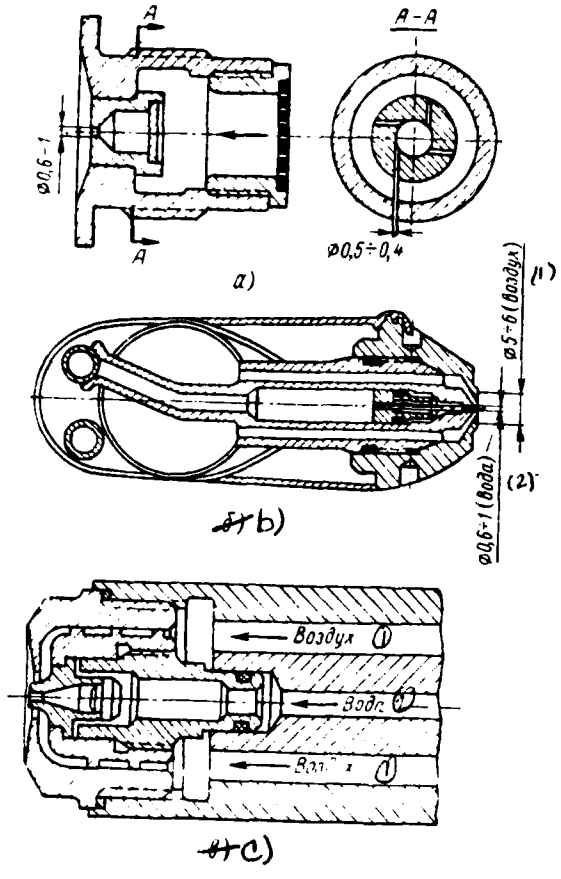

Fig. 11.1. Water-spattering injectors: a) the vortex/eddy type; b and c) ejector type.

Key: (1). air. (2). water.

Page 275.

Splashing of water in the centrifugal atomizers is

accomplished/realized by its supply to the center of the rotor (disk, cone, etc.), which has radial channels (drilling). During the rotation of rotor the water by centrifugal forces is thrown out from channels. This method requires the guarantee high speeds of rotation of sprayers. Installations for pulverization/atomization are bulky. However, valuable it is that the drops are very uniform in size/dimension; therefore this method sometimes finds a use in laboratory installations.

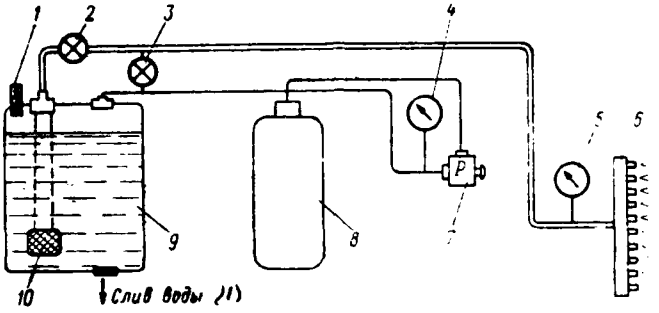

Fig. 11.2. The schematic diagram of the water-spattering system for the swirl jets, which effect with the aid of the compressed air: 1 - reduction valve; 2 - tap/crane; 3 - tap/crane; 4 - air pressure gage; 5 - water manometer; 6 - collector/receptacle with the injectors; 7 - air reducer; 8 - tank/balloon for the air; 9 - water tank; 10 - filter.

Key: (1). Drain of water.

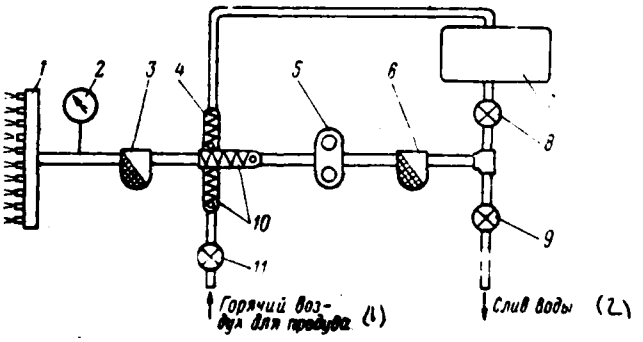

Fig. 11.3. Schematic diagram of water-spattering system for vortex

injectors with hydraulic pump:

1 - collector/receptacle with injectors; 2 - manometer; 3 - high-pressure filter; 4 - reduction valve; 5 - pump with drive; 6 - low-pressure filter; 7 - tank; 8 - tap/crane; 9 - tap/crane; 10 - check valves; 11 - tap/crane of purging.

Key: (1). Hot air for blowing through. (2). Drain of water.

Page 276.

Most widely during the creation of the conditions of artificial icing are applied different injectors, which by its construction/design and according to operating principle it is possible to divide into two fundamental forms: vortex/eddy ones [1] and ejector [90], [92].

FOOTNOTE [1]. The swirl jets sometimes also call centrifugal, but we will use latter/last term only with respect to the sprayers described above. ENDFOOTNOTE.

In the swirl jets the water supplied under pressure, passing through tangential openings/apertures or along spiral channels, untwists and is thrown out outside, creating the flame of

atomization. The example of the construction/design of vortex/eddy injector is represented in Fig. 11.1a. In order to avoid the freezing of water in injector, on them usually is established/installed electrical heating or is utilized the heated water. Fig. 11.2 gives the schematic diagram of water-pulverization system for the swirl jets. In it for water supply to injectors is applied the pressure of the compressed air. Is possible water supply, also, with the aid of pump (Fig. 11.3), but the compressed air is convenient fact that it makes it possible to easily provide a change of the pressure in entire operating range (usually 0.3-3 MN/m^2).

In ejector injectors (see Fig. 11.1b, 11.1c) atomization is produced due to the fragmentation of water by the flow of inducing air or vapor. The diagram of water-atomization for pneumo-ejector injectors (Fig. 11.4) is obtained considerably more complicated, since, besides the lines of water supply, are necessary other lines of the supply of the ejection gas, and also the sufficiently powerful/thick source of the compressed air or vapor.

Selection of a quantity of injectors.

The necessary quantity of injectors in collector/receptacle is determined from the condition of the uniform atomization of water all over area of collector/receptacle or subject of object. With the

atomization of the water through the injector the form of atomization is at first close to cone, and then is converted into shapeless cloud. Transition/transfer from cone to cloud occurs at a distance of approximately 30-50 cm.

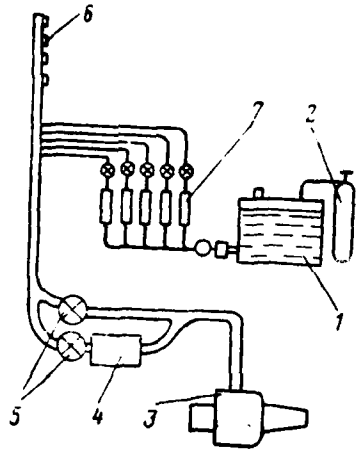

Fig. 11.4. The schematic diagram of the water-spattering system for the pneumo-ejector injectors: 1 - tank with the water; 2 - the compressed air tank; 3 - supercharger of the ejector air; 4 - heat exchanger; 5 - taps/cranes; 6 - collector/receptacle of the water sprayer; 7 - flow meters.

Page 277.

In order to ensure the uniformity of the field of atomization, the distance between injectors in collector/receptacle must be selected by such so that despite all modes/conditions of tests would be provided overlapping or at least contact of the spray cones of adjacent injectors.

Value of spray cone as the remaining parameters of the atomization: the flow rate of the water through injector and average size of the obtained drops, in many respects they depend on quality and individual characteristics of the manufacture of injectors and during layout they must be taken into consideration by preliminary calibration. Fig. 11.5 as an example depicts the dependence of the angle of atomization on the pressure of water for the swirl jets of average size. As is evident, the angle of atomization depends from pressure in the range to $3 MN/м^2$ (about 30 atm.), and further it is virtually equal to 90°.

Another condition which they must satisfy the selected injectors, is the guarantee of required flow rate $G_ф$ of water. For this it is necessary that each injector would provide the flow rate (it is not less)

Key: (1). kg/s.

$$q_i = \frac{G_ф}{n_ф} \text{ кг/сек}, \quad (11.1)$$

where $G_ф$ - required flow rate in kg/s, A conforming to ω_{max} according to formula (10.4);

$n_ф$ - quantity of injectors.

The flow rate of the water through injector g_i depends in

essence on the feed pressure of water and diameter of outlet and is determined by the calibration of injectors. Such dependences for several injectors are given in Fig. 11.6a.

Besides required flow rate, the selected injectors must provide the necessary atomization of drops according to sizes/dimensions.

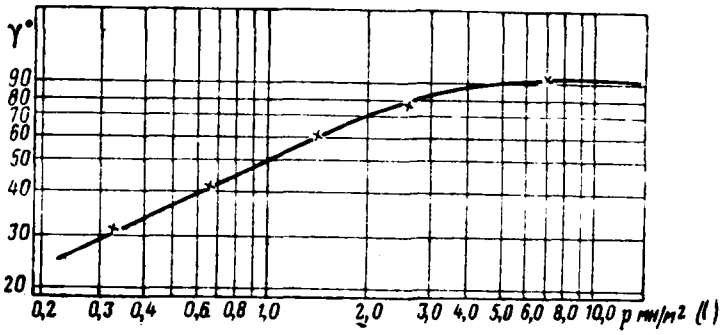

Fig. 11.5. Dependence of the angle of the spray cone of vortex/eddy injector on pressure.

Key: (1). MN/m².

Page 278.

For the swirl jets the diameter of drops depends also on the diameter of outlet, on the pressure of the supplied water. So (see Fig. 11.6b), with an increase in the pressure to 0.3 from 3 MN/m² the diameter of drops varies from 170-200 to 40-80 μ. True, at a pressure of more than 7 MN/m² the size/dimension of drops virtually remains constant and is not changed with an increase in the pressure.

For ejector injectors the size/dimension of drops is determined in essence by the ratio of the weight flow rate of water to the flow rate of air (Fig. 11.7).

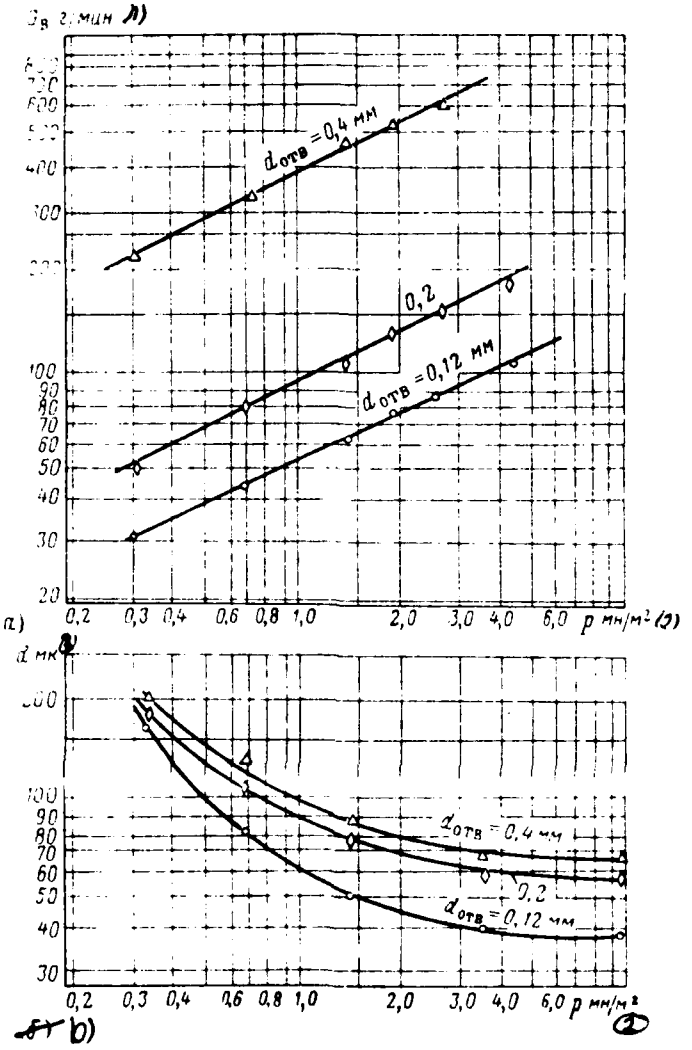

Fig. 11.6. Fundamental characteristics of the swirl jets: a) the minute flow rate of water $G_в$ in g/min; b) the size/dimension of drops $d_к$ in μ.

Key: (1). g/min. (2). мн/м². (3). μ.

Page 279.

Thus, in this case is opened/disclosed great possibility for variation by the flow rates of water and air for guaranteeing the required diameter of drops. In this case for guaranteeing the atomization there is no need for applying the high pressures of water and air, but it is possible to be bridged with pressures 0.1-0.3 MN/m² both for water and for air.

The comparison of Figs. 11.6 and 11.7 at first glance shows that the use/application of vortex injectors cannot ensure atomization necessary for a complete analogy with natural conditions (20-30 μ); however, this not entirely so. The data represented in Fig. 11.6 are acquired during the calibrations of the injectors, not blown out/blown off by the air; whereas during the incidence/impingement of drops into air flow they undergo supplementary fragmentation [116].

Thus, comparing between themselves these two forms of injectors, it is possible to arrive at the conclusion that the first provide great possibility in a change in the size/dimension of drops (due to the ratio of the flow rate of water to air), but they require the more complicated feed system of water and air, the second are more

limited on the possibility of guaranteeing the required sizes/dimensions of drops, but make it possible the more simple to ensure atomization water in air flow.

11.2. Determination of temperature and rate of evaporation of the drops of water in air flow.

With the existing methods and the ways of the checking of the conditions of icing to determine the temperature of drop in air flow by direct measurements it is not possible. Therefore it is determined by calculation on the base of known meteorological conditions and temperatures of the water before pulverization [110].

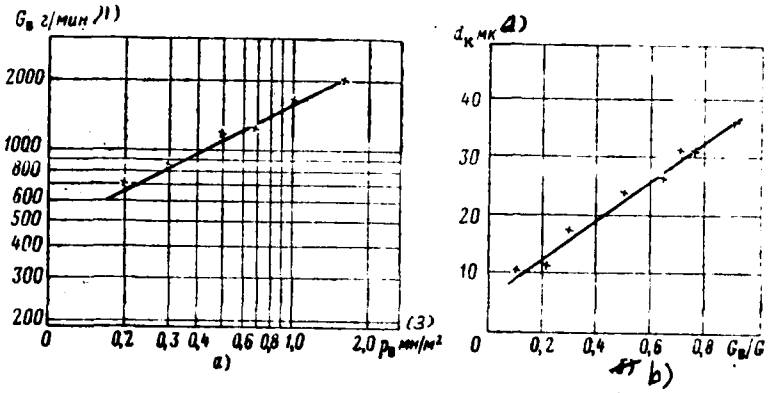

Fig. 11.7. Fundamental characteristics of the pneumo-ejector injector: a) the minute flow rate of water $G_в$ in g/min; b) the size/dimension of drops $d_к$ in μ.

Key: (1). g/min. (2). μ. (3). MN/m^2.

Page 280.

Pulverization water in the flow of cold (0 - -30°C) air usually produce at relatively high (to 50°C) temperature of water. Falling into flow, drop begins to be cooled, but so that it would achieve the necessary temperature, usually to the equal or close temperature of air, is necessary for a while. Cooling drop in flow occurs, on one hand, due to convective heat emission from drop into flow, and on the other hand, due to the evaporation of water. This cooling continues until the temperature of drop becomes somewhat less than the temperature of surrounding air, and then convection heat transfer will go from flow to drop and it will balance the heat losses due to evaporation. As a result will be established/installed certain equilibrium (somewhat different from the temperature of surrounding air) temperature.

The density of the flow of heat emission due to convection at the low relative speeds between air and drop can be represented the equation

$$q_к = 4\pi r^2 \lambda \frac{\partial t}{\partial r} \quad \text{W/m}^2 \qquad (11.2)$$

where r - a radial distance from the center of drop m;

λ - thermal conductivity of air in W/(m•deg).

Integration of equation for a sphere with a radius of $r_к$ gives

$$Q_к = 4\pi r_к \lambda (t_к - t_0) \text{ В.} \qquad (11.3)$$

The heat emission or drop due to evaporation is equal (see Chapter V)

$$Q_{βк} = q_β L_и F_к, \qquad (11.4)$$

where the density of the heat flow, spent on evaporation, is defined as

$$q_β = 0.622 \frac{\lambda L_и}{c_p r_к} \cdot \frac{e_к - e_0}{p_0}, \qquad (11.5)$$

where $e_к$ - an elasticity of vapor at temperature of the surface of drop.

Thus, cooling drop in air flow is determined by relationship/ratio (with $c_p = 1000$ J/kg•deg, $L_и$=25x10^5 J/kg)

$$\frac{4}{3}\pi r_к^3 \rho_в c_в \frac{dt_к}{d\tau} = 4\pi r_к \left[\lambda (t_к - t_0) \quad 1550\lambda \frac{e_к}{p_0} \frac{e_0}{p_0}\right],$$

where $\rho_в$ - water density in kg/m^3;

$c_в$ - heat capacity of water in J/kg·deg.

Page 281.

The time $\Delta\tau$, necessary so that the temperature of drop would fall from $t_{к0}$ to $t_{к1}$, it is equal

$$\Delta\tau = \frac{r_к^2 Q_в c_в}{3\lambda} \int_{t_{к0}}^{t_{к1}} \frac{dt_к}{(t_к - t_0) + 1550\left(\frac{e_к - e_0}{p_0}\right)}.$$

After integration and conversions we obtain

$$\Delta\tau = -\frac{r_к^2 Q_в c_в}{3X\lambda} \lg \frac{t_{к1} - t_0}{t_{к0} - t_0}, \qquad (11.6)$$

where X - the coefficient, determined by formula (5.39).

The equilibrium temperature of drop $t_к^*$ can be determined from the condition of equality heat fluxes (convection and evaporation)

$$-4\pi r_к \lambda (t_к^* - t_0) = 4\pi r_к \frac{0{,}622 \cdot L_н \lambda}{c_p} \cdot \frac{e_к - e_0}{p_0}, \qquad (11.7)$$

i.e. by the same method, as the equilibrium temperature of moist surface $t_{1\,вл}^*$ (see Section 5.5).

The time τ, for which the drop will be cooled from initial temperature $t_{к0}$ to equilibrium temperature $t_к^*$, is determined by successive approximations, selecting $t_{кi}$ and $t_{к(i+1)}$ sufficiently close, so that the coefficient X with change temperature to $t_{кi}$ from $t_{к(i+1)}$ virtually would not vary [104].

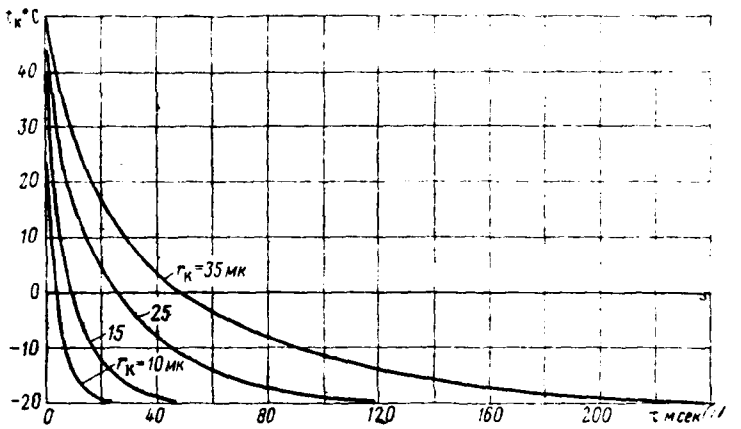

Fig. 11.8. Dependence of the time of cooling the drop of water on its size/dimension (temperature of surrounding air of -20°C, initial temperature of water of 50°C).

Key: (1). ms.

Page 282.

Method presented above makes it possible to rate/estimate the time of cooling drop in dependence on the temperature of air flow and size/dimension of drop. These data are necessary in order to correctly select distance from injectors to the experience/tested object, since as the transit time of this distance drop must be cooled to the equilibrium temperature or in any case to temperature, it is sufficient close to the temperature of air flow.

AD-A090 981 FOREIGN TECHNOLOGY DIV WRIGHT-PATTERSON AFB OH F/G 13/1
DE-ICING SYSTEMS OF FLIGHT VEHICLES. BASES OF DESIGN METHODS FO--ETC(U)
SEP 79 R K TENISHEV, B A STROGANOV, V S SAVIN
UNCLASSIFIED FTD-ID(RS)T-1163-79-PT-2 NL

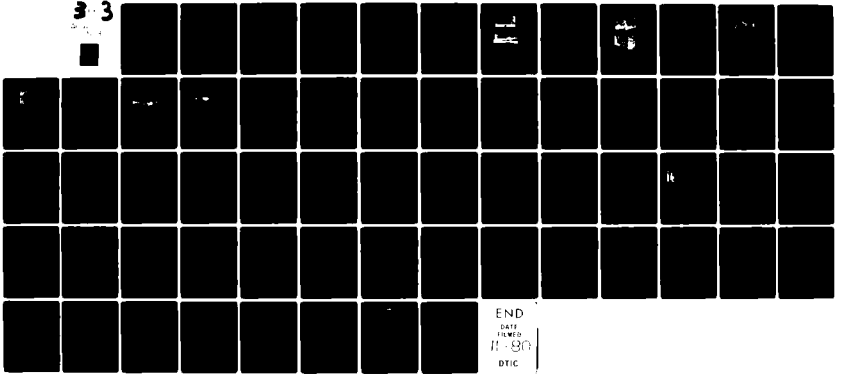

END
DATE FILMED
11-80
DTIC

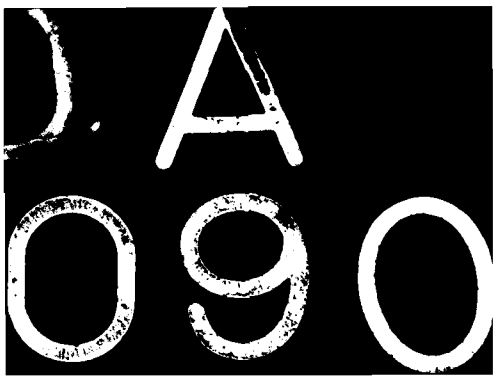
A
090

Fig. 11.8 depicts the graph/diagram of the dependence of temperature on time for the drops of different diameter at temperature of air flow of -20°C and initial temperature of water of 50°C, from which it is evident, for example, that the cooling time from 50 to -20°C will compose for the drop with a diameter of 20 μ of approximately 20 ms, and for the drop with a diameter of 50 μ of approximately 120 ms.

At velocity of incident flow 100 m/s the distance from the collector/receptacle of water sprayer to the experience/tested object must be not less than 2 m for drops 20 μ and 12 m for drops 50 μ.

One should consider that in view of neglect of that forced of the heat emissions of drop, which, it is doubtless, will occur in the beginning of motion, given calculation gives the high time of cooling drops and, consequently, also a somewhat high distance.

11.3. Conditions of the similarity of tests on models and nature.

With conducting tests in models and mock-ups whose size/dimension differs from the sizes/dimensions of full-scale samples/specimens, the results of these tests, other conditions being

equal, it is doubtless, they will differ from full-scale ones. In order to ensure conformity between tests on model and nature or to make possible to lead via conversion the results of model tests to nature, it is necessary to derive the criteria of similarity of the phenomena and to find the methods of their use [152]. In chapter IV was shown that such most important parameters of icing as the size/dimension of the zone of catching, coefficient of capture/grip and its surface distribution are determined by two parameters Re_0 and ψ. Let us present led in chapter IV equation (4.10) in the form of overall functional dependence (for one-dimensional flow)

$$\frac{d^2x_к}{d\tau^2} = f\left(c_x,\ \mathrm{Re},\ \psi,\ \mathrm{Re}_0,\ v_x,\ \frac{dx_к}{d\tau}\right).$$

Coefficient c_x is the function of number Re: $c_x = c_x(\mathrm{Re})$, which in turn, is determined depending on number Re_0; v_x and $\frac{dx}{d\tau}$.

Page 283.

The relative speed of flow v_x is in this case the function of coordinate x and aerodynamic airstream data. During the guarantee of aerodynamic similarity of flow, what is an indispensable condition of all tasks, connected with the studies of the flow around models, v_x will be identical both for the model and for nature.

As is evident, by the independent parameters, which are

determining the solution of the differential equation (if we consider that the similarity of airspeeds v_x is provided) are numbers Re_0 and ψ.

Led earlier in chapter of IV dependence of the fundamental characteristics of the catching of the drops: the interception coefficient and zone of catching on parameters Re_0 and ψ show their equivalence for a character catching.

Interception coefficient and size of the zone of catching depend substantially both on Re_0 and on ψ.

Thus, during model tests for retaining/preserving/maintaining the similarity it is necessary to observe equality numbers Re_0 and ψ for model and nature, i.e., if model will be two times less than nature, then for retaining/preserving/maintaining constancy ψ it is necessary to have drops two times less than during the tests of nature, in this case for retaining/preserving/maintaining the constancy Re_0 it is necessary two times to increase the speed.

These conditions are not always feasible; therefore it is expedient to carry out tests in certain range Re_0 and ψ, giving to them several values, and then to use extrapolation. This will

simplify conducting tests and will make it possible to obtain necessary for bringing to nature data.

11.4. Fundamental types of settings up (stands) for an artificial icing.

All installations (stands) for the creation of artificial icing can be in terms of design features and endeavor divided into the following groups or the types:

- flying laboratories,

- helicopter stands,

- stands for engines,

- refrigerated-wind tunnels,

- spiral stands,

- laboratory installations.

Most widely in practice are utilized installations of the first three types.

Flying laboratories.

The flying laboratories are very convenient for the investigations of icing and protection from it, since with their aid simply is solved a question about the guarantee of the necessary temperatures, heights/altitudes and flight speeds. Such flying laboratories are equipped on the basis of different aircraft and sufficiently widely they are applied both in our country and abroad.

Page 284.

In particular, they are utilized by firms "Napier", "Bristol", "Viking" in England; "Boeing" in the USA; "Turboneka" in France [86], [91], [93], [126].

as illustration in more detail let us pause at the investigations of firm "Napier" on aircraft "Lincoln MK" ($V_{крейс} = 450$ km/h, $H_{крейс} = 6700$ m, $H_{max} = 8500$ m). On the fuselage of this aircraft (Fig. 11.9) was established/installed the farm/truss with 49 pneumo-ejector injectors. At a distance of 1.8 m after it was arranged/located the tested section of wing or tail assembly (size/dimension of section comprised to 2.7 m on height/altitude and

2.1 m along chord). Fastening section was made rotary, so that during tests was provided a change in the angle of attack from -1.5 to +15.5°. Was provided for the possibility of the heating of sections both electricity and by air (the available power of heaters in section or on electric furnace for heating of air was equal to 80 kW).

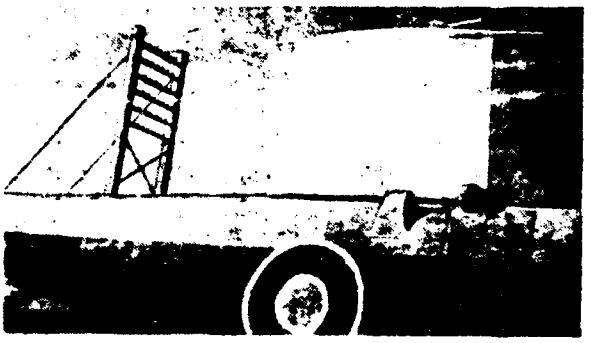

Fig. 11.9. Flying laboratory on aircraft "Lincoln MK" for the investigations of questions of icing.

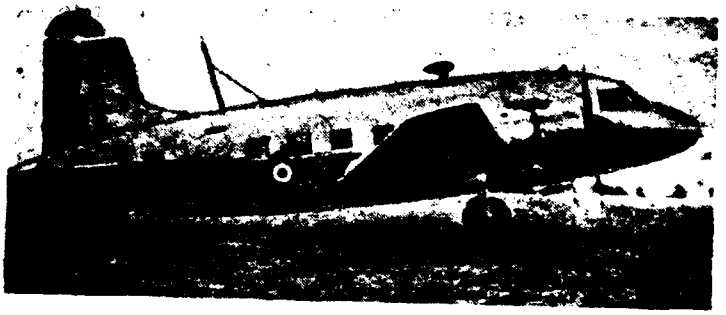

Fig. 11.10. Flying laboratory on aircraft "Viking".

Page 285.

Air for heating and atomization was taken from special supercharger. Sections were prepared by thermocouples and were drained/vented on span and along chord. This made it possible to establish/install the picture of icing under the varied conditions of flight, zone of

catching and spreading, to determine the character of the distribution of pressure according to the surface of section, to refine heat-transfer coefficients, required energy consumption, etc.

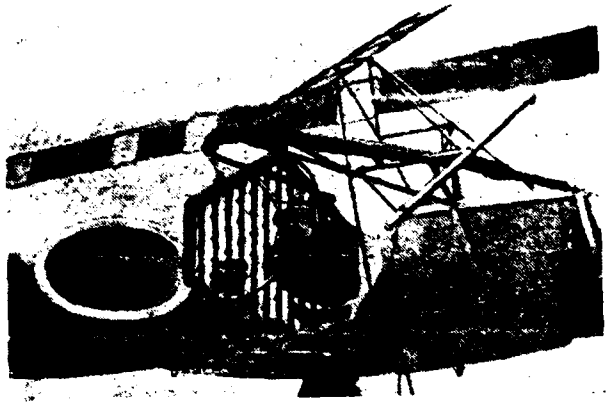

Fig. 11.11. Water-spattering installations on aircraft "comet" for the tests of engine "Avon R. A. 29".

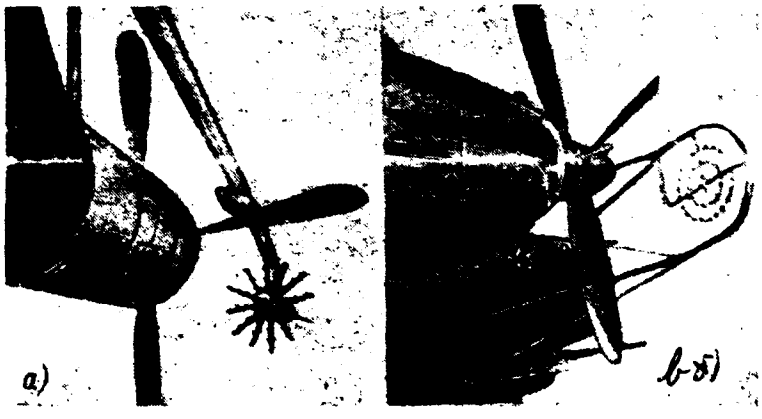

Fig. 11.12. Water-spattering installations for tests of TVD: a) engine "Nyad"; b) engine "Eland".

Page 286.

Special attention was given to the guarantee of water content and

fineness of atomization. For this purpose the sprayer was specially calibrated, comprised the graphs of the flow rates of water and sizes/dimensions of drops from the pressure of inducing air. On these graphs were established/installed the modes/conditions of the tests, which then were more precisely formulated and were checked in tests. Control/check of the size/dimension of drops was accomplished/realized via the taking of samples to microscope slide and their photography under microscope. Control/check of water content was accomplished/realized according to the real flow rate of water.

The especially widely flying laboratories are utilized for checking the protection from the icing of air intakes and intake parts of the power plants. As a result of their complex layout the theoretical calculation of the zones of the catching of ice and generally the development/detection of the surfaces, subjected to icing, is very hindered/hampered and all these questions are solved usually during tests under conditions of artificial icing.

Investigations on flying laboratories make it possible previously in mock-ups to master the construction/design of deicers and to select optimum version for its introduction into production. This practice makes it possible to avoid changes in the construction/design on real object and to accelerate its starting/launching into a series. Fig. 11.10, 11.11, 11.12, 11.13 show some flying laboratories, intended for the adjustment of de-icing systems.

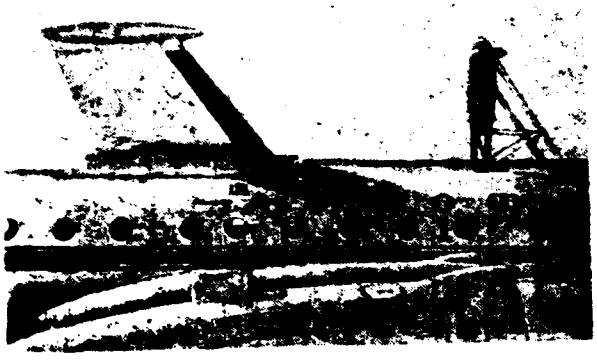

Fig. 11.13. Flying laboratory on the aircraft of Il-18 for the study of the icing of the full-scale sections of wing, tail assembly and other parts.

Page 287.

Helicopter stands.

For the tests of de-icing systems and study of the process of the icing of the carrying and tail rotors of helicopters under conditions of artificial icing are applied the setups or the helicopter stands, construction/design and technical characteristics of which they can be very different [141], [143], [144].

To some of them the investigation is produced only by the race of engine on the earth/ground, on others is provided the possibility

of the flight/span of helicopter or its hovering in the zone of artificial icing. Majority of helicopter stands functions only in winter time at natural minus temperatures, but in certain cases is provided for the possibility of cooling air in the location where is located helicopter (refrigerated-wind hangars, etc.).

In the majority of the cases such stands are the complicated engineering installations of very imposing sizes/dimensions. Fig. 11.14 shows the appearance of the helicopter stand of the national-research center in Canada. At farm/truss (in long approximately 20 m) is established/installed ejector type 161 injector (ejection of water is accomplished/realized by vapor). On steel mast the farm/truss is built up to the height/altitude of 15-20 m and with the atomization of water is created the clouds resulting from industry by the size/dimension from several ten to hundreds of meters, in which it is accomplished/realized hovering or flights/spans of helicopter.

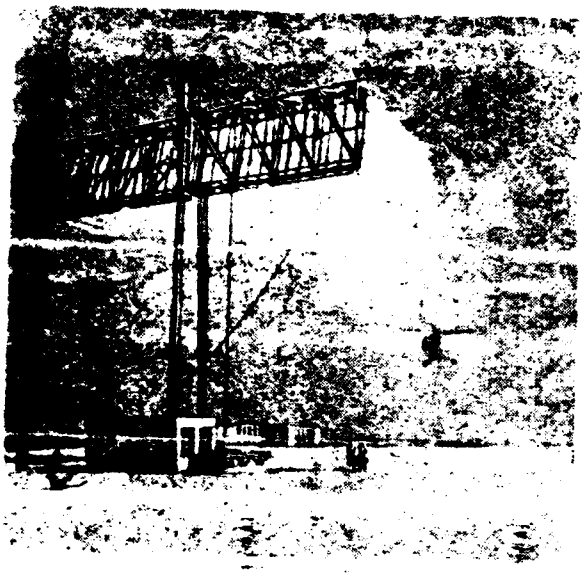

Fig. 11.14. Helicopter stand of the national research center of Canada.

Page 288.

Fig. 11.15 shows Soviet stand for the investigation of the icing of the heavy helicopters.

However, in a number of cases can be used sufficiently simple installations. As an example of this installation can serve stand for the icing of rotors, average/mean and light helicopters, shown in Fig. 11.16.

It consists of two struts (masts), stretched by two braces from each side. The water-spattering device/equipment is made from the tube, suspended/hung from two cables and butted from the series/row of sections.

Water-pressure system is established/installed in the movable van which can be utilized also for other installations.

Helicopters test while hovering, moreover for increasing the safety of experiment they must be moored. A similar stand successfully was applied, for example, for the investigation of the icing of such helicopters as Mi-4, Mi-1, Ka-15.

During the studies of the icing of helicopter screws/propellers under artificial conditions should be focused attention on the fact that to ensure uniform water content in clouds resulting from industry is virtually very difficult, since as a result of evaporation into the surrounding cloud dry air water content on the periphery of cloud is always less than in its central part.

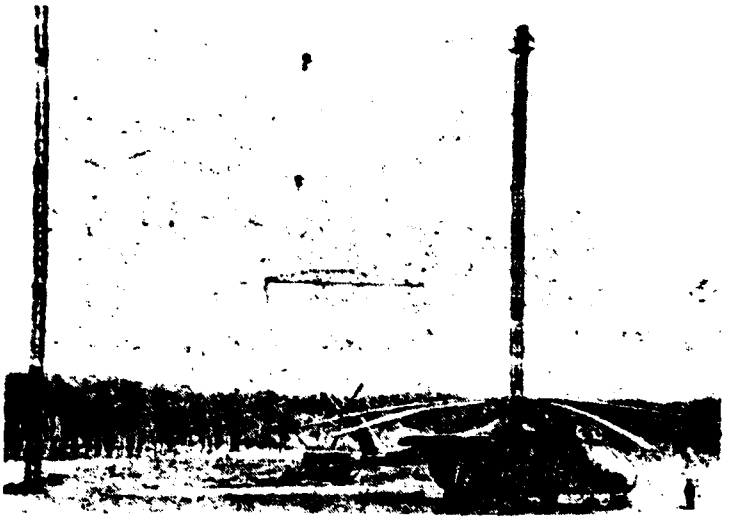

Fig. 11.15. Stand for the investigation of the icing of the heavy helicopters of the type of Mi-6, etc.

Page 289.

For the described above stand of the simplified construction/design it is necessary to consider one additional special feature/peculiarity. The speed of the sucked through screw/propeller air varies along the length of blade/vane from zero to maximum value on an end radius. If in this case injectors along the tube of stand are arranged/located with identical space, the water content and, consequently, also intensity ices formation on blade/vane will be respectively decreased from its root toward the end, curve 1 in Fig. 11.17.

Arranging/locating injectors with the changing according to the specific law space, it is possible to to a considerable extent decrease the described phenomenon (curve 2 in Fig. 11.17).

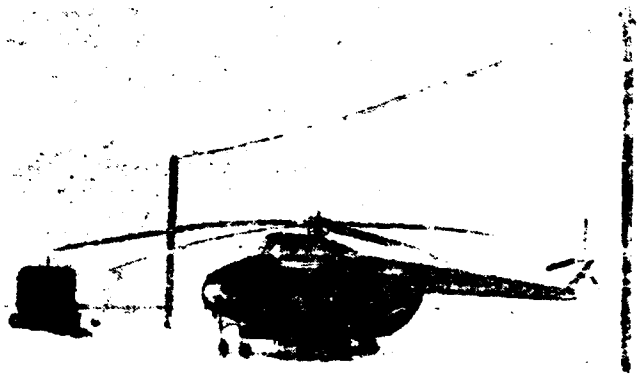

Fig. 11.16. Simplified version of helicopter stand for the investigation of the icing of average/mean and light helicopters.

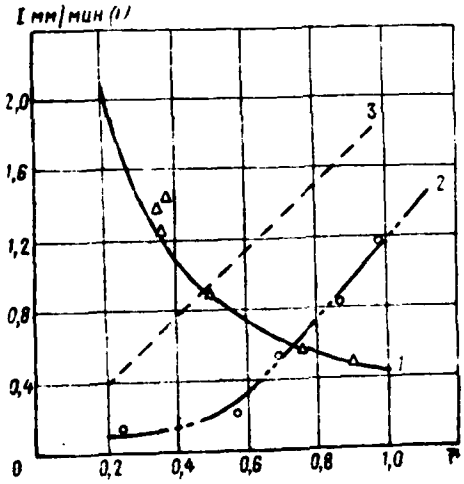

Fig. 11.17. Intensity of ice formation along the length of blade/vane with icing on stand: 1 - with even pitch of injectors; 2 - with injector grid according to specific law; 3 - with hovering under natural conditions of icing of high above earth/ground.

Key: (1). mm/min.

Page 290.

However, in any event essential effect have wind gusts, reflected from the earth/ground the airflow, etc., thanks to which of the condition of icing differ somewhat from natural ones. In particular this affects the root sections where air-intake velocity is low; therefore the significant part of the drops is related and icing intensity is understated (curve 2 in Fig. 11.17). "Therefore tests are produced usually as follows: helicopter for a certain period of time is subjected to icing on stand without the start of de-icing system. Then is produced its landing and measurment of thickness of ice in different cross sections throughout a radius of blade/vane. According to this thickness of ice is produced the calculation of the intensity of ice formation and local water content, which is usually different in a radius. After this are fulfilled already "working" modes/conditions in :accordance with study program. (The reference performance regarding the thickness of ice, analogous described above, they are produced periodically during entire time of tests).

Stands for engines.

Are known several types of installations for the investigation of icing and effectiveness of the de-icing system of engines with artificial icing, for example the open stand, equipped by the special water-spattering system (Fig. 11.18); the stand, equipped with cooling installation (Fig. 11.19); the thermobaric chamber, in which the tests are conducted through stagnation parameters (M=0) (Fig. 11.20); the thermobaric chamber, in which the tests are conducted under conditions of the free flow, with the blowout of power plant (Fig. 11.21).

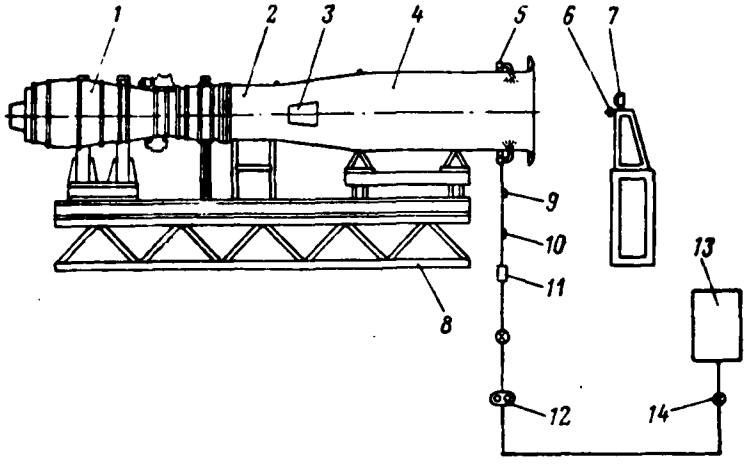

Fig. 11.18. The open stand, equipped by the water-spattering system: 1 - engine; 2 - the input device; 3 - inspection window; 4 - tube; 5 - collector/receptacle with the injectors; 6 - camera; 7 - projector; 8 - machine tool; 9 - thermometer for water at the entry into the collector/receptacle; 10 - manometer for water at the entry into the collector/receptacle; 11 - filter mesh; 12 - high-pressure pump; 13 - water tank; 14 - tap/crane.

Page 290a.

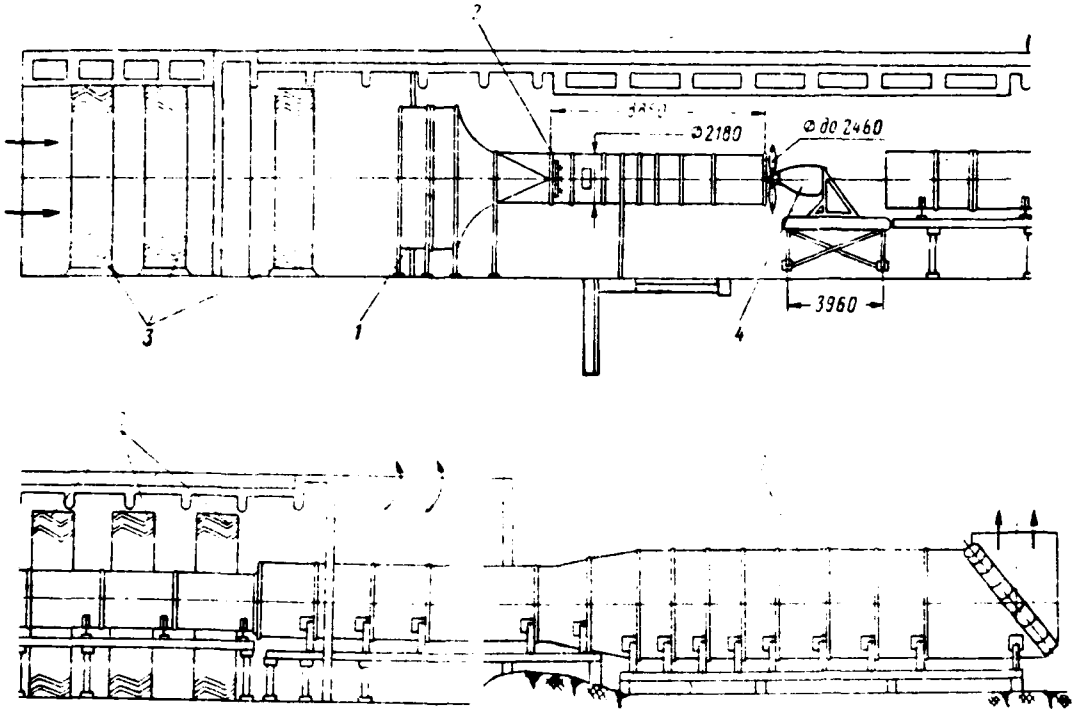

Fig. 11.19. Stand with cooling installation for study of icing of power plants: 1 - cooler; 2 - water sprayer; 3 - mufflers; 4 - power plant.

Page 291.

The advantage of the open stand is its simplicity and possibility of rapid installation and conducting entire cycle of

tests [78]. As this stand usually is utilized the stand, used for the ground tests of engines which for these purposes is additionally equipped by system of water-pulverization/water-atomization and by corresponding monitoring and measuring equipment. A shortcoming in this stand is the possibility of conducting the tests of the effectiveness of POS of engine only under winter conditions at negative free-air temperatures.

This shortcoming is removed in the case of the tests of engine in thermobaric chamber. Air into thermobaric chamber at a necessary minus temperature is supplied from compressor station.

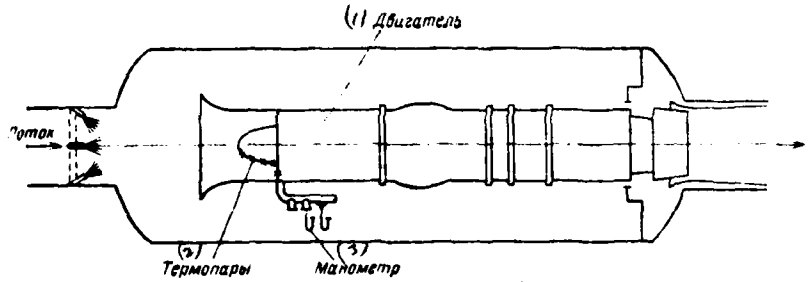

Fig. 11.20. Thermobaric chamber for the tests of engine on parameters of braking.

Key: (1). Engine. (2). Thermocouples. (3). Manometer.

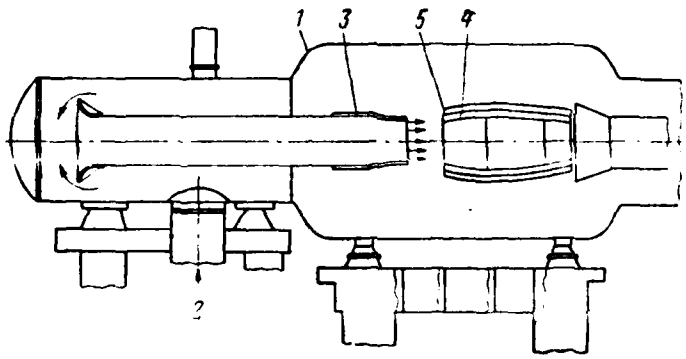

Fig. 11.21. Thermobaric chamber in which power plant is blown out/blown off by flow: 1 - chamber/camera; 2 - supply of cold air; 3 - nozzle with heating; 4 - engine; 5 - engine nacelle.

Cooling air usually is produced in the special cooling turbine, then in order to exclude the supply of the saturated by moisture air into the thermobaric chamber (which is with difficulty considered quantitatively), is produced its drying usually in special silica gel devices/equipment. Besides the possibility of conducting the tests at any time of year, the essential advantage of the thermobaric chamber over the open stand is also the possibility of conducting the tests under altitude-speed conditions. Conducting such tests makes it possible to produce the evaluation of the effectiveness of POS of engine under operating conditions according to height/altitude and flight speed.

The third type of installation - thermobaric chamber, in which the tests are conducted under conditions of the free flow with blow-through of the power plant, allows, besides the effectiveness of POS of engine, to test also the effectiveness of POS of aircraft air intake.

Checking the effectiveness of POS of engine is produced in the following trimmed/steady-state modes/conditions: idling, about 0.6 nominal ones, nominal and maximum.

Testing it is expedient to carry out at three values of temperature of air at the inlet into engine in the

prescribed/assigned temperature range of surrounding air at the appropriate standard values of water content.

The required flow rate of water is determined from formulas (10.4), moreover in certain cases in flow itself can be certain initial water content $\omega_{нач}$, taking into account which through injectors is supplied the quantity of water, equal to

$$G_{ф} = \omega_{ф} \cdot W, \qquad (11.8)$$

where

$$\omega_{ф} = \omega - \omega_{нач}.$$

Testing it is expedient to carry out with the imitation of all available on engine devices for air bleed.

Engine must be prepared by thermocouples for measuring the temperature of the walls of the elements/cells of inlet duct and fairing about the engine nacelle.

Under conditions of icing the engine with connected POS of inlet parts and engine nacelle is maintained/withstood in all modes/conditions, except maximum, not less than 10 min, and under maximum conditions - the permissible for this engine time (usually not more than 5 min). In this case must be carried out continuous

visual observation of ice formation on the elements/cells of inlet duct with its periodic photography and of the parameters of engine, which characterize began icing (reduction/descent in the thrust, increase in the temperature of the gas before the turbine, incidence/drop in the efficiency/cost-effectiveness and others).

Page 293.

In the presence of dangerous icing the system of atomization is turned off/disconnected and engine immediately stops.

It is necessary to focus attention on some special features/peculiarities of the tests of POS of power plants in comparison with testing of other parts which consist of the following.

1. In connection with presence of rotating parts of testing they must be carried out so that would be provided permanent visual control/check after ices formation or knowingly ice formation was insignificant according to sizes/dimensions, i.e., tests were limited on time, which more narrowly was discussed earlier.

2. As a result of difficult survey/coverage after engine components, that undergo icing, it is necessary to usually utilize

special remote devices, which check beginnings and process of icing on elements/cells of inlet duct of engine, about which it was mentioned in preceding/previous chapter.

3. Due to decrease in temperature of air in intake diffuser of engine which can comprise in takeoff conditions of order of 20°C, is possible icing of elements/cells of inlet duct, also, at positive temperature to +5-+10°C; therefore checking effectiveness of POS of engine must be carried out to temperatures of +10°C.

4. For prevention of icing of sensors and instruments, adjusted in inlet duct, they must be shielded from icing or, if it is possible, to be established/installed in such a way, that would not occur settling ice. Furthermore, in view of the increased vibrations from engine such instruments must possess the necessary vibration stability and vibration stability.

The special features/peculiarities of the tests of POS of engines indicated must be considered during preparation/training and compilation of test procedure, and also with designing of stands.

Page 294.

Chapter XII.

TESTINGS WITH THE IMITATION OF ICING[1].

FOOTNOTE [1]. Written by R. Kh. Tenishev and B. A. Stroganov.
ENDFOOTNOTE.

12.1. Purpose and system of tests.

Research of the effect of icing on aerodynamic characteristics it is desirable to conduct into two stages: in the beginning of experiment on model in wind tunnel, then - on full-scale aircraft (or helicopter) in flight.

Are especially important investigations in tube for new aircraft types which yet there is not experiment of flights under conditions of icing. Such investigations make it possible to isolate most dangerous flight conditions and thereby to raise the safety of further flight experiments and to organize them are more rational.

However, to this is not limited the value of preliminary testings of model in wind tunnel with the imitators of icing. Their results are of large interest during the design of de-icing systems.

Rating/estimating icing from the point of view of flight safety, it is necessary to consider the fact that different aircraft types and helicopters to different degree react to icing; therefore they can be shielded to different degree, which more narrowly was discussed in II and III chapters.

Moreover, analysis of aerodynamic tests with the imitators of ice in tubes and in flight it can show that in the individual sections of wing or tail assembly the de-icing system can generally prove to be unnecessary. Especially this is developed on contemporary high-speed aircraft, whose icing is possible only under conditions of landing approach or climb, i.e., on time it is very brief (under cruising conditions of the flight of such aircraft icing usually is not observed). As an example it is possible to give aircraft "Boeing 727", in which completely is absent the de-icing system of tail assembly, since, in the opinion, designers, in it there is no special need [101].

As a result of investigations in tubes are obtained primary aerodynamic characteristics: $c_y = f(\alpha)$; $m_z = f(\alpha, \delta_{\text{р.в}}\delta_{\text{э}})$; $m_{\text{ш.р.в.}} = f(\alpha, \delta_{\text{р.в}})$ etc., which make it possible to rate/estimate the effect of ice formation on lifting surfaces to stability and aircraft handling during different flight conditions. Special attention is given by flight conditions with the released high-lift device of wing, since

in this case tail assembly usually works at the angles of attack, close to critical ones, and even small ice formation on stabilizer can sharply change the longitudinal-behavior characteristics and controllability (see Chapter II).

During flight tests with the imitators of icing is more precisely formulated the effect of icing on aerodynamic characteristics of aircraft (helicopter). Since direct ice hazard consists in a deterioration in the stability, and controllability on some flight conditions with the specific sizes/dimensions and forms of ice, then first of all it is necessary to rate/estimate these deviations and to determine the modes/conditions, in which they are greatest. Taking into account that the great effect of icing frequently is developed under conditions of pre-landing glide, especially with maximally bow heaviness, in test program compulsorily must be reflected the modes/conditions, which correspond to pre-landing glide and drift to the second circle.

Page 295.

In this case should be rated/estimated the effect of icing with different vertical g-forces which can occur with landing approach due to the pilot s error, wind gusts and so forth, etc.

If deviations in stability and controllability do not leave the permissible limits, then it is necessary to test the effect of icing on the tactical flight and operating characteristics of aircraft. As has already been spoken in chapter II, icing, making aerodynamics worse of lifting surfaces, can lead to changes in such flight characteristics (rate of climb, cruising and maximum speed, ceiling, modes of operation of engine and consumption of fuel), which, without having directly effect on flight safety, nevertheless affect the efficiency/cost-effectiveness, the selection time of base altitude, duration of flight and other stages of flight mission.

Determining characteristics indicated above is done by methods generally accepted in flight tests [8].

12.2. Forms of imitators.

The form of imitator and its sizes/dimensions must correspond to the heaviest icing which can be encountered during the operation of aircraft (helicopter). As noted above, the forms of ices formation are exclusively diverse and depend both on the ambient conditions of icing and on the flight speed, at which occurs the icing. Furthermore, with the insufficient effectiveness of de-icing system are possible local ice formations, to rate/estimate which is possible only after tests under conditions of icing.

However, for the comparison of the results of tests with imitators (tube and flight) it is necessary to select general/common/total (standard) forms and sizes/dimensions of the imitators which would be sufficiently close to real ices formation on lifting surfaces (or they provided analogous aerodynamic effect), were simple in manufacture and convenient in the operation (i.e. they did not require special equipping for their manufacture and installation on aircraft).

It is possible to propose the following types of imitators:

1) imitators in the failure or absence of the de-icing system, which correspond to the forms of ice, indicated in Fig. 2.1, i.e., the imitators of tapered and horn-shaped ice. Imitators for this case it is expedient to make with triangular ones in the cross section (which is convenient in production). Location of imitators and their significant dimensions are given in Fig. 12.1a and b.

Page 296.

2) the imitators, which correspond to barrier ice, which is obtained, if zone heating has insufficient size/dimension, and also

the ice formation, which are formed periodically on the boundary of "thermal knife" with the work of cyclic deicer (with the large duration of cycle and intense icing these built-up edges they can reach considerable thickness). Imitators for this case can be made with trapezoidal ones in cross section (cm of Fig. 12.1c and d).

Tests must be carried out into several stages: at first with the imitators of form a of the small height/altitude h, then (into 2-3 receptions) their height/altitude increases and finally after the analysis of the results of the first stage - with the imitators of form b (also beginning from smaller sizes/dimensions). Need and system of investigations with second type imitators (c and d) is established/installed in accordance with the design features of the system of the heating of the experience/tested part of the flight vehicle.

It is logical that the forms, sizes/dimensions and location of imitators must be more precisely formulated for specific aircraft (or the screws/propellers of helicopters) on the basis of the examination of the construction/design of their POS, form and sizes/dimensions of the parts being investigated, results of tests under conditions of artificial and natural icing, etc. In proportion to the storage of such data the system of tests and their space can be changed (it is reduced or increased toward investigation of the forms of imitators, characteristic for the icing of the experience/tested aircraft).

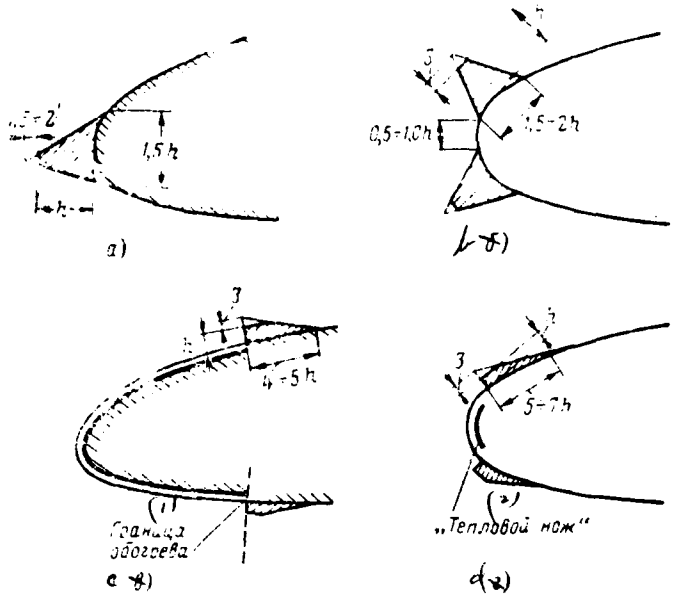

Fig. 12.1. Forms and significant dimensions of the imitators of ice on the lifting surfaces: a) are wedge-shaped; b) horn-shaped; c) barrier ice; d) barriers from "thermal knife".

Key: (1). Boundary of heating. (2). Thermal of knife".

Page 297.

12.3. Methods of manufacture and examples of the use/application of imitators.

The imitators of icing can be made from the most varied

materials: rubber, Textolite, foam plastic, tree/wood, elastic cords and so forth, etc. Especially part is utilized foam plastic due to the ease/lightness of its working/treatment. Imitators usually adhere on surface. But in separate cases, when cannot be guaranteed safe landing with imitators, should be with changed other methods of fastening, which ensure their jettisoning in flight. For guaranteeing of larger strength and facilitation of technology of gluing the imitators, arranged/located on both sides from the leading edge (see Fig. 12.1, b, c and d), can be connect/joined together by connectors or cover plates.

As examples of tests with imitators according to the evaluation of the effect of the conditions of icing on aerodynamic characteristics it is possible to give the tests of aircraft "Boeing 707" [123] and the screw/propeller of aircraft "Barracuda" [109].

The tests of aircraft "Boeing 707" were conducted with target the determination of the behavior of aircraft in the case of the failure of the deicers of the tail assembly. Representation about the sizes/dimensions of imitators and their form gives Fig. 12.2. The forms of imitators were selected on the basis of the analysis of different types of the ices formation, from which were selected the most dangerous, which corresponded to the severe conditions, which were being encountered in practice. Imitators were made from

fiberglass and established/installed on fuller's earth and left half the stabilizer (it was imitated failure of 1/8 deicers of the tail assembly).

Tests were carried out under conditions of takeoff and landing also in entire range of service speed (from $V_{...}$ to V_{max}). Their results showed that the maneuverability of aircraft virtually does not change, i.e., failure of the de-icing system of the tail assembly of this aircraft cannot lead to dangerous consequences from the point of view of stability and aircraft handling. During tests was established/installed certain decrease in the velocity of flight in comparison with noniced aircraft, which is connected with an increase in the drag.

The tests of the screw/propeller of aircraft "Barracuda" (diameters of 3.5 m were carried out with purpose of the determination of losses in thrust during icing. Sizes/dimensions and form of ice for three sections by radius are shown in Fig. 12.3. To relative radius $\bar{R}$=0.7 the sizes/dimensions of imitator (extent on the small arc of profile/airfoil, thickness at critical point) remained constants. The propagation of ice on $\bar{R}$=0.7 reached to 27o/o of chord. From radius $\bar{R}$=0.7 and further the sizes/dimensions of ice were decreased proportional to blade thickness.

Page 298.

In order to more accurately transmit the character of "rough" ice, on the surface of imitator along diagonal were plotted/applied the grooves in deep approximately 3 mm with space 12 mm. This form and sizes/dimensions of ice correspond to very heavy icing.

As a result of tests was obtained a change propeller efficiency, thrust coefficients and moment/torque of the iced over screw/propeller in comparison with noniced one. The change propeller efficiency, obtained as a result of these tests, is represented in Fig. 2.9 (see Chapter II). According to data these tests it is possible to ascertain that the icing of screw/propeller will lead to an incidence/drop in the speed (in the range of flight speeds from 270 to 540 km/h) by 12-22 km/h. This shows that such investigations are important during the solution of a question about need and degree of the protection of engine-propeller combination.

Sometimes the evaluation of stability and controllability is produced by the obtained in a artificial manner icing of lifting surfaces. So, during the investigation of the effect of icing on the flight characteristics of the helicopter of Mi-4 helicopter first underwent icing with hovering on stand, and then was fulfilled flight with increased to definite limits ice. During such tests the form and

the sizes/dimensions of ices formation, which correspond to this type of the helicopter (for aircraft this method is hardly applicable), are obtained by themselves. As far as helicopter is concerned of Mi-4, then, as it was said in Section 2.5, control of helicopter became slack and somewhat deteriorated the maneuverability of apparatus.

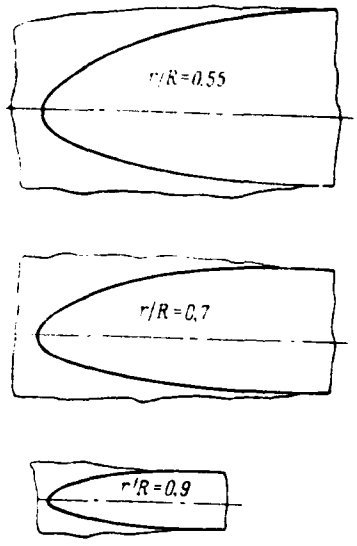

Fig. 12.2. Imitators of ice on aircraft "Boeing 707" during checking of stability and controllability with failure of POS.

Fig. 12.3. Imitator of 1 types ice on blade of propeller of aircraft "Barracuda".

Page 299.

Table 1. Fundamental parameters of the saturated water vapor.

(1) Температура t, °C	(2) Парциальное давление e н/м² (5)		(6) мм рт. ст.		(3) Плотность ρ_s	(4) Абсолютная влажность M_s	
	(7) надо льдом	(8) над водой	(7) надо льдом	(8) над водой		(7)	(8)
—40	28,7	—	0,097	—	2,60	0,268	
—30	38,2	—	0,286	—	2,58	0,342	—
—29	42,3	—	0,317	—	2,57	0,376	—
—28	46,8	—	0,351	—	2,57	0,416	
—27	51,8	—	0,389	—	2,57	0,457	—
—26	57,3	—	0,430	—	2,57	0,503	—
—25	63,4	—	0,476	—	2,56	0,555	—
—24	70,1	—	0,526	—	2,56	0,610	—
—23	77,3	—	0,580	—	2,56	0,672	—
—22	85,3	—	0,640	—	2,56	0,737	—
—21	94,0	—	0,705	—	2,55	0,810	—
—20	103,5	—	0,776	—	2,55	0,888	—
—19	113,9	—	0,854	—	2,55	0,975	—
—18	125,2	—	0,939	—	2,55	1,065	—
—17	137,5	—	1,031	—	2,54	1,165	—
—16	151,0	—	1,132	—	2,54	1,277	—
—15	165,5	191,5	1,241	1,436	2,54	1,390	1,610
—14	181,5	208,0	1,361	1,560	2,54	1,523	1,713
—13	198,6	225,5	1,490	1,691	2,53	1,660	1,880
—12	217,5	244,5	1,632	1,834	2,53	1,810	2,035
—11	238,0	265,0	1,785	1,987	2,53	1,970	2,200
—10	260,0	286,0	1,950	2,147	2,53	2,150	2,360
—9	284,0	310,0	2,131	2,326	2,52	2,340	2,540
—8	310,0	335,0	2,326	2,514	2,52	2,530	2,740
—7	338,0	362,0	2,537	2,715	2,52	2,860	2,955
—6	368,5	391,0	2,765	2,931	2,52	2,990	3,180
—5	402,0	421,3	3,013	3,163	2,51	3,260	3,410
—4	437,0	454,5	3,280	3,410	2,51	3,530	3,660
—3	476,0	489,5	3,568	3,673	2,51	3,820	3,940
—2	517,0	527,0	3,880	3,956	2,51	4,140	4,220
—1	562,0	568,0	4,217	4,258	2,50	4,490	4,530

Page 300.

Continuation table 1.

0	610,0	610,0	4,579	4,579	2,50	4,850	4,850
1	—	656,0	—	4,926	2,50	—	5,200
2	—	705,4	—	5,294	2,50	—	5,550
3	—	758,0	—	5,685	2,50	—	5,960
4	—	813,0	—	6,101	2,49	—	6,360
5	—	873,0	—	6,543	2,49	—	6,820
6	—	934,0	—	7,013	2,49	—	7,260
7	—	1000,0	—	7,500	2,48	—	7,750
8	—	1072,0	—	8,040	2,48	—	8,270
9	—	1146,0	—	8,600	2,48	—	8,810
10	—	1228,0	—	9,209	2,48	—	9,430
11	—	1310,0	—	9,820	2,48	—	10,000
12	—	1400,0	—	10,500	2,47	—	10,680
13	—	1495,0	—	11,210	2,47	—	11,340
14	—	1597,0	—	11,980	2,47	—	12,080
15	—	1720,0	—	12,890	2,47	—	12,880
16	—	1870,0	—	14,100	2,46	—	14,050
17	—	1935,0	—	14,500	2,46	—	14,500
18	—	2040,0	—	15,290	2,46	—	15,200
19	—	2195,0	—	16,480	2,46	—	16,300
20	—	2340,0	—	17,540	2,45	—	17,330
22	—	2640,0	—	19,700	2,45	—	19,500
24	—	2982,0	—	22,370	2,44	—	21,800
26	—	3360,0	—	25,200	2,44	—	24,400
28	—	3775,0	—	28,100	2,43	—	27,250
30	—	4240,0	—	31,800	2,43	—	30,100
35	—	5615,0	—	42,100	2,42	—	39,600
40	—	7370,0	—	55,300	2,40	—	51,100
45	—	$95,8 \cdot 10^2$	—	71,850	2,39	—	65,500
50	—	$123,5 \cdot 10^2$	—	92,800	2,38	—	83,000
55	—	$157,5 \cdot 10^2$	—	118,3			
60	—	$199,0 \cdot 10^2$	—	149,4			
65	—	$250,0 \cdot 10^2$	—	187,6			
70	—	$311,0 \cdot 10^2$	—	233,4			
75	—	$385,0 \cdot 10^2$	—	289,0			
80	—	$473,0 \cdot 10^2$	—	355,0			

Key: (1). Temperature. (2). Partial pressure e. (3). Heat of vaporization L and M J/kg. (4). Absolute humidity M in g/m³. (5). N/m². (6). mm Hg. (7). it is must by ice. (8). above water.

Page 301.

Table 2. Fundamental physical characteristics of the materials, utilized for thermocouples.

(1) Наименование металла или сплава	(2) Термоэлектродвижущая сила в паре с платиной мв	(3) Температура применения в °С: (10) для термометров сопротивления	для термопар: (12) длительная	(13) кратковременная	(4) Температура плавления °С	(5) Удельный вес г/см³	(6) Теплоемкость ккал/кг °С	(7) Теплопроводность ккал/м·час °С	(8) Удельное сопротивление ом·мм²/м	(9) Температурный коэффициент электросопротивления (0—100°С)
Алюминий (14)	+0,40	—	—	—	658	2,7	0,167	175	0,025—0,278	$4,3 \cdot 10^{-3}$
Алюмель (15)	От —1,05 до —1,38	—	1000	1250	1450	8,5	0,225 —	—	0,33—0,35	$1,0 \cdot 10^{-3}$
Железо химически чистое (16)	+1,8	150	600	800	1528	7,86	0,12	40	0,0907	$6,25 \cdot 10^{-3}$ — $6,57 \cdot 10^{-3}$
Золото (17)	+0,8	—	—	—	1063	19,25	0,0312	265	0,022	$3,97 \cdot 10^{-3}$
Иридий (18)	+0,65	—	—	—	2350	—	0,058	—	—	$3,93 \cdot 10^{-3}$
Константан (19)	—3,5	—	600	800	1220—1280	8,9	0,098	20	0,45—0,5	$0,01 \cdot 10^{-3}$
Копель (20)	—4,0	—	600	800	1250	9,0	—	—	0,49	$-0,1 \cdot 10^{-3}$
Кадмий (21)	+0,9	—	—	—	321	—	—	—	—	—
Медь химически чистая (22)	+0,76	150	350	500	1083	8,95	0,0936	340	0,0156—0,0168	$4,33 \cdot 10^{-3}$
Медь проводниковая (23)	+0,75	150	350	500	—	8,9	0,0936	300—340	0,017	$4,25 \cdot 10^{-3}$ — $4,28 \cdot 10^{-3}$
Манганин (24)	+0,8	—	—	—	910	8,1	—	—	0,42	$0,006 \cdot 10^{-3}$
Нихром (25)	От +1,5 до +2,5	—	1000	1100	1500	8,2	—	—	0,95—1,05	$0,14 \cdot 10^{-3}$
Никель (26)	От —1,5 до —1,51	300	1000	1100	1455	8,75	0,108	50	0,118—0,138	$6,21 \cdot 10^{-3}$ — $6,34 \cdot 10^{-3}$

Page 302.

Continuation table 2.

Олово (27)	+0,43	—	—	—	232	7,4	0,0564	55	0,143	$4,4 \cdot 10^{-3}$
Платина «Экстра» (28)	0	660	1300	1600	1779	21,32	0,032	59	0,0981—0,106	$3,94 \cdot 10^{-3}$ —$5,8 \cdot 10^{-7}$
Платинородий (29)	+0,64	—	1300	1600	—	—	—	—	0,190	$1,67 \cdot 10^{-3}$
Платиноиридий (30)	+1,3	—	1000	1200	—	—	—	—	—	—
Палладий (31)	—0,57	—	—	—	1553	—	—	—	—	—
Свинец (32)	+0,44	—	—	—	327	11,3	0,0316	30	0,227	$4,11 \cdot 10^{-3}$
Серебро (33)	+0,72	—	600	700	960,5	10,5	0,057	360	0,0147	$4,1 \cdot 10^{-3}$
Хромель (34)	(36) От +2,76 (37) до +3,13	—	1000	1250	1450	8,7	—	—	0,7	$0,5 \cdot 10^{-3}$
Цинк (35)	+0,7	—	—	—	419,5	6,86	0,096	95	0,062	$3,9 \cdot 10^{-3}$

Key: (1). Designation of metal or alloy. (2). Thermoelectromotive force in vapor with platinum mV. (3). Temperature of use/application in °C. (4). Melting point of °C. (5). Specific gravity/weight g/cm³. (6). Heat capacity kcal/kg of °C. (7). Thermal conductivity kcal/m•h of °C. (8). Specific resistance of Ω•mm²/m. (9). Temperature coefficient of electrical resistance (0-100°C). (10). for resistance thermometers. (11). for thermocouples. (12). prolonged. (13). short-term. (14). Aluminum. (15). Alumel. (16). Iron chemically pure. (17). Gold. (18). Iridium. (19). Constantan. (20). Copel. (21). Cadmium. (22). Copper chemically pure. (23). Copper conductor. (24). Manganin. (25). Nichrome. (26). Nickel. (27). Olovo. (28). Platinum of "extra ones". (29). Platinum-rhodium. (30). Platinum-iridium. (31). Palladium. (32). Lead. (33). Silver. (34). Chromel. (35). Zinc. (36). from (37). to.

Page 303.

Table 3. Dependence of coefficient $\frac{c_D Re_K}{24}$ on Reynolds number.

Re	$\frac{c_D Re_K}{24}$	Re	$\frac{c_D Re_K}{24}$	Re	$\frac{c_D Re_K}{24}$	Re	$\frac{c_D Re_K}{24}$
0	1,000	8,0	1,678	200	6,52	6 000	96,8
0,05	1,009	10,0	1,782	250	7,38	8 000	130,6
0,1	1,018	12,0	1,901	300	8,26	10 000	166,3
0,2	1,037	14,0	2,008	350	9,00	12 000	204,0
0,4	1,073	16,0	2,109	400	9,82	14 000	243,0
0,6	1,108	18,0	2,198	500	11,46	16 000	285,0
0,8	1,142	20,0	2,291	600	12,97	18 000	325,0
1,0	1,176	25,0	2,489	800	15,81	20 000	365,0
1,2	1,201	30,0	2,673	1 000	18,62	25 000	470,0
1,4	1,225	35,0	2,851	1 200	21,3	30 000	574,0
1,6	1,248	40,0	3,013	1 400	24,0	35 000	674,0
1,8	1,267	50,0	3,327	1 600	26,0	40 000	778,0
2,0	1,285	60,0	3,60	1 800	29,8	50 000	980,0
2,5	1,332	80,0	4,11	2 000	32,7	60 000	1175,0
3,0	1,374	100,0	4,59	2 500	40,1	80 000	1552,0
3,5	1,412	120,0	5,01	3 000	47,8	$1,0 \cdot 10^5$	1905,0
4,0	1,447	140,0	5,40	3 500	55,6	$1,2 \cdot 10^5$	2234,0
5,0	1,513	160,0	5,76	4 000	63,7	$1,4 \cdot 10^5$	2549,0
6,0	1,572	180,0	6,16	5 000	80,0	$1,6 \cdot 10^5$	2851,0

Table 4. The design conditions of icing, accepted in England for an aircraft (prolonged maximum)

Температура (1) °С	(2) Водность г/м³	(3) Диаметр капель мк	(4) Высота м
0	0,8	20	0÷6000
—10	0,6		900÷8400
—20	0,3		900÷9000
—30	0,2		900÷9000

Note. The conditions of icing at temperature of 0°C can be related to the altitude range of 900-6000 m.

Key: (1). Temperature. (2). Water content g/m³. (3). Diameter of drops μ. (4). Height/altitude.

Table 5. The design conditions of icing, accepted in England for power plant (short-term maximum).

Температура (1) °С	Водность (2) г/м³	Диаметр капель (3) мк	Высота (4) м
0	2,5		3000÷6000
—10	2,2		6000÷8400
—20	1,7	20	4500÷9000
—30	1,0		4500÷10 700
—40	0,2		4500÷12 200

Note. Conditions table 5 are real:

a) at heights/altitudes from 3000 to 9000 m - in sections 5 km, with the gaps/intervals between them on 5 km in which should be accepted the conditions on table 4:

b) at heights/altitudes from 9000 to 12000 in sections 5 km, with the gaps/intervals between them on 32 km without icing.

Key: (1). Temperature. (2). Water content g/m³. (3). Diameter of drops μ. (4). Height m.

Page 304.

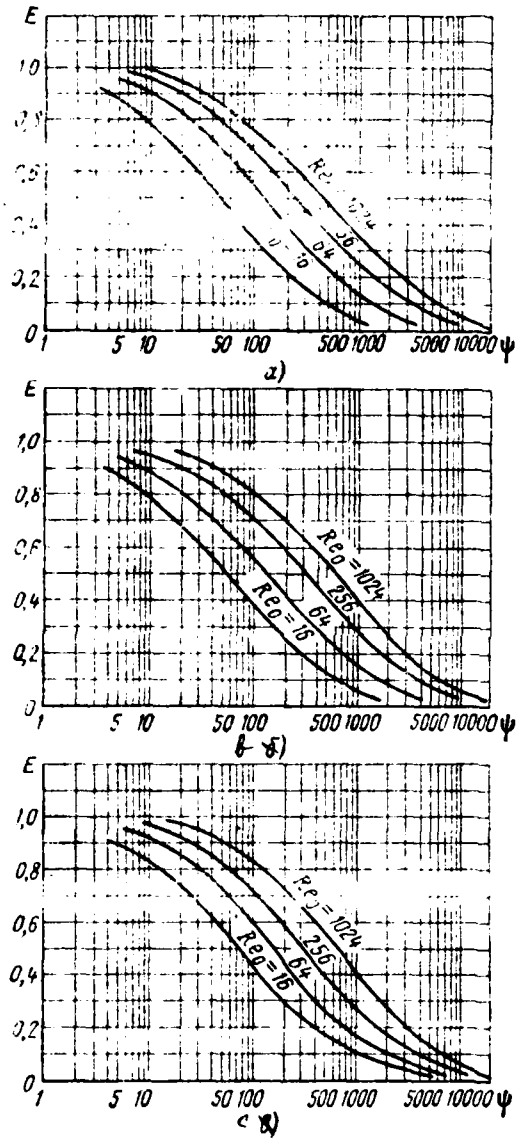

Fig. 1. Interception coefficient of drops of 15o/o symmetrical Zhukovskiy profile: a) $\alpha=0$, $c_y=0$; b) $\alpha=2°$, $c_y=0.22$; c) $\alpha=4°$, $c_y=0.44$.

Page 305.

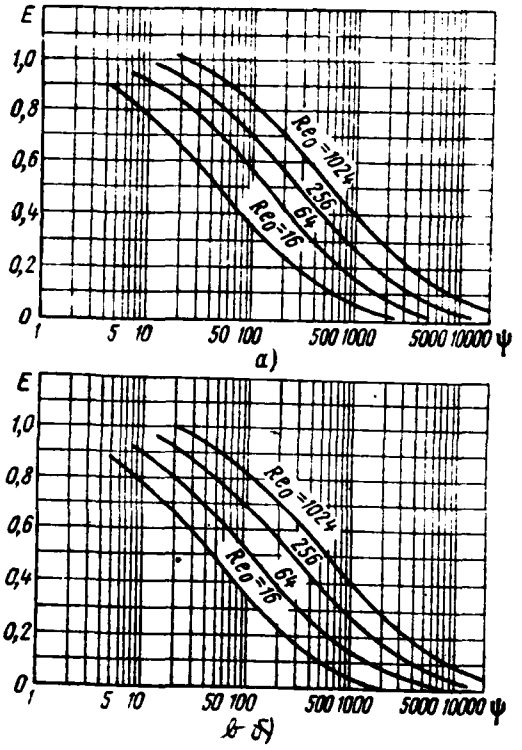

Fig. 2. Coefficient of capture of drops: a) 15o/o bent Zhukovskiy profile, $\alpha=4^\circ$, $c_y=0.44$; b) profile/airfoil NACA-65_2-0.15, $\alpha=4^\circ$, $c_y=0.44$.

Page 306.

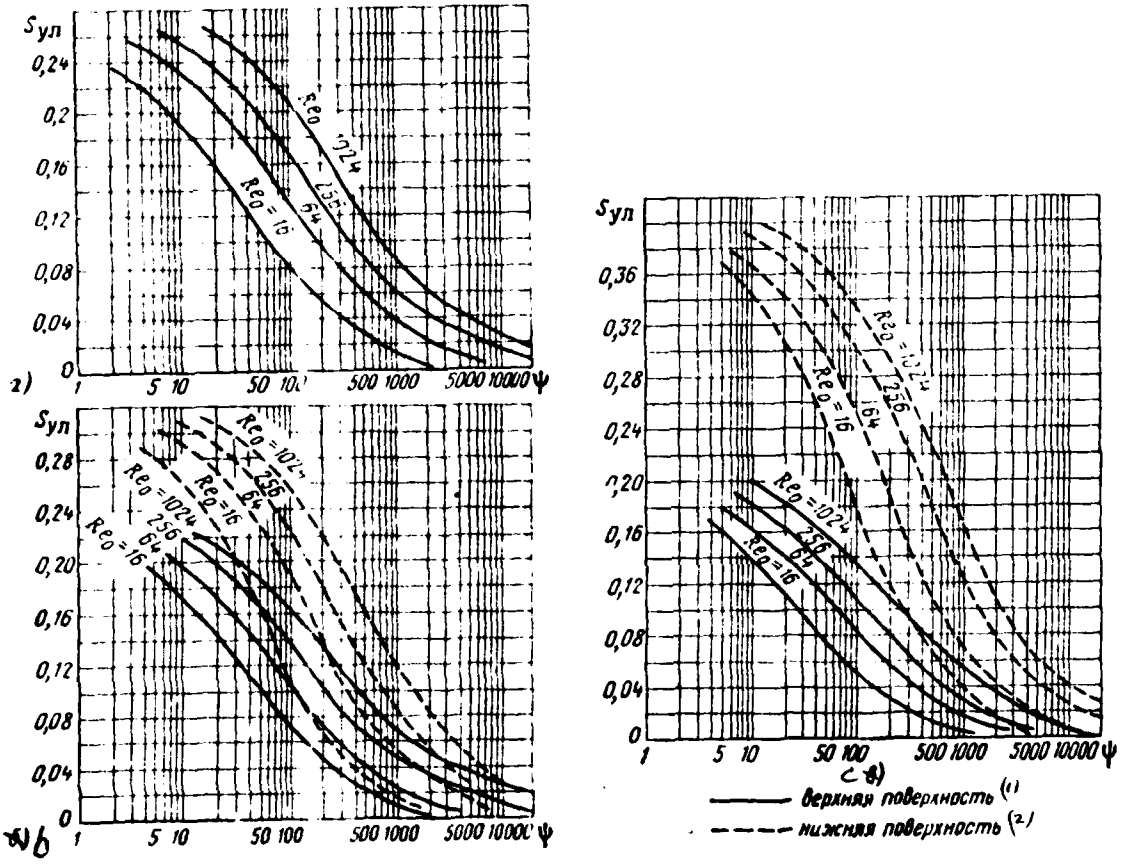

Fig. 3. Extent of zone of catching of drops on 15o/o symmetrical Zhukovskiy profile: а — $\alpha = 0$, $c_y = 0$; б — $\alpha = 2°$, $c_y = 0,22$; в — $\alpha = 4°$, $c_y = 0,44$

Key: (1). upper surface. (2). lower surface.

Page 307.

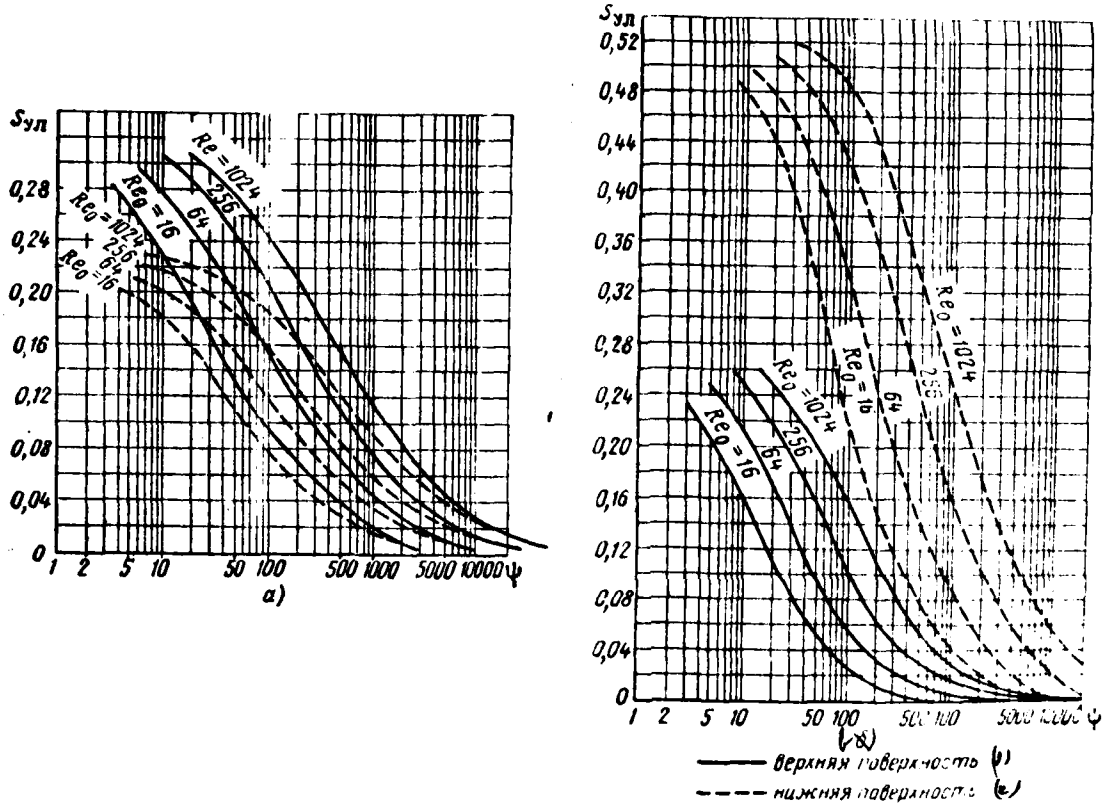

Fig. 4. Extent of zone of catching of drops: a) on 15o/o bent Zhukovskiy profile, $\alpha=4°$, $c_y=0.44$; b) on profile/airfoil NACA-65_2-0.15, $\alpha=4°$, $c_y=0.44$.

Key: (1). upper surface. (2). lower surface.

Page 308.

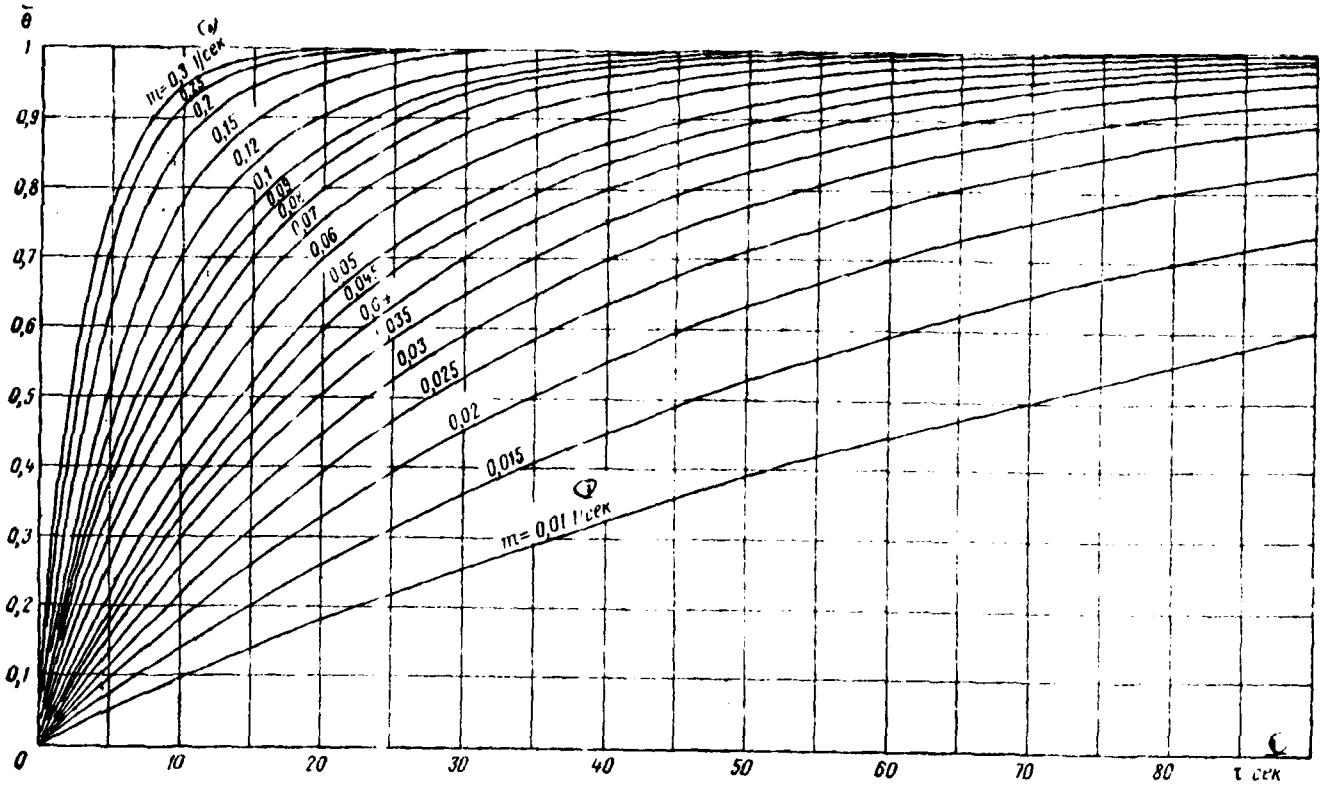

Fig. 5. Curves of dimensionless temperature in time at different rates of heating.

Key: (1). s.

Page 309.

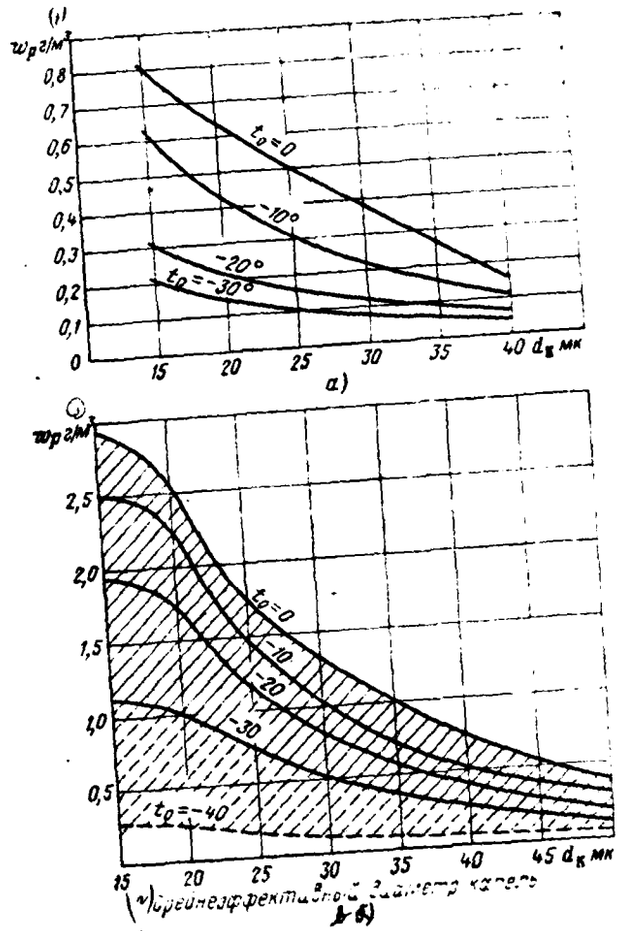

Fig. 6. Dependence of water content on temperature and size/dimension of drops, accepted under design conditions of USA: a) prolonged icing; b) short-term icing.

Key: (1). g/m³. (2). Mean-effective diameter of drops.

Notes. 1. Prolonged conditions are related to altitude range from 0 to 6700 m. The maximum thickness of a cloud layer is equal to 2000 m. Conditions on water content are prescribed/assigned for standard horizontal distance - 28 km.

2. Short-term conditions are related to altitude range from 1200 to 6700 m. Conditions on water content are prescribed/assigned for standard horizontal distance - 4000 m.

Page 310.

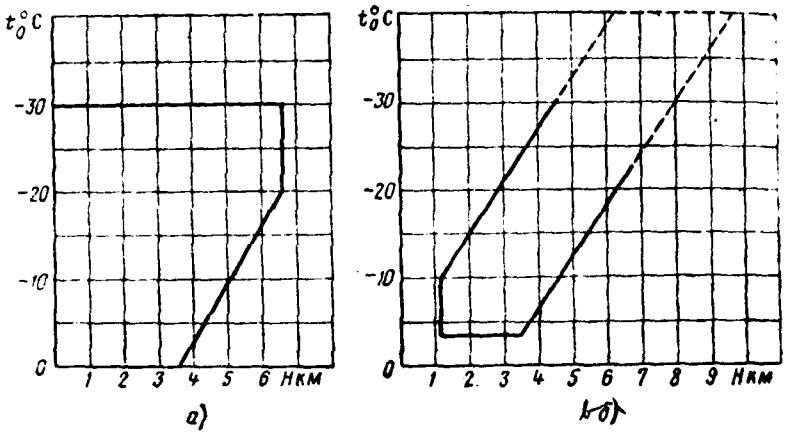

Fig. 7. Temperature range of icing in dependence on height/altitude: a) prolonged icing; b) short-term icing.

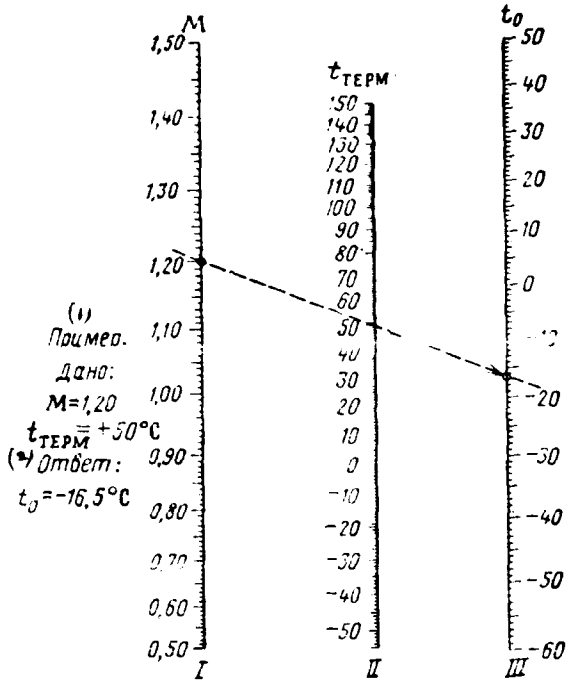

Fig. 8. Nomogram for determining the actual temperature of surrounding air with speeds of flight $0,5 < M < 1,5; N = 0,978$: I - scale of Mach numbers (flight speed); II - temperature scale, shown by the thermometer; III - scale of actual temperature.

Key: (1). An example. it is given. (2). Response/answer.

Page 311.

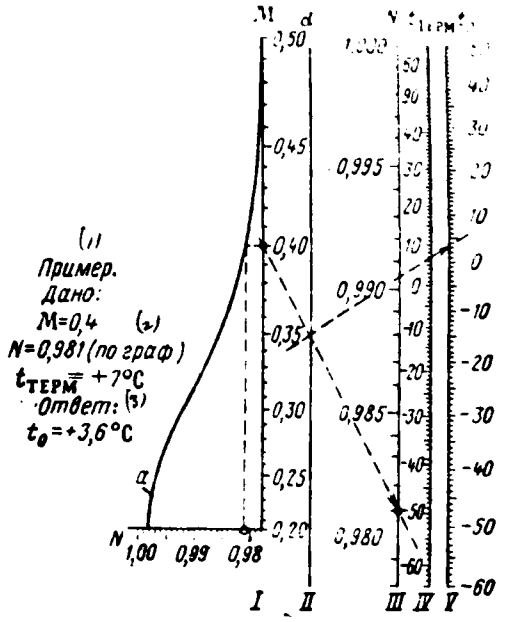

Fig. 9. Nomogram for determining actual temperature of surrounding air at low speeds of flight $0.2 \leq M \leq 0.5$: a) curve of dependence of coefficient N; I - scale of Mach numbers (flight speed), II - auxiliary scale; III - scale of coefficient N; IV - temperature scale, shown by thermometer; V - scale of actual temperature.

Key: (1). An example. it is given. (2). On graph/count. (3). Response/answer.

Page 312.

REFERENCES.

1. Абрамович Г. Н., Прикладная газовая динамика, ГИТТЛ, 1953
2. Берман Л. Д., Испарительное охлаждение циркуляционной воды Госэнергоиздат, 1957.
3. Боровиков А. М., Физика облаков, Гидрометеоиздат, 1961.
4. Боровиков А. М., Некоторые результаты изучения облачных элементов, Труды ЦАО, вып. 3, 1948.
5. Босворт Р. Л., Процессы теплового переноса, ГИТТЛ, 1957.
6. Бронштейн И. Н. и Семендяев К. А., Справочник по математике, ГИТТЛ, М., 1953.
7. Ван-Драйст, Проблема аэродинамического нагрева, «Вопросы ракетной техники», 1957, № 5 (11).
8. Ведров В. С. и Гайц М. А., Летные испытания самолетов, Оборонгиз, 1951.
9. Гольдштейн С., Современное состояние гидроаэродинамики вязкой жидкости, т. 1—2, ИЛ, 1948.
10. Горбачев В. А. и Мелкобродов Е. А., Физические основы устройства и работы авиационных приборов, Оборонгиз, 1953.
11. Гребер Г., Эрк и Григулль У., Основы учения о теплообмене, ИЛ, 1958.
12. Гугенмахер Л. И., Электрические модели, АН СССР, 1949.
13. Диткин В. А. и Кузнецов П. П., Справочник по операционному исчислению, Гостехиздат, 1951.
14. Дружинин Г. В., Надежность устройств автоматики, изд-во «Энергия», 1964.
15. Епифанов А. Д., Надежность автоматических систем, изд-во «Машиностроение», 1964.
16. Заварина М. В., Аэроклиматические факторы обледенения самолетов, Гидрометеоиздат, Л., 1961.
17. Зайцев В. А. и Ледохович А. А., Приборы и методика исследования облаков с самолета, Гидрометеоиздат, 1960.
18. Идельчик И. Е., Справочник по гидравлическим сопротивлениям, Госэнергоиздат, М.—Л., 1960.
19. Каменев П. Н., Отопление и вентиляция, ч. II. Вентиляция, Стройиздат, 1964.
20. Капица П. Л., Волновое течение тонких слоев вязкой жидкости, ЖЭТФ АН СССР, 1948, т. 18, вып. 1.
21. Карплюс У., Моделирующие устройства для решения задач теории поля, ИЛ, 1962.
22. Карслоу Х. С., Теория теплопроводности, ГИТТЛ, 1947.
23. Качурин Л. Г., Электрические измерения аэрофизических величин, ЛГУ, 1962.
24. Кобринский Н. Е. и Трахтенброт Б. А., Введение в теорию конечных автоматов, Физматгиз, 1962.
25. Кожарин В., Оценка условий обледенения самолетов в слоистых и слоисто-кучевых облаках, «Гражданская авиация», 1957, № 11.

26. Кондратьев Г. М., Регулярный тепловой режим, Гостехиздат, 1954.
27. Кондратьев Г. М., Тепловые измерения, Машгиз, М., [illegible]
28. Котик М. Г., Павлов А. В., Пашковский И. М., [illegible] новский Ю. С., Щитаев Н. Г., Летные испытания самолетов [illegible] «Машиностроение», 1965.
29. Лавров В. В., Вопросы физики и механики льда, [illegible] «Морской транспорт», 1962.
30. Лебедев Н. В., Борьба с обледенением самолетов, Оборонгиз, [illegible]
31. Левин Л. М., Об осаждении частиц аэрозоля из потока [illegible] ствие, ДАН СССР, 1953, т. XCI, № 6.
32. Левин Л. М., О функции распределения облачных и дождевых капель по размерам, ДАН СССР, 1954, т. XCIV, № 6.
33. Левин В. Г., Физико-химическая гидродинамика, АН СССР, 1952.
34. Лин Ц. Ц., Турбулентное течение и теплопередача, ИЛ, 1963.
35. Лыков А. В., Теория теплопроводности, Гостехиздат, 1962.
36. Мазин И. П., Методы оценки эффективности работы самолетных термических противообледенителей с учетом водности и температуры облаков, Труды ЦАО, вып. 39, 1962.
37. Мазин И. П., Физические основы обледенения самолетов, Гидрометеоиздат, 1957.
38. Мак-Адамс В. Х., Теплопередача, Металлургиздат, 1961.
39. Мельников А. П., Аэродинамика больших скоростей, Воениздат, 1961.
40. Мейсон Б. Дж., Физика облаков, Гидрометеоиздат, Л., 1961.
41. Минервин В. Е., Мазин И. П., Бурковская С. М., Некоторые новые данные о водности облаков, Труды ЦАО, вып. 19, 1958.
42. Миронов К. А. и Шипетин Л. И., Теплотехнические измерительные приборы, Машгиз, 1958.
43. Михеев М. А., Основы теплопередачи, Госэнергоиздат, 1956.
44. Николаев Н. С. и др., Аналоговая математическая машина УСМ 1 (для решения краевых задач математической физики), Машгиз, 1962.
45. Пашковский И. М., Особенности устойчивости и управляемости скоростного самолета, Воениздат, 1961.
46. Петухов Б. С., Опытное изучение процессов теплопередачи, Госэнергоиздат, М.—Л., 1962.
47. Преображенский В. П., Теплотехнические измерения и приборы, Госэнергоиздат, 1946.
48. Пчелко И. Г., Метеорологические условия полетов на больших высотах, Гидрометеоиздат, 1957.
49. Пчелко И. Г., Боровиков А. М., Результаты обработки данных микроструктурных наблюдений для облаков с обледенением и без обледенения, Труды ЦИП, № 80, Гидрометеоиздат, М., 1959.
50. Решетов Г. Д., Облачность в верхней тропосфере, Труды ЦИП, № 81, 1961.
51. Рыкалин Н. И., Расчеты тепловых процессов при сварке, Машгиз, 1951.
52. Скацкий В. И., Самолетный измеритель водности капельножидких облаков, ИАН СССР, сер. геофизическая, 1963, № 9.
53. Соломонов П. А., Вопросы надежности авиационной техники, Воениздат, 1965.
54. Стечкин Б. С. и др., Теория реактивных двигателей. Лопаточные машины, Оборонгиз, 1958.
55. Сунцов Н. Н., Методы аналогий в аэродинамике, Физматгиз, 1958.
56. Тесленко А. И., Обледенение авиационных газотурбинных двигателей, Воениздат, 1961.
57. Тетельбаум И. М., Электрическое моделирование, Физматгиз, 1951.

58. Трунов О. К., Обледенение самолетов и средства борьбы с ним' изд-во «Машиностроение», 1965.
59. Туричин А. М., Электрические измерения неэлектрических величин, Госэнергоиздат, 1951.
60. Фильчаков П. Ф., Панчишин В. И., Интеграторы ЭГДА. Моделирование потенциальных полей на электропроводной бумаге, АН УССР, 1961.
61. Халтинер Дж., Мартин Ф., Динамическая и физическая метеорология, ИЛ, 1960.
62. Хинце И. О., Турбулентность, ИЛ, 1964.
63. Хргиян А. Х., Физика атмосферы, ГИФМЛ, М., 1958.
64. Шак А., Промышленная теплопередача, Металлургиздат, М., 1961.
65. Шейнин В. М., Весовая и транспортная эффективность пассажирских самолетов, Оборонгиз, 1962.
66. Шифрин К. С., О возрастании среднего радиуса в облаке с высотой, Труды ГГО, вып. 31 (93), 1961.
67. Шлихтинг Г., Возникновение турбулентности, ИЛ, 1962.
68. Эккерт Э. Р. и Дрейк Р. М., Теория тепло- и массообмена, Госэнергоиздат, М.—Л., 1961.
69. Якоб М., Вопросы теплопередачи, ИЛ, 1960.
70. Abel G. C., Report of the first (+ second + third) year on development of flight testing techniques for finding and measuring natural icing conditions, ARC C. P., 1956—1958, No. 221—223.
71. Abramson A. E., Calculation of droplet trajectories using an electronic analog computer. The Third Midwestern Conference on Fluid Mechanics, Minneapolis, 1953.
72. Aerospace Safety, 1963, vol. 19, No. 11, pp. 18—19.
73. Aircraft Engineering, 1964, vol. 36, No. 6.
74. Airplanes airworthiness, Transport categories FAA, Washington, 1962, September.
75. Anderson B. H., Improved technique for measuring heat transfer coefficients, Planetary and Space Science, 1961, vol. 4, No. 1.
76. Ballard O. R. and Guan B., Ice cristals — a new icing hazard, Canadian Aer. Journal, 1958, No. 1.
77. Bannon J. K., Aircraft icing at very low temperature, The Meteorological Magazine, 1955, vol. 84, No. 997.
78. Barlett D., Gas turbine icing tests at Mt. Washington, SAE Journal, 1951, January.
79. Beckwith I. E. and Gallagher J. J., Local heat transfer and recovery temperature on a yawed cylinder at Mach number of 4, 15 and high Reynolds numbers, NASA TR R-104, 1961.
80. Bergrun N. R., General results of NACA flight research in natural icing conditions during the winter 1945—1946, Astronaut. Eng. Rev., 1948, January.
81. Bergrun N. R., An empirically derived basis for calculating the area, rate and distribution of water-drop impingement on airfoils, NACA Report, 1952, No. 1107.
82. Best A. C., Occurence of high rates of ice accretion on aircraft, Meteorological Office Professional Notes, London, 1952, No. 106.
83. Bigg F. J., Day D. J., McNaughton I. I., The measurement of ice crystal clouds, Aircraft Ice Protection Conference, 1959.
84. Bolke F. L. and Paselk F. L., Icing problems and thermal anti-icing systems, JAS, 1946, vol. 13, No. 9.
85. Bolley E., Icing on aircraft, Handbook of meteorology, New-York—London, 1945.
86. Bourrillon M., Les essais en vol de givrage artificiel appliques au turbo-propulseur turbomeca «Bastan», Technique et Science Aeronautiques, 1961, No. 2.
87. Brun R. J., Mergler H. W., Impingement of water droplets on a cylinder in an incompressible flow field, NACA TN No. 2904, 1953.

88. Brun R. J., Cloud-droplet ingestion in engine inlets with inlet velocity ratios of 1,0 and 0,7, NACA Report No. 1317, 1957.

89. Brun R. J., Lewis W., Perkins P. J., Impingement of cloud droplets on a cylinder and procedure for measuring liquidwater content and droplet sizes in supercooled clouds by rotating multicylinder method, NACA Report, 1955, No. 1215.

90. Chappell M. S., A resume of simulation techniques and icing activities at the engine laboratory of the National Research Council (Canada), Ottawa, 1953.

91. Cheverton B. T., The icing research aircraft, Aircraft Ice Protection Conference, 1960.

92. Cheverton B. T., Sharp C. R., Badham L. G., Spray nozzles for the simulation of cloud conditions in icing tests of jet engines, N. A. E. C., Ottawa, 1951, No. 14.

93. Cheverton B. T., Icing flight development, Journal of RAS, 1959, vol. 63, No. 587.

94. Collingwood D. G., Electrically-heated transparancies, Aircraft Engng, 1963, No. 4.

95. Crick R. D., Electrical de-icing of helicopter blades, Aircraft Ice Protection Conference, 1961.

96. Curle N., Heat transfer through a constant property laminar boundary layer, ARC R & M, 1962, No. 3300.

97. Dellaye J., Le givrage des turbo-réacteurs, Bulletin Assoc. Ingrs. issus Ecole applic. artill. et genie, Bruxelles, 1957, No. 1.

98. Dorsch R. G., Brun R. J., A method for determining clouddroplet impingement on swept wings, NACA TN, 1953, No. 2931.

99. Drake R. M., Investigation of the variation of point unit heat transfer coefficients for laminar flow over an inclined flat plate, Journal of Appl. Mech., 1949, vol. 16, No. 1.

100. Drake R. M. and others, Local heat transfer coefficients on the surface of an elliptical cylinder, axis ratio 1 : 3, in high speed air stream, Trans. of the ASME, 1953, vol. 75, No. 7.

101. Flight International, 1963, 9 May, p. 687.

102. Giedt W. H., Investigation of variation of point unit heat transfer coefficients around a cylinder normal to an air stream, Trans. of the ASME, 1949, vol. 71, No. 4.

103. Goland L., The theoretical investigation of heat transfer in the laminar flow regions of airfoils, JAS, 1950, vol. 17, No. 7.

104. Golitzine N., Sharp C. R., Badham L. G., Spray nozzles for the simulation of cloud conditions in icing tests of jet, N. A. E. C. Report, Ottawa, 1951, No. 14.

105. Golitzine N., Method for measuring the size of water droplets in clouds, fogs and sprays, Ottawa, 1951.

106. Goodman T. R., Linearized theory of water drop impingement, J. A. S., 1956, vol. 23, No. 4.

107. Greenly K. H., Recent developments in aircraft ice protection, Aircraft Engng, 1963, vol. 35, No. 4.

108. Guilbert A. G., Thermal anti-icing survey on Mt. Washington, Trans. of the ASME, 1947, vol. 69, No. 8.

109. Hainess A. B., Comparative tests on propellers with simulated ice and with de-icing overshoes in 24-ft tunnel, ARC R & M, 1946, No. 2397.

110. Hardy J. R., Evaporation of drops of liquid, ARC R & M, 1947, No. 2805.

111. Hardy J. R., Kinetic temperature of propeller blades in conditions of icing, ARC R & M, 1947, No. 2806.

112. Hardy J. R., Kinetic temperature of wet surfaces, ARC R & M, 1945, No. 2830.

113. Hardy J. R., An analysis of the dissipation of heat in conditions of icing from a section of the wing of the C-46 airplane, NACA Report, 1946, No. 831.

114. Hauger H. H., Intermitten heating of airfoil for ice protection, utilising hot air, Trans. of ASME, 1954, vol. 76, No. 2.

115. Howlett D. P., Ice detectors, Aircraft Ice Protection Conference, 1961.

116. Jenkins D. C., The acceleration of water drops by an airstream of constant relative velocity, ARC CP, 1961, No. 539.

117. Knuth E. L., Comments on flight measurements of aerodynamic heating and boundary layer transition on the Viking nose cone, Jet Propulsion, 1956, vol. 26, No. 12.

118. Koh J. C. J. and Harnett J. P., Measured pressure distribution and local heat transfer rates for flow over concave hemisphere, ARS Paper 1460—60, 1960.

119. Ledford R. L., A device for measuring heat transfer rates in hypervelocity wind tunnels, Сб. «Advances in hypervelocity techniques», N. Y., 1962.

120. Le Sueur H. E., Icing standard and methods used to determine the suitability of aircraft to fly in icing conditions, Aircraft Ice Protection Conference, 1958.

121. Liebmann G., Solution of transient heat transfer problems by the resistance—network analog method, Trans. of the ASME, 1956, vol. 78, No. 6.

122. Lovesey A. C., Les methodes modernes d'essais des turboréacteurs, Revue Universelle de Mines, 1954, No. 12.

123. Melt-profe «ice», Boeing Magazine, 1960, vol. 30, 11.

124. Messinger B. L., Equilibrium temperature of an unheated icing surface as a function of air speed, JAS, 1953, vol. 20, No. 1.

125. Messinger B. L. and Werner S. B., Design and development of the ice protection systems for the Lockneed «Electra», Aircraft Ice Protection Conference, 1959.

126. Napier & Son Limited, Проспекты фирмы №№ LTP 11-1-1; LTP-27; LTP-67.

127. Palmer, «Palmer Airfoil De-Icer Equipment» проспект фирмы «Пальмер». London, 1965.

128. Payne C. E. G. and Pitts G. F., Proteus icing experience, Aircraft Ice Protection Conference, 1959.

129. Perls T. A. and Hartog S. S., Pyroelectric transducers for heat transfer measurements, Сб. Acta IMEKO, Budapest, 1961, vol. 4.

130. Richardson D. A. and others, Solutions for helicopter rotor blade icing, JAS Paper 810, 1958.

131. Robinson H. G., An analogue computer for convective heating problems, A. R. C. Technical Report C. P. 1957, No. 374.

132. Schaefer V. J., Heat requirements for instruments and airfoils during icing storms of Mt. Washington, Trans. of the ASME, 1947, vol. 69, No. 8.

133. Schaetzel S. S., A rapid method of estimating the severity of icing, Aircraft Engng, 1950, vol. 22, No. 258.

134. Seban R. A. and Drake R. M., Local heat transfer coefficients on the surface of an elliptical cylinder in a high speed stream, Trans. of the ASME, 1953, vol. 75, No. 2.

135. Seban R. A. and Bond R., Skin-friction and heat-transfer characteristics of a laminar boundary layer on a cylinder in axial incompressible flow, JAS, 1951, vol. 18, No. 10.

136. Serafini J. S., Impingement of water droplets on wedges and double wedges airfoils at supersonic speeds, NACA Report, 1954, No. 1159.

137. Sherlaw W., Some aspects of engine icing, Aircraft Ice Protection Conference, 1958.

138. Shires G. L., Munns G. E., The icing of compressor blades and their protection by surface heating, ARC R & M. 1955, No. 3041.

139. Smith A. G. and Jones C., Anti-icing and boundary layer control by slit blowing, Aircraft Ice Protection Conference, 1961.

Page 317.

140. Squire H. B., Heat transfer calculation for [illegible] A.R.C. R. & M. 1942, No. 1986.

141. Stallabrass J. R., Some aspects of helicopter [illegible] Aeron. Journal 1957, vol. 3, No. 8.

142. Stallabrass J. R., Price R. D., On the adhesion of [illegible] rious materials, Canadian Aeron. and Space Journal, 1963, vol. 9, No. 7.

143. Stallabrass J. R., Flight tests of an experimental helicopter rotor blade electrical de-icer, National Research Council of Canada, Aeronautical Report, 1959, November.

144. Stallabrass J. R., Canadian research in the field of helicopter icing, The Journal of the Helicopter Ass. of Gr. Britain, 1958, vol. 12, No. 4.

145. Tanner D. C., Fluid de-icing, Aircraft Ice Protection Conference, London, 1961.

146. Teslenko A. J., Jivraful la turbomotoare, Revista Transporturilor, Bucuresti, 1960, No. 8.

147. The College of Aeronautics Cranfield Note, 1959, No. 77.

148. The Thunderstorm, Washington, 1949.

149. Thompson J. K., Les problemes de givrages, Shell Aviation News, No. 213.

150. Tribus M., Young G. B. W., Boelter L. M. K., Analysis of heat transfer over a small cylinder in icing conditions on Mt. Washington, Trans. of the ASME, 1948, vol. 70, No. 8.

151. Tribus M., Guibert A., Impingement of spherical water droplets on a wedge of supersonic speeds in air, J. A. S., 1952, vol. 19, No. 6.

152. Tribus M., Young G. B. W., Boetter L. M. K., Limitations and mathematical basis for predicting aircraft icing characteristics from scale-model studies, Trans. of the ASME, 1948, vol. 70, No. 8.

153. Tribus M., Intermittent heating for aircraft ice protection with application to propellers and jet engines, Trans. of the ASME, 1951, November, vol. 73, No. 8.

154. Trunov O. K., Tenishev R. H., Some problems of aircraft and helicopter ice protection, Aircraft Ice Protection Conference, 1961.

155. Weiner F., Further remarks on intermittent heating for aircraft ice protection, Trans. of ASME, 1951, vol. 73, No. 8.

156. Wiser G. J., Design and operational experience with electrically heated windshields and conopies, Aircraft Ice Protection Conference, 1959.

Pages 318-320.

No typing.

DISTRIBUTION LIST

DISTRIBUTION DIRECT TO RECIPIENT

ORGANIZATION		MICROFICHE
A205	DMATC	1
A210	DMAAC	2
B344	DIA/RDS-3C	9
C043	USAMIIA	1
C509	BALLISTIC RES LABS	1
C510	AIR MOBILITY R&D LAB/FIO	1
C513	PICATINNY ARSENAL	1
C535	AVIATION SYS COMD	1
C591	FSTC	5
C619	MIA REDSTONE	1
D008	NISC	1
H300	USAICE (USAREUR)	1
P005	DOE	1
P050	CIA/CRB/ADD/SD	2
NAVORDSTA (50L)		1
NASA/NST-44		1
AFIT/LD		1
LLL/Code L-389		1
NSA/1213/TDL		2

ORGANIZATION		MICROFICHE
E053	AF/INAKA	1
E017	AF/RDXTR-W	1
E403	AFSC/INA	1
E404	AEDC	1
E408	AFWL	1
E410	ADTC	1
	FTD	
	CCN	1
	ASD/FTD/NIIS	3
	NIA/PHS	1
	NIIS	2